NTNU – Trondheim
Norwegian University of
Science and Technology

Effects of Particle Shape on Mechanical Properties of Aggregates

Stefán Benediktsson

Geology
Submission date: May 2015
Supervisor: Børge Johannes Wigum, IGB

Norwegian University of Science and Technology
Department of Geology and Mineral Resources Engineering

Summary

Aggregates are one of the primary building material used in the world. The durability of construction aggregates will therefore depend upon the quality of aggregate mechanical properties. It is therefore important to understand how particle shape will effect mechanical properties of aggregates, measured by the Los Angeles and micro-Deval values. In order to assess the influence of particle shape on aggregate mechanical properties, the proportion of flaky and cubic particles, measured by the flakiness index (FI), was artificially varied in a series of tests for six different rock types. All in all 69 Los Angeles and 69 micro-Deval tests were performed according to European standards.

The main findings are that the standard Los Angeles (LA) and micro-Deval (MD) test methods which measure the amounts of fines ($<$1.6 mm) produced by impact and/or wear are generally not sensitive to variations in the flakiness index (FI). The LAx and MDx values, which are measured by the amounts of material passing the lower fraction of the size range, are more sensitive to variations in the flakiness index (FI). Sieve analysis also shows that the standard LA and MD method of measuring production of fines is not always a good indicator of aggregate breakdown and may in some cases ignore increased breakdown of the aggregate coarser than 1.6 mm. The LAx and MDx values better demonstrate the behavior of the aggregate coarser than 1.6 mm and give better information about the extent of aggregate breakdown.

Preface

This master thesis titled ”Effects of Particle Shape on Mechanical Properties of Aggregates” is my final requirement for fulfillment of masters degree in Geology with specialization in Environmental and Geo-technology from the Norwegian University of Science and Technology (NTNU). The main focus for the thesis is the relationship between particle shape measured by the flakiness index (FI) and mechanical properties of rock aggregates measured by the Los Angeles and micro-Deval tests.

The thesis work was done in the winter of 2014 - 2015, from September 1st - May 15th, under supervision from Professor Børge Johannes Wigum, to which I owe my gratitude for his guidance that made this thesis come together. Furthermore, I would like to thank Eyolf Erichsen (NGU) for wise input, discussions and for making the project possible. Special thanks go to Roald Tangstad (NGU) for assisting me greatly in collecting all the aggregate samples and Henry Vongraven (NGU) for his contribution to the laboratory testing. Finally, I would like to thank Nils S. Uthus (Statens vegvesen), employees at the Norwegian Geological Survey (NGU) and workers in the rock quarries for all the help.

Table of Contents

List of Tables

List of Figures

Abbreviations

LA	=	Los Angeles value
LAr	=	Los Angeles value residue
LAx	=	100% - LAr
MD	=	Micro-Deval value
MDr	=	Micro-Deval value residue
MDx	=	100% - MDr
FI	=	European standard flakiness index
I_F	=	British standard flakiness index
AIV	=	Aggregate impact value
AIVR	=	Aggregate impact value residue
ACV	=	Aggregate crushing value
ACVR	=	Aggregate crushing value residue
S	=	Norwegian impact value

Chapter 1

Introduction

1.1 Background

Aggregates are defined as particles of rock used for building and construction. Aggregates are one of the primary building material in the world, they are for example the main ingredient in asphalt (>95 %) and concrete (60-75 %). The durability of construction aggregates will therefore depend upon the quality of aggregate mechanical properties. Demand for aggregate is high and will only increase in the future as cities grow and demand for infrastructure increases. The yearly per capita consumption of aggregates in Norway 2013 was 12 tonnes (NGU, 2014). Crushed aggregates have steadily been taking over natural aggregates, from sand and gravel deposits, as the main supply of aggregates in Norway and worldwide. The main reason for this are more restrictive regulations aimed at preserving natural aggregates. In this study all aggregates will be crushed aggregates, that is bedrock excavated by blasting (shot rock) and reduced in size by crushers into various particle size fractions.

The research and development program "Environmentally Friendly Pavements" was aimed at lowering road tire noise and road dust emissions of road surfaces, related to vehicle traffic. One of the researches main findings was that road tire noise levels decrease as the aggregate particle size in the road surface decreases. Increased wear was, however, detected as the aggregate size decreased in the road surface, which can result in increased road dust emission (Aksnes and Evensen, 2009). Further investigation by Erichsen et al. (2010) showed aggregate strength decreasing with decreasing aggregate particle size and increasing flakiness index (FI). There has long been a question as to the effect of aggregate shape on mechanical properties of aggregates. Dhir et al. (1971) artificially varied the proportion of flaky particles from 0 to 85 percent and ran a series of aggregate impact and crushing tests. Little research has, however, been performed to establish flakiness index relationship to the Los Angeles and micro-Deval test methods.

1.2 Objective and Scope

Main objectives of this study are to:

- Examine the influence of particle shape on Los Angeles and micro-Deval test values.
- Suggest revision of today's requirement of flakiness index. Requirement for each size fractions, not average of all fractions.
- Evaluate how different geological parameters that is mineralogy, texture and mineral grain size effects the particle shape and mechanical properties of rock aggregate.

The scope of the project involves:

- Los Angeles (LA) and micro-Deval (MD) testing methods will be performed to test the mechanical properties of the material. Size fractions 4/8 mm, 8/11.2 mm and 11.2/16 mm with different proportions of flaky particles will be tested on predetermined rock types.
- Review of existing theory for the relationship between aggregate mechanical properties and flakiness index.

1.3 Methodology of the Study

The following methodology was applied during the study:

1. Literature review
    - The purpose of the literature review was to collect and review relevant domestic and foreign literature, research findings and other information relative to flakiness index relation to aggregate mechanical properties.
2. Aggregates collection and tests
    - Six hard-rock aggregate sources from four regions in Norway: Sør-Trøndelag, Nord-Trøndelag, Vestfold and Rogaland were chosen for study.
    - The micro-Deval (MD) and Los Angeles (LA) tests were conducted on all source samples.
3. Data processing and analyses
    - All data is processed and plotted using Microsoft Excel.
4. Conclusion and recommendations
    - Summary of research findings as well as recommendations.

1.4 Limitations of the Study

The analysis is limited to the few number of rock types collected. Collected samples may not be representative of the whole rock deposit (quarry).

Main challenge for the study was to collected enough material to carry out testing on various artificial mixtures for all size fractions. However, in this study, additional size fractions were analyzed, e.g. more size fractions than required in the standards.

Chapter 2

Literature Review

The purpose of the literature review was to collect and review relevant domestic and foreign literature, research findings and other information relative to flakiness index relation to aggregate mechanical properties. Also to familiarize the reader with the test methods mentioned and used in the thesis.

2.1 Aggregate Mechanical Tests

Mechanical tests have been developed to assess the durability of the rock material. These test can give an indication of the rocks performance in-service and service life. Various test methods have been developed to test different characteristics of the rock, in this literature review the focus will be on the Los Angeles (resistance to impact and abrasion), micro-Deval (resistance to abrasion), aggregate impact value (resistance to impact) and aggregate crushing value (resistance to crushing). Figure 2.1 shows how these different rock fracturing mechanisms work.

2.1.1 Los Angeles test (LA)

About

The Los Angeles test was developed during the 1920s at the Municipal Laboratory in the city of Los Angeles, it measures aggregate resistance to crushing and abrasive wear (Prowell et al., 2005). The lower the LA value is, the better the aggregate is at resisting impact and abrasion. The LA value is calculated as percentage of mass passing the 1.6 mm sieve after controlled impact and abrasion, thus the higher the LA value is, the higher the production of fines is. The Los Angeles test is an European Standard test method (EN 1097-1:2011) and is used worldwide as an aggregate qualification test (Meininger, 1994). Todays requirement according to the Norwegian Public Road Administration (NPRA) handbook N200 for the LA value ranges from $\leq$15 to $\leq$40 (Statens vegvesen, 2014) depending on the purpose of the material and annual average daily traffic (AADT). Some concerns

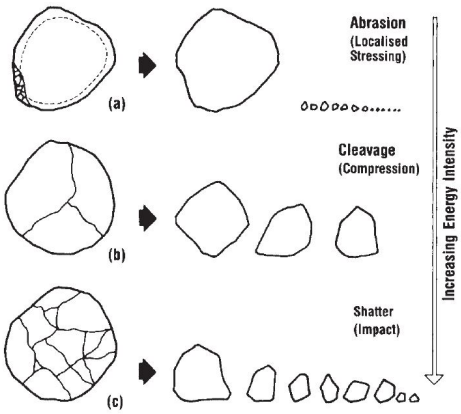

Figure 2.1: Rock fracturing mechanism (Barksdale, 1991).

about LA correlation to field performance have arisen over the years due to its high impact loading of the aggregate and not abrasion which happens in the field, on for example highways. Good example is coarse grained granites which give good field performance but often obtains poor results from the Los Angeles test. Due to the brittleness of the material. On the other hand, softer material and therefore material with worse abrasion resistance can obtain good results from the Los Angeles test. This is due to the material absorbing the impact and not braking but deforming, resulting in good LA value but poor field performance (Senior and Rogers, 1991). A recent study by Nålsund (2014) found the Los Angeles test method to categorize aggregates quality clearly, based on their mechanical properties. Poor correlation was, however, found between the LA value and field performance of aggregate ballast.

Erichsen (2014) investigated the degradation of aggregates during the Los Angeles test and raises the question if the Los Angeles value residue (LAr) is better at demonstrating aggregate breakdown. Fernlund (2005) writes that rocks types do not fragment equally. Different rock types can have the same LA value but the way they break down can differ greatly. She states that sieve analysis cannot distinguish between these differences. Ramsay et al. (1974, 1977) Spence et al. (1974) write that sieving and measuring the fines passing a sieve size much smaller than the original particle size range does not represent a realistic measurement of aggregate strength. The same methodology is used for the Los Angeles value and micro-Deval value where the breakup is measured by the amount of material passing 1.6 mm sieve size.

Test Procedure

Los Angeles test was conducted at Norwegian Geological Survey (NGU) material lab according to the European standard (EN 1097-2:2010). The test procedure for the Los Angeles test starts by placing a 5000±5 g (M_0) aggregate sample inside a drum rotating about its horizontal axis. The drum is closed at both ends with internal diameter of (711

Figure 2.2: Los Angeles test machine used in study.

$\pm$ 5) mm and an internal length of (508 $\pm$ 5) mm. The support system for the machine consists of two horizontal stub axles connected to the walls of the drum but do not enter into the drum. The machines must be based on a level concrete or stone block floor. To insert and remove test material and steel balls from the drum a dust-proof opening (150 $\pm$ 3) mm wide is made available over the whole length of the drum. 11 spherical steel balls are put inside the drum with the test material. A single ball has a diameter of between 45 mm and 49 mm and weighs between 400 g and 445 g. Total weight of the 11 balls must weigh between 4690 g and 4860 g.

In this study size fractions other than the standard 10/14 mm were tested. In order to produce results similar to the standard 10/14 mm fraction an alternative narrow range classification method has been made to the Los Angeles test. Table 2.1 shows how number of balls and mass of ball load varies for each range classification. It must be stressed that the results will not be exactly like the 10/14 mm reference method.

Inside the drum there is a single rigid shelf with length equal to that of the drum. The purpose of this shelf is to pick up the aggregates and steel balls as the drum rotates. At a certain height the aggregates and steel balls drop from the shelf on to the opposite side

of the drum causing impact and crushing to the aggregates. Additionally the aggregates are subjected to abrasion and grinding as the drum rotates. The drum rotates at a constant speed between 31 and 33 rounds per minute for 500 revolutions. After the machine test is completed the material is collected, washed and sieved using a 1.6 mm sieve. The material left on the 1.6 mm sieve is dried at a temperature of (110 $\pm$ 5) °C and then weighed (m).

Table 2.1: Alternative narrow range classifications for the Los Angeles test.

Range classification (mm)	Intermediate sieve size (mm)	Percentage passing intermediate sieve (%)	Number of balls	Mass of ball load (g)
4 to 8	6.3	60 to 70	8	3410 to 3540
8 to 11.2	10	60 to 70	10	4250 to 4420
11.2 to 16	14	60 to 70	12	5120 to 5300

Equations

The Los Angeles value (LA) is calculated with the following equation (2.1):

$$LA = \frac{M_0 - m}{M_0} \times 100 \tag{2.1}$$

where,
M_0 is the initial mass of sample, in grams.
m is the sum of mass >1.6 mm, in grams.

The Los Angeles value residue (LAr) is the percentage of mass retained on a sieve size with same aperture size as the lower fraction of the size range. LAr is calculated with the following equation (2.2):

$$LAr = \frac{M_1}{M_2} \times 100 \tag{2.2}$$

where,
M_1 is the mass retained on a sieve size with same aperture size as the lower fraction of the size range, in grams.
M_2 is the initial mass of the sample, in grams.

The LAx is the percentage of mass passing a sieve size with same aperture size as the lower fraction of the size range. The lower the LAx value is, the better the aggregate is at resisting impact and abrasion. LAx is calculated with the following equation (2.3):

$$LAx = 100\% - LAr \tag{2.3}$$

2.1.2 Micro-Deval test (MD)

About

The micro-Deval test was developed during the 1960s in France. The micro-Deval test method measures aggregate resistance to wear by subjecting the aggregates to inter-particle abrasion and an abrasive charge in the form of steel balls. The micro-Deval test is performed with water inside the drum. This could result in micro-Deval giving more accurate field performance in comparison to the Los Angeles test, which is performed dry (Senior and Rogers, 1991). Many aggregate decrease in strength when wet, resulting in poor field performance (Prowell et al., 2005). The lower the micro-Deval value (MD) is, the better the aggregate is at resisting abrasive wear. Todays requirement according to the NPRA handbook N200 for the MD value ranges from $\leq$15 to $\leq$20 (Statens vegvesen, 2014) depending on the purpose of the material and AADT. Recent research by Nålsund (2014) found a correlation between amount of soft minerals and MD value. As amounts of soft minerals (low hardness) increases in an aggregate particle, the MD value increases (poor resistance against abrasive wear).

Figure 2.3: Micro-Deval test machine used in study.

Test Procedure

Micro-Deval test was conducted at NGU's material lab according to European standard (EN 1097-1:2011). The test procedure for the micro-Deval starts by placing a 500±2 g (M_0) aggregate sample inside a drum with an inside diameter of (200 ± 1) mm and an internal length of (154 ± 1) mm. An abrasive charge in the form of steel balls (5000 ± 5) g is also added to the drum, the diameter of each steel ball shall be (10 ± 0.5) mm.

In this study size fractions other than the standard 10/14 mm were tested. In order to produce results similar to the standard 10/14 mm fraction an alternative narrow range classification method has been made to the micro-Deval test. Table 2.2 shows how mass of ball load varies for each range classification. It must be stressed that the results will not be exactly like the 10/14 mm reference method.

Water (2.5 ± 0.05) liters is added to the drum and the drum is closed by a watertight and dust-tight lid seal. The drum is then rotated around its horizontal axis at a speed of 100 rounds per minute for (12000 ± 10) revolutions. After the test, the material sample is washed and sieved using a 1.6 mm sieve and a 8 mm guard sieve to separate the aggregates from the steel balls. Magnet is then used to pick up the steel balls. The material left on the 1.6 mm sieve is dried at a temperature of (110 ± 5) °C and then weighed (m).

Table 2.2: Alternative narrow range classifications for the micro-Deval test.

Range classification (mm)	Intermediate sieve size (mm)	Percentage passing intermediate sieve (%)	Mass of ball load (g)
4 to 8	6.3	60 to 70	2800 ± 5
8 to 11.2	10	60 to 70	4400 ± 5
11.2 to 16	14	60 to 70	5400 ± 5

Equation

The micro-Deval value (MD) is calculated with the following equation (2.4):

$$MD = \frac{M_0 - m}{M_0} \times 100 \tag{2.4}$$

where,
M_0 is the initial mass of sample, in grams.
m is the sum of mass >1.6 mm, in grams.

The micro-Deval value residue (MDr) is the percentage of mass retained on a sieve size with same aperture size as the lower fraction of the size range. MDr is calculated with the following equation (2.5):

$$MDr = \frac{M_1}{M_2} \times 100 \tag{2.5}$$

where,
M_1 is the mass retained on a sieve size with same aperture size as the lower fraction of the size range, in grams.
M_2 is the initial mass of the sample, in grams.

The MDx is the percentage of mass passing a sieve size with same aperture size as the lower fraction of the size range. The lower the MDx value is, the better the aggregate is at resisting abrasion. MDx is calculated with the following equation (2.6):

$$MDx = 100\% - MDr \tag{2.6}$$

2.1.3 LAx and MDx values

The LAx and MDx values are calculated as the amount of material passing the lower size fraction of the size range. Figure 2.4 shows test fraction 8/11.2 mm used as an example to better understand the process behind the LAx and MDx values. After the 8/11.2 mm test fraction has been run through the LA and MD testing machines it is collected and analyzed in a column of sieves. For size fraction 8/11.2 mm the uppermost sieve size in the column is 8 mm, the LAx and MDx value is then calculated as percentage of mass passing the uppermost sieve size. The uppermost sieve size is always the lower size fraction of the size range. The higher the LAx and MDx values are, the more material is breaking down and leaving the original size range. Increasing LAx and MDx values therefore indicate increased breakdown of material. The x in LAx and MDx represents the size of the uppermost sieve, hence the name of the values:

- LA4: Percentage mass of the test fraction (4/8 mm) passing through the 4 mm sieve size
- LA8: Percentage mass of the test fraction (8/11.2 mm) passing through the 8 mm sieve size
- LA11: Percentage mass of the test fraction (11.2/16 mm) passing through the 11.2 mm sieve size

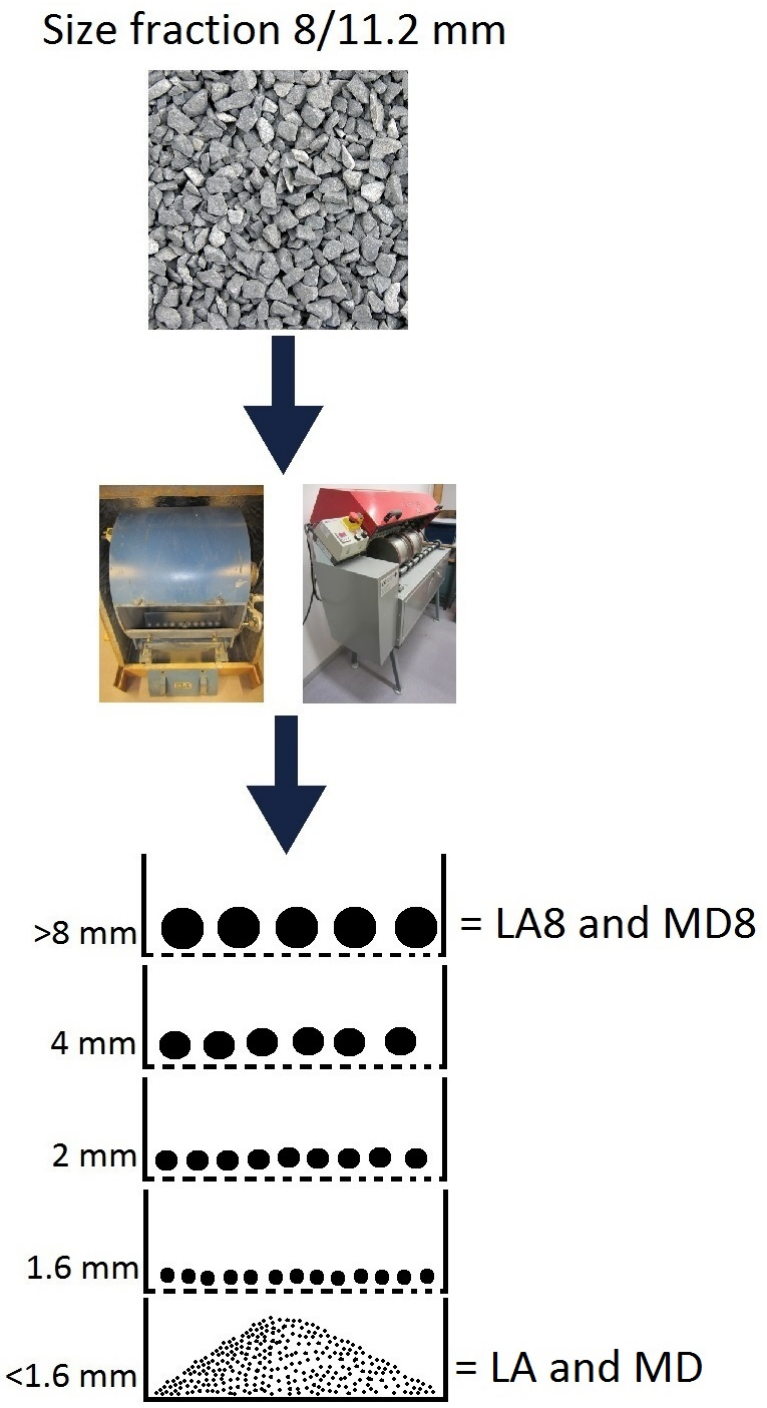

Figure 2.4: Outline of the steps that lead to the calculation of LA, LAx, MD and MDx. Particle size fraction 8/11.2 is used as an example.

2.1.4 Aggregate Impact Value (AIV) and Aggregate Crushing Value (ACV)

The aggregate impact test apparatus (BS 812-112:1990) is a simple aggregate test machine allowing it to be taken into the field to do testing, see figure 2.5. The test machine is basically a weight in the form of a hammer or a piston, weighing from 13.5 kg to 14.1 kg. When the hammer is released it falls down 385 ± 6.5 mm, this is repeated 15 times for each test. This repeated impact to the aggregate material will give a measure of the materials resistance to granulation. Only two aggregate impact values are enough for each sample due to its high reproducibility. The aggregate impact value is calculated as a percentage of sample material passing 2.36 mm sieve relative to initial weight. The lower the aggregate impact value is, the better the aggregate is at resisting granulation (Smith and Collis, 1993).

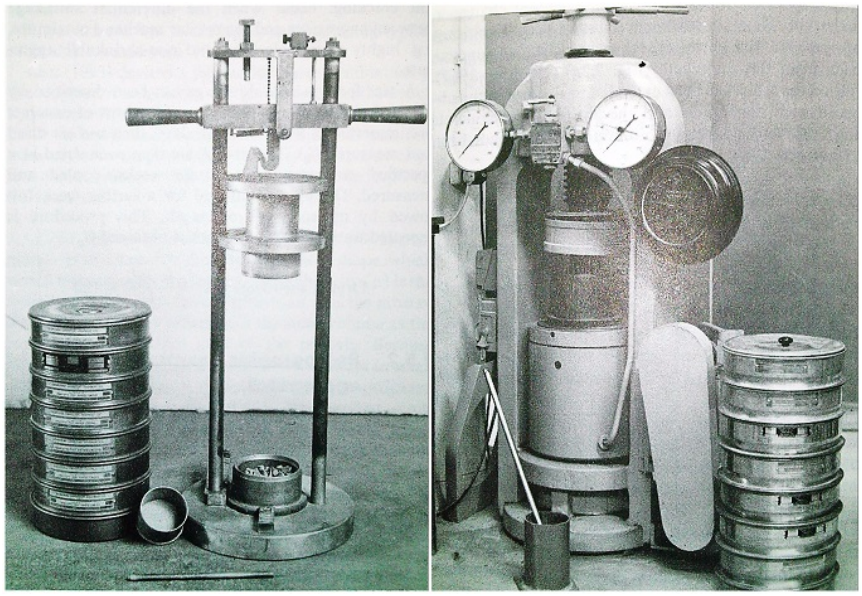

Figure 2.5: AIV test apparatus on the left and ACV test apparatus on the right (Smith and Collis, 1993).

The aggregate crushing test apparatus (BS 812-110:1990) is a compression machine, see figure 2.5. A sample weighing around 2 kg is put under a continuous load by a piston. The aggregate material is subjected to this load for 10 minutes resulting in a total load of 400 kN. Only two aggregate crushing values are enough for each sample due to its high reproducibility. The aggregate impact value is calculated as a percentage of sample material passing 2.36 mm sieve relative to initial weight. The lower the aggregate crushing value is, the better the aggregate is at resisting crushing (Smith and Collis, 1993).

2.1.5 Norwegian Impact Test (S)

The Norwegian impact test method (Statens vegvesen 1997, chapter 14.451) is very similar to the aggregate impact test, it was first developed in Sweden and its intended use was to measure rock strength properties. Modified versions of the test have been developed and one of them is the Norwegian impact test also called Brittleness value or Sprøhetstall, see figure 2.6. A piston weighing 14 kg falls down 250 mm onto the sample, 20 times. The S value is then calculated as a percentage passing the original size range. The S8 value would therefore be calculated as percentage of material passing 8 mm sized sieve and S2 passing 2 mm sized sieves. The lower S value is, the better the aggregate is at resisting crushing by repeated impacts (Dahl et al., 2012).

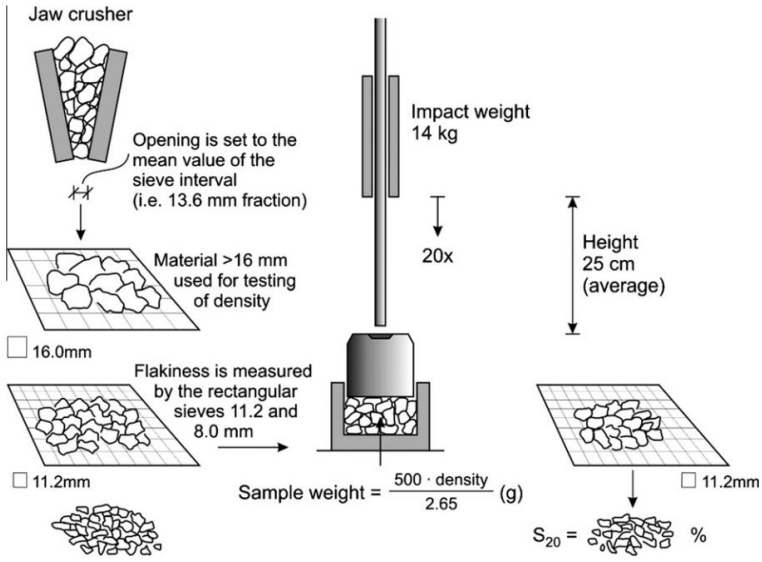

Figure 2.6: Procedure for the Norwegian impact test value (S_{20}) (Dahl et al., 2012).

Around 2005 the Norwegian impact test was replaced by the Los Angeles test for determining resistance to crushing for road aggregates in Norway. The relationship between the Los Angeles and the Norwegian impact test was studied, correlation between these two test methods was made using the correlation coefficient (r). The correlation coefficient is the square root of R^2 which is calculated from regression analysis, values close to zero suggest poor correlation while values close to 1 or -1 suggest high correlation. The results gave good correlation coefficient of r = 0.90. The results on the plot were, however, very spread out and scattered. The Los Angeles test uses 1.6 mm sieve to calculate the value, therefore a 2 mm sieve (S2) was used to calculate the Norwegian impact value instead of 8 mm sieve. The results from S2 plotted against the LA value gave better correlation coefficient of r = 0.96 and less scattered plot (Erichsen, 2013).

2.2 Petrographic Properties

Rocks are divided into three main groups by how they are formed: igneous, sedimentary and metamorphic. Each group is then subdivided, mainly by the rocks mineralogy and texture. Sedimentary and metamorphosed rocks normally show more variation than igneous rocks due to layering of the strata (Dunlevey and Stephens, 1998). Deere and Miller (1966) state that rocks with low strength are usually very porous, chemically altered, sedimentary rocks with weak bonds or strongly foliated igneous and metamorphic rocks.

Researches have shown that mineral grain size can have large impact on mechanical properties of rock. Investigations by Brattli (1992) and Liu et al. (2005) have shown that as mineral grain size decreases, the better the aggregate is at resisting fragmentation and abrasion. Nålsund and Jensen (2013) investigated a large collection of igneous, metamorphic and consolidated/metamorphosed sedimentary rocks (fine- to very fine-grained). The results found poor correlation between textural properties (mineral grain size, mineral grain size distribution and micro-cracks) and mechanical properties (Los Angeles value and micro-Deval value). Haraldsson (1984) also did not find strong correlation between mineral grain size (fine- and coarse-grained basalts) and mechanical properties. Micro cracks inside the mineral grains have also been identified to be an important factor when it comes to mechanical properties of aggregates (Nålsund and Jensen, 2013).

2.3 Aggregate Flakiness

Flaky aggregate shape is considered to be unfavorable due to low strength, which will in return lower the strength of the product, for example concrete and asphalt. The most favorable shape is cubic or spherical shape, cubic shape gives maximum strength to the aggregate. Other reasons why it is the most favorable shape is that cubic aggregates pack more, resulting in low void ratio and more compact material (Prowell et al., 2005). A flaky aggregate particle is basically a particle with one axis considerably smaller than the other two axis, see figure 2.7.

More than 95 percent of asphalt pavement consists of aggregates. Brown et al. (1989), Kandhal et al. (1992) and Kim et al. (1992) researches state that particle size, shape and texture have large impact on the performance of hot-mix asphalt pavement. Bouquety et al. (2007) states that aggregate shape is one of the key factors when describing the quality of aggregates. Bouquety et al. (2007) states that as the proportion of flaky particles increases: concrete compression strength decreases, consumption of cement increases, concrete workability decreases, asphalt packing density decreases and asphalts compressive- and tensile strength decreases. Akbulut and Gürer (2007) investigation reviled that flaky particles have low tensile strength and should therefore be limited in asphalt concrete as it increases deformation.

The particle shape of crushed aggregates are known to be controlled by the geology (petrography) of the aggregate and the production factors at the quarry. More flaky particles are produced when crushing strong and hard or brittle rocks than weak rocks (Smith and

Collis, 1993). He also writes that fine grained igneous rocks are more brittle than coarse grained and give higher proportion of flaky particles, the stronger the rock is the higher the proportion of flaky aggregate particles is. He also says mineral grains with high directional dependence (anisotropy) such as quartz and feldspar increase the flakiness of the aggregate. Production factors can be modified to produce less flaky aggregate particles, some of these main factors are:

- Gyratory crushers and impactors produce superior aggregate shape compared to jaw crushers (Czarnecka and Gillott, 1982)
- Choke feed the crusher (compression crushers) with constant feed to boost inter-particle crushing (Prowell et al., 2005)
- Reduce the reduction ratio in each stage, instead have multiple stages (Wigum, 2014)
- The closed side setting of compression crushers should be equal to the size of the desired product and should be monitored, the bowl and head liner will wear out with time and particles could go through the open side setting without being fully crushed. Gyration speed in gyratory crushers can also be increased to limit particles going through the open side setting without being fully crushed (Prowell et al., 2005)
- Vertical shaft impact crushers (VSI) have proven to produce more cubic aggregates (Prowell et al., 2005)

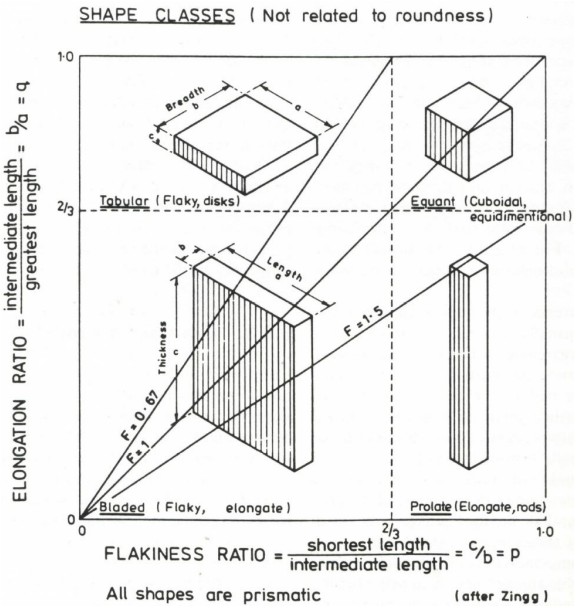

Figure 2.7: Shape categories (Smith and Collis, 1993).

Flakiness index (FI)

About

The flakiness index is a physical test method for determination of aggregate particle shape. The lower the flakiness index number is, the closer the aggregate is to cubic shape. Flakiness index was first introduced to the NPRA handbook 018 in 2005. Todays requirement according to the NPRA handbook N200 for the flakiness index (FI) ranges from $\leq$25 to $\leq$35 (Statens vegvesen, 2014) depending on the purpose of the material and AADT.

Test Procedure

Flakiness index was conducted at NGU's material lab according to the European standard (EN 933-3:1997+A1). The test procedure for flakiness index consist of double sieving with square hole sieves and bar sieves, see figure 2.8. First the sample is separated into different particle size fractions, then it is screened with a bar sieve. The distance between the bars in the bar sieve are half the size of the square hole sieves diameter, see table 2.3.

Figure 2.8: Particle size 8/10 mm being screened by 5 mm bar sieve.

Table 2.3: Bar sieves used in this study.

Particle size fraction (mm)	Width of slot in bar sieve (mm)
14/16 mm	8 mm
11.2/14 mm	7 mm
10/11.2 mm	5.6 mm
8/10 mm	5 mm
6.3/8 mm	4 mm
4/6.3 mm	3.15 mm

Equation

$$FI = (\frac{M_2}{M_1}) \times 100 \tag{2.7}$$

where,
M_1 is the total weight, in grams.
M_2 is the sum of particles passing through the corresponding bar sieves, in grams.

British standard flakiness index (I_F)

The British standard flakiness index (I_F) (BS 812: 1989) is measured and calculated similarly to the European standard flakiness index, see equation 2.7. However the relationship between the square hole sieve diameter and distance between the bars in the bar sieve is calculated as 0.6 times the mean dimension (Smith and Collis, 1993). For example, 8/10 mm particle size would be calculated as 0.6×((8+10)/2) = 5.4 mm gap between bars.

2.4 Relationship Between FI and Mechanical Properties of Aggregates

Research on aggregate shape relation to mechanical properties dates all the way back to 1949 when Selmer-Olsen revealed how aggregate shape can effect various rock types, see figure 2.9. Certain rock types show substantial variation with aggregate shape, others less. Erichsen (2013) evaluated the methods used to test aggregates and correlated the Norwegian impact value S8 to the LA value (8/11.2 mm), the results reviled good correlation coefficient (r = 0.90). The report also reveled good correlation between the flakiness number (flisighetstall) and flakiness index (FI), although, correlation varied for each particle size fraction. Particle size fraction 8/11 mm had good correlation (r = 0.95), size fraction 10/14 mm had fair correlation (r = 0.87) and particle size fraction 11/16 mm had the lowest r-value of them all (r = 0.84). Correlation can clearly be seen between these test methods and therefore similar results can be expected when LA value is plotted against FI.

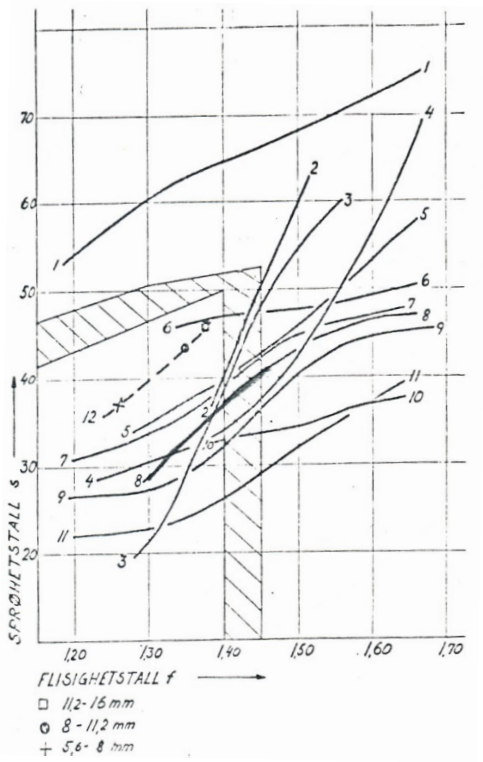

Figure 2.9: The Norwegian impact value (S) (sprøhetstall) versus the flakiness-number (flisighetstall) (Selmer-Olsen, 1949).

Selmer-Olsen (1980) states that particle breakdown is not only tied to aggregate strength but also aggregate shape. Figure 2.10 shows how the Norwegian impact value (S) varies and generally increases as the flakiness-number (flisighetstall) increases. From the results in figure 2.10 he states that rock types with large mineral grain size, generally have higher S value compared to fine grained rock types. Large variations in the S value and flakiness-number (flisighetstall) are observed within each rock type. Medium- to fine-grained gabbros have lower S value than similar granitic rock types. Selmer-Olsen (1980) also correlated the LA value to the S value, see figure 2.10. He states that the Los Angeles test method is not as sensitive to changes in aggregate flakiness, compared to the Norwegian impact test method. Although, the two test methods have good correlation when the flakiness-number is around 1.45. When the flakiness-number goes above 1.50 or under 1.30 the correlation gets poorer.

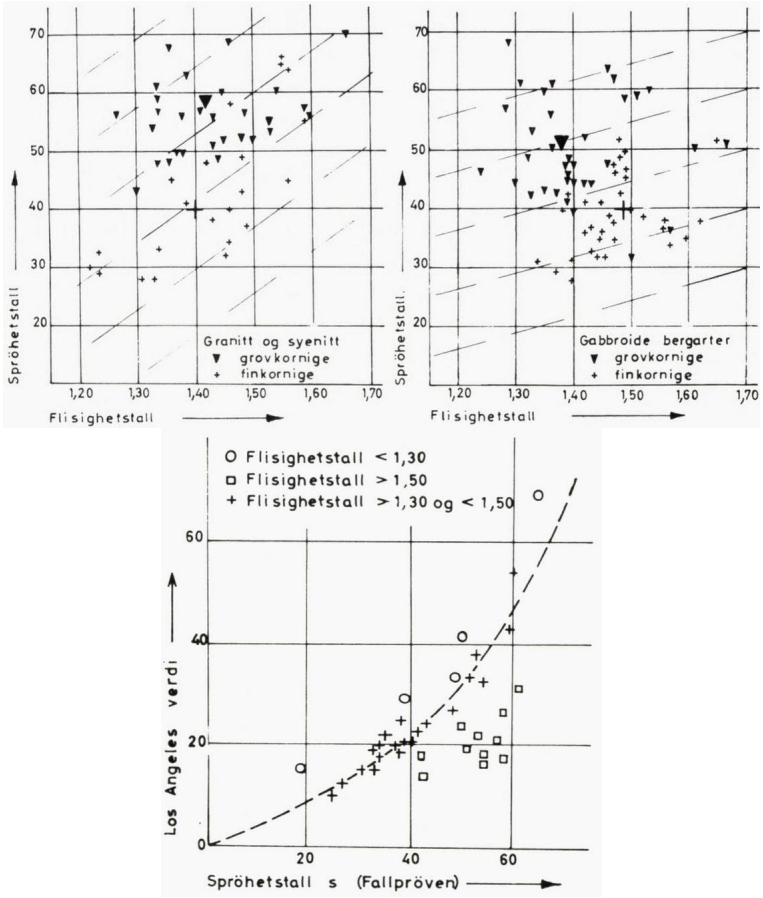

Figure 2.10: The Norwegian impact value (S) (sprøhetstall) versus the flakiness-number (flisighetstall) for different rock types. Also the relationship between S and LA, with variations in the flakiness-number (Selmer-Olsen, 1980).

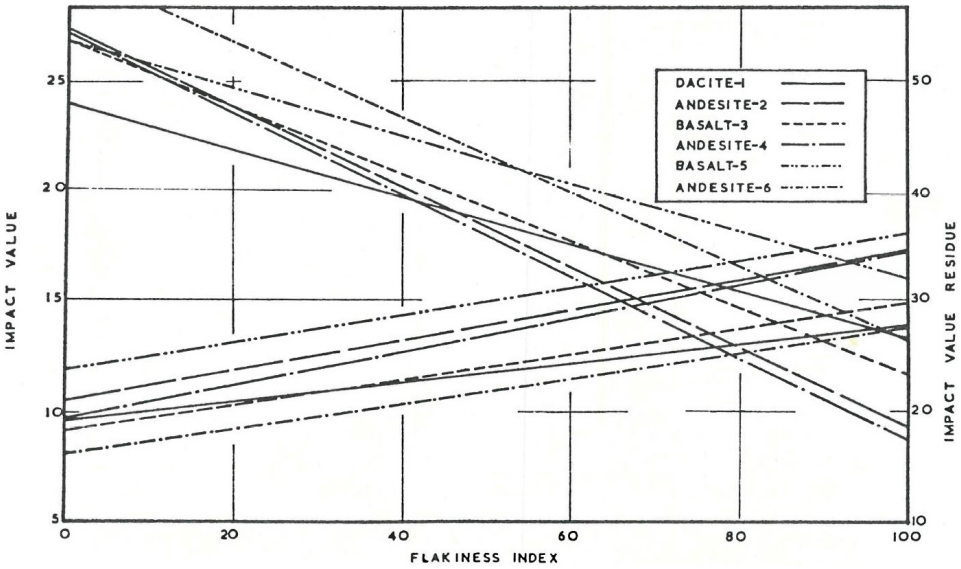

Figure 2.11: The aggregate impact value (AIV) and impact value residue (AIVR) versus the British standard flakiness index (I_F) (Dhir et al., 1971).

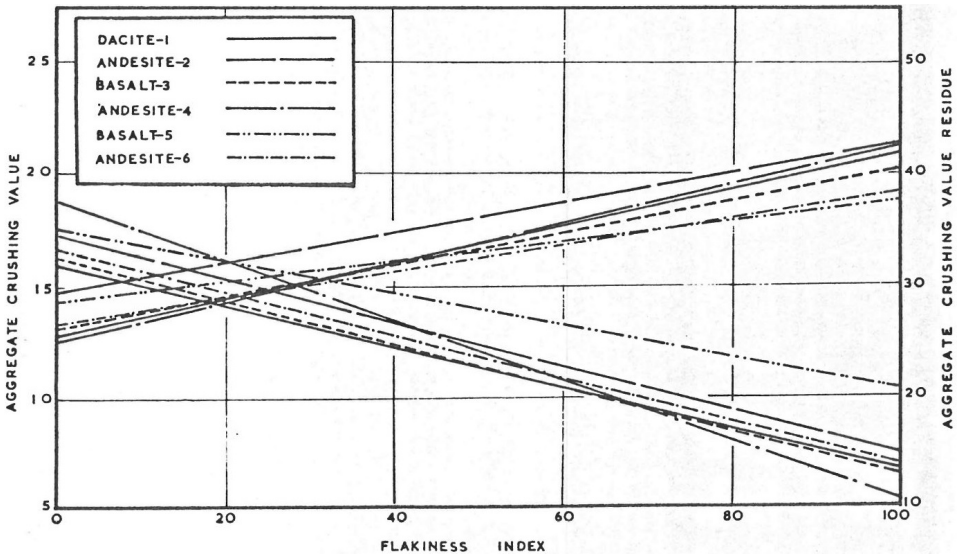

Figure 2.12: The aggregate crushing value (ACV) and crushing value residue (ACVR) versus the British standard flakiness index (I_F) (Dhir et al., 1971).

A study made by Dhir et al. (1971) investigated fine-grained basic igneous rocks. The relationship between the aggregate impact value and aggregate crushing value were investigated and how particle shape and petropgraphy affects those two values. To determine the influence of particle shape on these two values, I_F was artificially varied from 0 to 85 percent. The results of this work can be seen in figure 2.11, where the relationship between the aggregate impact value (AIV) and I_F can be seen to have linear relationship with overall statistical analysis of AIV = 9.7813 + 0.0571 I_F, r = 0.7969. Furthermore, the impact value residue (AIVR) was investigated and was shown to be much more sensitive to changes in aggregate particle shape AIVR = 54.17557 - 0.3067 I_F, r = 0.9249, compared to the standard aggregate impact value. Figure 2.12 shows similar results for the aggregate crushing value and crushing value residue. Overall statistical analysis result in ACV = 13.5055 + 0.0677 I_F, r = 0.9462 and ACVR = 34.2024 + 0.2035 I_F, r = 0.9266. It can bee seen that aggregate crushing value residue (ACVR) is also more sensitive to variations in aggregate shape. Dhir et al. (1971) therefore recommend the residual values to be used when analyzing aggregate quality.

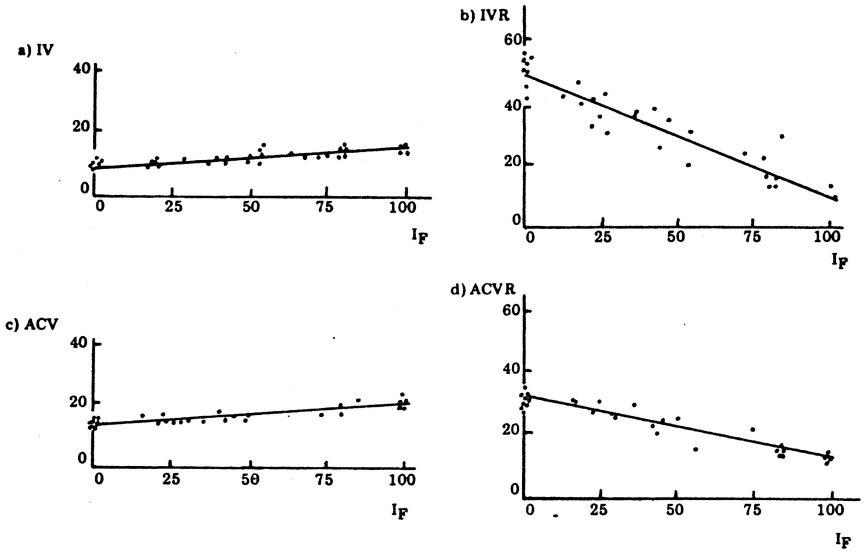

Figure 2.13: (a) Aggregate impact value (AIV), (b) Aggregate impact value residue (AIVR), (c) Aggregate crushing value (ACV), (d) Aggregate crushing value residue (ACVR) versus the flakiness index (I_F) (Spence et al., 1974).

Ramsay et al. (1974, 1977) and Spence et al. (1974) state that the residue value is more sensitive to changes in particle shape and can be used to better assess the influence of particle shape on mechanical properties, see figure 2.13. From that figure it can clearly be seen that the residue values have much steeper slopes and are much more sensitive to change in particle shape. Ramsay et al. (1974) also found a relationship between rock strength and aggregate shape. Rocks that are considered to be weak (AIV much higher than 25) were not as affected by aggregate shape as rocks that are considered to be strong.

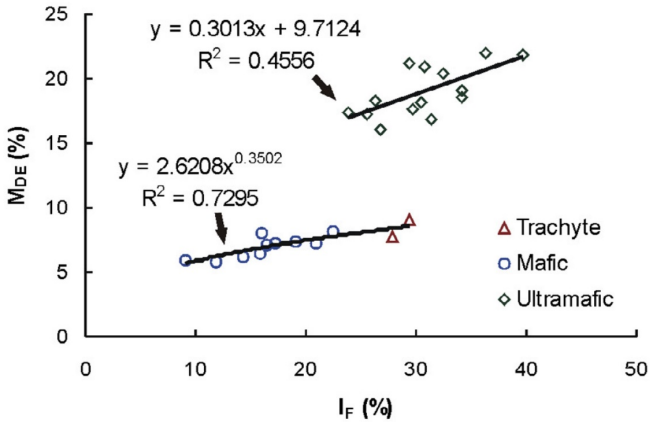

Figure 2.14: MD versus the flakiness index (I_F) (Rigopoulos et al., 2013).

Recent research by Rigopoulos et al. (2013) investigated construction aggregates from Greece and the relationship between their physical and mechanical properties. The research revealed that the I_F and MD values correlate positively with each other. Figure 2.14 shows that as the flakiness index increases, aggregates resistance to wear decreases. The two different trends that can be observed between ultra-mafic and mafic-trachytic samples was suggested to be due to high tectonic deformation, which the ultra-mafic samples have been subjected to and lowers their mechanical strength.

A research made by Erichsen et al. (2010) investigated three rock types (porphyry, gabbro and monzonite) with dissimilar mechanical properties regarding resistance to crushing and abrasive wear. Particle size fractions 4/8 mm, 8/11.2 mm, 10/14 mm and 11.2/16 mm for each rock type were tested using Los Angeles and micro-Deval test methods.

Figure 2.15 shows MD versus FI for different particle size fractions. The MD value is seen to increases steadily with decreasing particle size and increase in FI value. Figure 2.16 shows the LA versus FI for different particle size fractions. The LA value is seen to increases steadily with decreasing grain size and increase in FI value. Wieden and Augustin (1977) ran Los Angeles tests with different proportions of flaky and elongated particles for various rock types. Regardless the rock type, increase in proportion of flaky and elongated particles caused increase in the LA value. Röthlisberger et al. (2005) reported that increase in the percentage of flaky particles, increases the LA value. Figure 2.17 shows FI plotted against different size fractions. The results indicate that the FI increases steadily as aggregate size decreases. Also FI calculated for each particle size fractions is seen here to give better and more detailed information about the aggregate flakiness of a rock type compared to FI calculated for a wide particle range (4/16 mm).

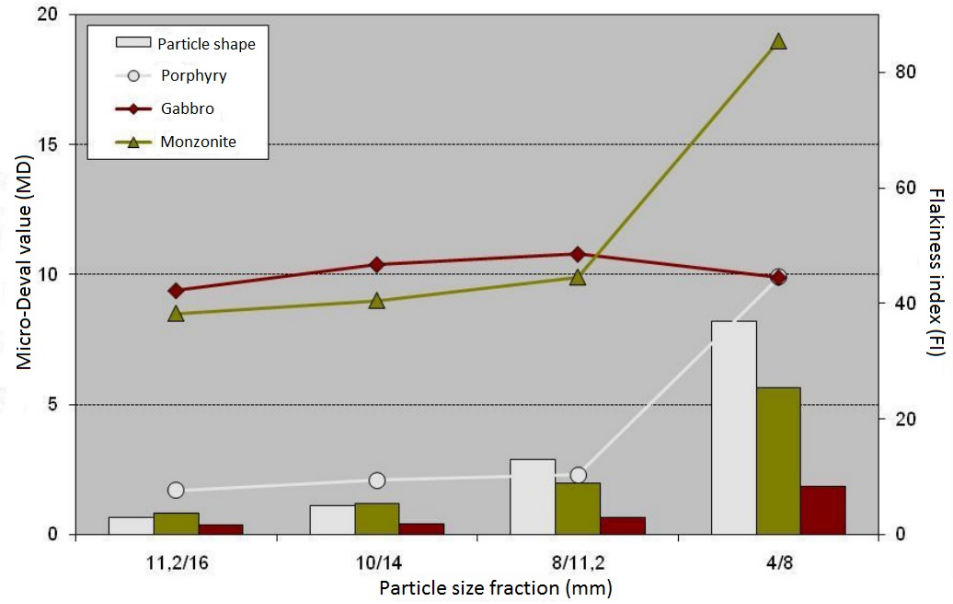

Figure 2.15: MD versus the flakiness index (FI) (Erichsen et al., 2010).

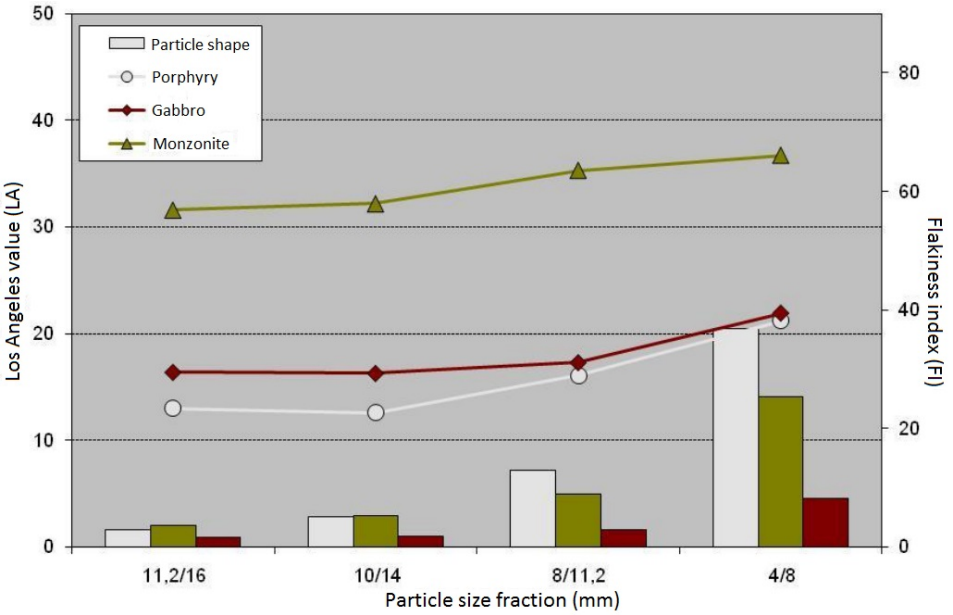

Figure 2.16: LA versus the flakiness index (FI) (Erichsen et al., 2010).

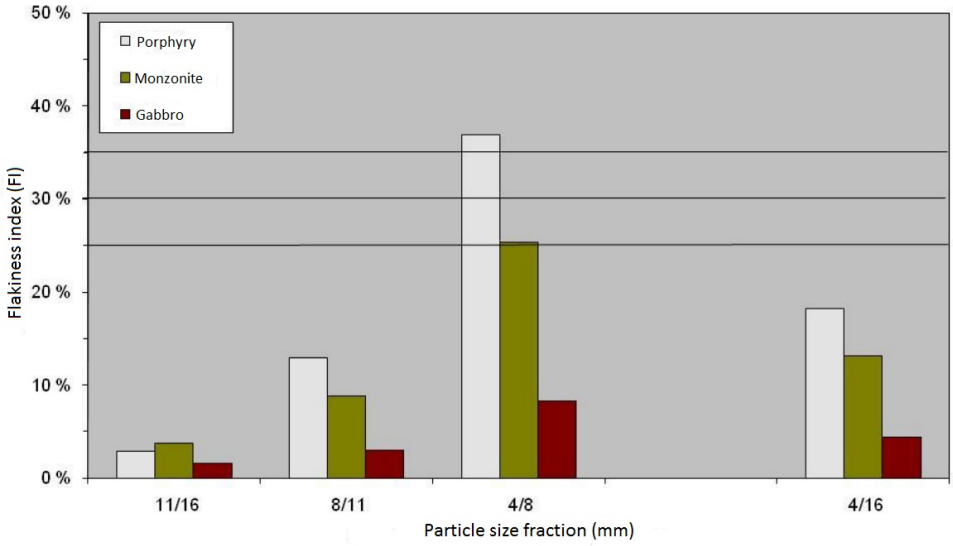

Figure 2.17: The flakiness index (FI) versus particle size fractions. Black lines mark the requirement for FI (Erichsen et al., 2010).

Test results from Erichsen et al. (2010) indicate that current test methods, Los Angeles abrasion test and micro-Deval, vary with aggregate shape and particle size fractions, see figure 2.15 and 2.16. Although, he concludes that it can not be ascertained if mechanical strength varies with aggregate particle size fractions. The test methods do not use the same number of steel balls for each particle size fraction. The size and weight of each steel balls are the same, smaller size particles are therefore loaded with larger force per area compared to larger sized particles.

2.5 Summary

- Flakiness index (FI) calculated for each particle size fractions gives better and more detailed information about the aggregate flakiness of a rock type compared to flakiness index (FI) calculated for a wide particle range.
- Aggregate impact value (AIV) increases with increasing flakiness index (I_F).
- Aggregate crushing value (ACV) increases with increasing flakiness index (I_F).
- Aggregate impact value residue (AIVR) proven to be more sensitive to changes in flakiness index (I_F) compared to the standard aggregate impact value (AIV).
- Aggregate crushing value residue (ACVR) proven to be more sensitive to changes in flakiness index (I_F) compared to the standard aggregate crushing value (ACV).
- Los Angeles value residue (LAr) more sensitive to particle breakdown compared to standard Los Angeles value (LA).
- Positive correlation found between micro-Deval (MD) and flakiness index (I_F).

Chapter 3

Fieldwork

Fieldwork was carried out between 14th October and 3rd November 2014 in six bedrock quarries located in Sør-Trøndelag, Nord-Trøndelag, Vestfold and Rogaland. The goal was to gather enough flaky and cubic material from six bedrock quarries, each with different rock types, to run Los Angeles and micro-Deval laboratory tests. Minimum two rock hand samples were taken at each location which were used to prepare thin-section for further mineralogical study additionally, 30 kg of size fraction 4/8 mm, 8/11.2 mm and 11.2/16 mm was collected for standard (normal) procedure testing. The rock material collected was taken from stockpiles in the quarries.

Figure 3.1: Transporter and piles of crushed aggregate 4/8 mm, 8/11.2 mm and 14/16 mm.

After a suitable location for the transporter was found in the quarry, see figure 3.1, a wheel-loader came with less than half a bucket containing crushed aggregates of size fractions 4/8 mm, 8/11.2 mm and 11.2/16 mm. The aggregates size fractions were then split up into different size fractions by hand sieving, see table 3.1. Bar sieve was then used to screen the material into flaky and cubic aggregate particles.

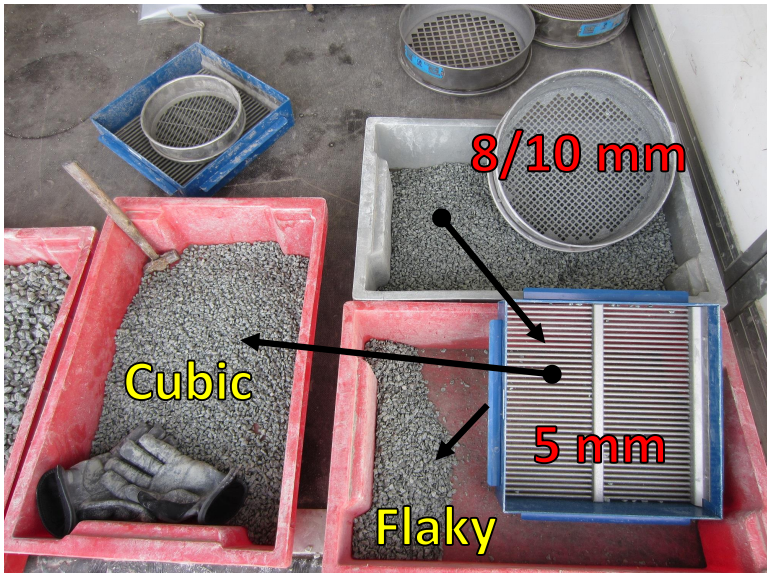

Figure 3.2: Shows particle size fraction 8/10 mm being screened with a 5 mm bar sieve.

Table 3.1: Sieve sizes used to split the original size fractions and corresponding bar sieves.

Size fraction (mm)	Sieve size used to split (mm)	Size fractions after split (mm)	Bar sieves (mm)
11.2/16 mm	14 mm	14/16 mm	8 mm
		11.2/14 mm	7 mm
8/11.2 mm	10 mm	10/11.2 mm	5.6 mm
		8/10 mm	5 mm
4/8 mm	6.3 mm	6.3/8 mm	4 mm
		4/6.3 mm	3.15 mm

Table 3.2: Table of minimum amount of aggregates required to run laboratory tests.

Particle size fraction (mm)	Bar sieve (mm)	Version A (g)	Version B (g)	Version C (g)
14/16	8	5250	3150	2100
11.2/14	7	9750	5850	3900
10/11.2	5.6	5250	3150	2100
8/10	5	9750	5850	3900
6.3/8	4	5250	3150	2100
4/6.3	3.15	9750	5850	3900

Screening out enough flaky material proved to be the biggest challenge as can be seen in figure 3.2, there particle size 8/10 mm is being sieved with a 5 mm bar sieve. A minimum amount of aggregate material was required to be able to run different artificial flakiness index mixtures in Los Angeles and micro-Deval laboratory tests, see table 3.2. For example to be able to run version A of laboratory tests on size fraction 14/16 mm; 5250 g of both cubic and flaky aggregates material had to be screened out. In case of weighing errors due to the material being wet and/or sandy; additional 500 - 700 g were added to the minimum amount required. Version A allows for four different artificial mixture designs of the flakiness index, that is 0 %, 25 %, 50 %, 75 % and 100 %. Version B allows for three different artificial mixture designs of the flakiness index, that is 25 %, 50 % and 75 %. Version C allows for two different artificial mixture designs of the flakiness index, that is 25 % and 75 %.

3.1 Aggregate Sampling

The selection of quarries (rock type) was based on representing a wide variation in the Los Angeles- and micro-Deval mechanical properties tests. The sampling took place in the quarries from stockpiles containing commercial product.

3.1.1 Gabbro

Fieldwork was accomplished between the 14th and 15th of October. The number of crushing stages the sampled material has been subjected to can be seen in table 3.3. The version achieved, to run various artificial mixtures of the flakiness index, for each particle size fraction for gabbro can be seen in table 3.4.

Figure 3.3: Gabbro.

Table 3.3: Number of crushing stages for each particle size fraction collected at gabbro quarry.

Size fraction (mm)	Number of crushing stages
11.2/16 mm	Primary and secondary
8/11.2 mm	Primary and secondary
4/8 mm	Primary, secondary and tertiary

Table 3.4: Versions achieved for each particle size fraction.

Size fraction (mm)	Version
11.2/16 mm	C
8/11.2 mm	C
4/8 mm	C

3.1.2 Greywacke

Fieldwork was accomplished the 3rd of November. Only one day was needed because size fractions 8/11.2 mm and 11.2/16 mm were not produced at the quarry, therefore six large sacks of 8/16 mm were taken to NGU for further laboratory testing. Size fraction 4/8 mm was hand sieved at the quarry and the requirement for minimum amount of version A of cubic and flaky material was achieved relatively quickly due to the flakiness of the material. The number of crushing stages the sampled material has been subjected to can be seen in table 3.5. The version achieved, to run various artificial mixtures of the flakiness index, for each particle size fraction for greywacke can be seen in table 3.6.

Figure 3.4: Greywacke.

Table 3.5: Number of crushing stages for each particle size fraction collected at the greywacke quarry.

Size fraction (mm)	Number of crushing stages
8/16	Primary and secondary
4/8	Primary and secondary

Table 3.6: Versions achieved for each particle size fraction.

Size fraction (mm)	Version
11.2/16 mm	C
8/11.2 mm	B
4/8 mm	A

3.1.3 Rhomb porphyry

Fieldwork was accomplished between the 22nd and 23rd of October. The number of crushing stages the sampled material has been subjected to can be seen in table 3.7. The version achieved, to run various artificial mixtures of the flakiness index, for each particle size fraction for rhomb porphyry can be seen in table 3.8.

Figure 3.5: Rhomb porphyry.

Table 3.7: Number of crushing stages for each particle size fraction collected at the rhomb porphyry quarry.

Size fraction (mm)	Number of crushing stages
11.2/16	Primary, secondary and tertiary
8/11.2	Primary, secondary and tertiary
4/8	Primary, secondary and tertiary

Table 3.8: Versions achieved for each particle size fraction.

Size fraction (mm)	Version
11.2/16 mm	C
8/11.2 mm	C
4/8 mm	C

3.1.4 Monzonite 1

Fieldwork was accomplished between the 24th and 25th of October. The number of crushing stages the sampled material has been subjected to can be seen in table 3.9. Two months later it was discovered that not enough material had been collected to run artificial mixing tests. Therefore, additional 30 kg was sent to NGU. The version achieved, to run various artificial mixtures of the flakiness index, for each particle size fraction for monzonite 1 can be seen in table 3.10.

Figure 3.6: Monzonite 1.

Table 3.9: Number of crushing stages for each particle size fraction collected at monzonite 1 quarry.

Size fraction (mm)	Number of crushing stages
11.2/16	Primary and secondary
8/11.2	Primary and secondary
4/8	Primary and secondary

Table 3.10: Versions achieved for each particle size fraction.

Size fraction (mm)	Version
11.2/16 mm	C
8/11.2 mm	C
4/8 mm	C

3.1.5 Monzonite 2

Fieldwork was accomplished between the 27nd and 28th of October. Screening out flaky material proved to be too time-consuming, therefore 6 sacks of 4/16 mm aggregate material were taken for further laboratory tests. The number of crushing stages the sampled material has been subjected to can be seen in table 3.11. The version achieved, to run various artificial mixtures of the flakiness index, for each particle size fraction for monzonite 2 can be seen in table 3.12.

Figure 3.7: Monzonite 2.

Table 3.11: Number of crushing stages for each particle size fraction collected at monzonite 2 quarry.

Size fraction (mm)	Number of crushing stages
4/16	Primary

Table 3.12: Versions achieved for each particle size fraction.

Size fraction (mm)	Version
11.2/16 mm	C
8/11.2 mm	C
4/8 mm	C

3.1.6 Mylonite

Fieldwork was accomplished between the 30th and 31st of October. The number of crushing stages the sampled material has gone through can be seen in table 3.13. The version achieved, to run various artificial mixtures of the flakiness index, for each particle size fraction for mylonite can be seen in table 3.14.

Figure 3.8: Mylonite.

Table 3.13: Number of crushing stages for each particle size fraction collected at mylonite quarry.

Size fraction (mm)	Number of crushing stages
11.2/16	Primary, secondary, tertiary and quaternary (VSI)
8/11.2	Primary, secondary, tertiary and quaternary (VSI)
4/8	Primary, secondary, tertiary and quaternary (VSI)

Table 3.14: Versions achieved for each particle size fraction.

Size fraction (mm)	Version
11.2/16 mm	C
8/11.2 mm	C
4/8 mm	B

Table 3.15: Overview of versions achieved to run artificial mixtures and number of crushing stages for each particle size.

Rock type		11.2/16 mm	8/11.2 mm	4/8 mm
Gabbro	Crushing stages	2	2	3
	Version	C	C	C
R. porphyry	Crushing stages	3	3	3
	Version	C	C	C
Monzonite 1	Crushing stages	2	2	2
	Version	C	C	C
Monzonite 2	Crushing stages	1		
	Version	C	C	C
Mylonite	Crushing stages	4	4	4
	Version	C	C	C
Greywacke	Crushing stages	2		2
	Version	C	B	A

Chapter 4

Materials and Methods

Chapter 2 describes the main test methods used in this study: the Los Angeles (LA), micro-Deval (MD) and flakiness index (FI).

4.1 Standard Procedure Tests

For each rock type a standard (normal) procedure Los Angeles and micro-Deval tests was performed on size fractions 10/14 mm, 11.2/16 mm, 8/11.2 mm and 4/8 mm. The flakiness index (FI) was also measured prior to each test. In the results chapter the standard procedure tests are given a triangle symbol in the graphs to differentiate them from the artificial mixing tests. See Appendix C for detailed standard procedure test results.

4.2 Artificial Mixing

In order to assess the influence of particle shape, the proportion of flaky and cubic particles was artificially varied from 0 to 100 percent in a series of tests for each rock type. Table 4.1 shows artificial mix design for each particle size fraction, for both the Los Angeles and micro-Deval test methods. Not enough material was collected to run all artificial mix versions of the flakiness index. Therefore, a decision was made to focus on 25 and 75 percent flakiness index mix design rather than 0 and 100 percent flakiness index. The decision was based on that 0 and 100 percent flakiness indexes are very uncommon and extreme flakiness index values. However, at few quarries enough material was collected to run additional flakiness index mix designs. Table 4.2 shows the number of artificially mixed Los Angeles and micro-Deval tests performed on each particle size fraction. All in all 45 Los Angeles and 45 micro-Deval tests were performed.

Table 4.1: Artificial mixing procedure to achieve various flakiness indexes, for both the Los Angeles and micro-Deval test methods.

Size fraction		Bar sieve	In-situ	Flakiness index (FI)							
(mm)	(mm)	Q (mm)		0	25		50		75		100
				> Q	> Q + < Q		> Q + < Q		> Q + < Q		< Q
11.2/16	16/14	> 8	35%	35,0%	26,3%		17,5%		8,7%		
		< 8				8,7%		17,5%		26,3%	35,0%
	14/11.2	> 7	65%	65,0%	48,7%		32,5%		16,3%		
		< 7				16,3%		32,5%		48,7%	65,0%
8/11.2	10/11.2	> 5.6	35%	35,0%	26,3%		17,5%		8,7%		
		< 5.6				8,7%		17,5%		26,3%	35,0%
	8/10	> 5	65%	65,0%	48,7%		32,5%		16,3%		
		< 5				16,3%		32,5%		48,7%	65,0%
4/8	6.3/8	> 4	35%	35,0%	26,3%		17,5%		8,7%		
		< 4				8,7%		17,5%		26,3%	35,0%
	4/6.3	> 3.15	65%	65,0%	48,7%		32,5%		16,3%		
		< 3.15				16,3%		32,5%		48,7%	65,0%

Table 4.2: Number of artificial tests performed on each particle size fraction.

Rock type	Particle size fraction 11.2/16 mm									
	Los Angeles (LA)					Micro-Deval (MD)				
	0 FI	25 FI	50 FI	75 FI	100 FI	0 FI	25 FI	50 FI	75 FI	100 FI
Gabbro	1	1		1		1	1		1	
R. porphyry		1		1			1		1	
Monzonite 1		1		1			1		1	
Monzonite 2		1		1			1		1	
Mylonite		1		1			1		1	
Greywacke		1		1			1		1	
Rock type	**Particle size fraction 8/11.2 mm**									
	Los Angeles (LA)					Micro-Deval (MD)				
	0 FI	25 FI	50 FI	75 FI	100 FI	0 FI	25 FI	50 FI	75 FI	100 FI
Gabbro	1	1		1		1	1		1	
R. porphyry		1		1			1		1	
Monzonite 1		1		1			1		1	
Monzonite 2		1		1			1		1	
Mylonite	1	1		1		1	1		1	
Greywacke		1	1	1			1	1	1	
Rock type	**Particle size fraction 4/8 mm**									
	Los Angeles (LA)					Micro-Deval (MD)				
	0 FI	25 FI	50 FI	75 FI	100 FI	0 FI	25 FI	50 FI	75 FI	100 FI
Gabbro	1	1		1		1	1		1	
R. porphyry		1		1			1		1	
Monzonite 1		1		1			1		1	
Monzonite 2		1		1			1		1	
Mylonite		1	1	1			1	1	1	
Greywacke	1	1	1	1	1	1	1	1	1	1

Chapter 5

Results and Discussion

5.1 Thin Section Analysis

Twelve thin sections were made at Norwegian university of science and technology (NTNU) department of geology and mineral resources engineering laboratories. Petrographic thin section analysis was performed by Eirik Pettersen at NGU. The hand-samples gathered for mylonite proved to be non-representative of the aggregate production, mylonites results are therefore based on a previous thin section analysis by Marker (2005). Relative hardness is calculated using the Mohs scale of mineral hardness. Thin-section photographs can be seen in appendix A.

Table 5.1: Results from thin section analysis performed by Eirik Pettersen, NGU. The table shows mineralogical composition for each rock type. Mylonite results are based on previous field investigation by Marker (2005).

Rock type	Quartz	Orthoclase (K-feldspar)	Plagioclase	Clinopyroxene	Orthopyroxene	Actinolite	Hornblende	Chlorite	Epidote	Biotite	Muscovite	Sericite	Olivin	Calcite	Apatite	Titanite	Rutile	Tremolite	Kyanite	Other	Relative hardness
Gabbro			30	10	15	8	19	2	10		5	1									5,46
Rhomb porphyry	1	70	10					1	1			5		1	1			2		8	5,77
Monzonite 1	1	5	73	1	2	2				10		2			1		1	2			5,57
Monzonite 2		10	74	4						8		1		1	1		1				5,64
Greywacke	6							1	2			45		45						1	3,1
Mylonite	30		60	3					6		1										6,16
Mylonite	35		55	5					5												6,18
Mylonite	35		55	5					5												6,18
Mylonite	30		60	5					4											1	6,12

Table 5.2: Results from thin section analysis performed by Eirik Pettersen, NGU. Mylonite results are based on previous field investigation by Marker (2005).

								Grain Size				Grain boundary	
Test nr.	Type	Rock type	Color	Structure	Foliation	Texture	Matrix (mm)	Porfyroblast (mm)	Recrystallized (%)	Grain variation	Old grains	Recrystallized	Plagioclase alteration
2	Igneous (Plutonic)	Gabbro	Multiple	Massive	None	Granular	Fine-grained (< 1 mm)	Fine- to med.-grained	40	Equigranular	Dentate	Straight	Strong
3	Igneous (Volcanic)	R. porphyry	Red	Massive	None	Porphyritic	Fine-grained (< 1 mm)	Med.-grained (1-5 mm)	10	Inequigranular	Lobate	Straight	Strong
5	Igneous (Plutonic)	Monzonite 1	Med. gray	Massive	Weak	Granular	Fine-grained (< 1 mm)	Med.- to coarse-grained	3	Equigranular	Embayed	Straight	None
7	Igneous (Plutonic)	Monzonite 2	Med. gray	Massive	None	Granular	Fine-grained (< 1 mm)	Coarse-grained (> 5 mm)	2	Equigranular	Lobate	Straight	None
9	Sedimentary (Arenaceous)	Greywacke	Green	Bandet	Good	Mylonitic	Fine-grained (< 1 mm)	Fine-grained (< 1 mm)	85	Equigranular	-	-	-
MM 026334	Metamorphic	Mylonite	Light gray	Foliated	Good	Porphyritic	0.1-0.3	0.9-2.0	20	-	Lobate	Polygonal	Advanced
MM 026335	Metamorphic	Mylonite	Ligth gray	Foliated	Good	Porphyritic	0.1-0.2	0.3-1.1	30	-	Lobate	Polygonal	Strong
MM 026336	Metamorphic	Mylonite	Light gray	Foliated	Moderate	Porphyritic	0.1-2.0	-	25	-	Lobate	Polygonal	Strong
MM 026337	Metamorphic	Mylonite	gray	Foliated	Moderate	Porphyritic	0.1-1.8	-	10	-	Lobate	Polygonal	Strong

5.2 LA Versus MD

Figure 5.1 shows all Los Angeles values (LA) versus micro-Deval values (MD). Mylonite, r. porphyry and gabbro have overall low LA and MD values. Greywacke has the highest MD values but similar LA values compared to gabbro. Monzonite 1 and 2 have the highest LA values, monzonite 2 has although overall higher LA and MD values. No large variations in the LA and MD values are observed when influenced by varying particle size and shape, the dots pack close to one another for each rock type. Figure 5.2 shows all 69 LAx values versus 69 MDx values. The results show large variations in the LAx and MDx values when influenced by varying particle size and shape, the dots have a large spread for each rock type. Detailed results are available in Appendix B.

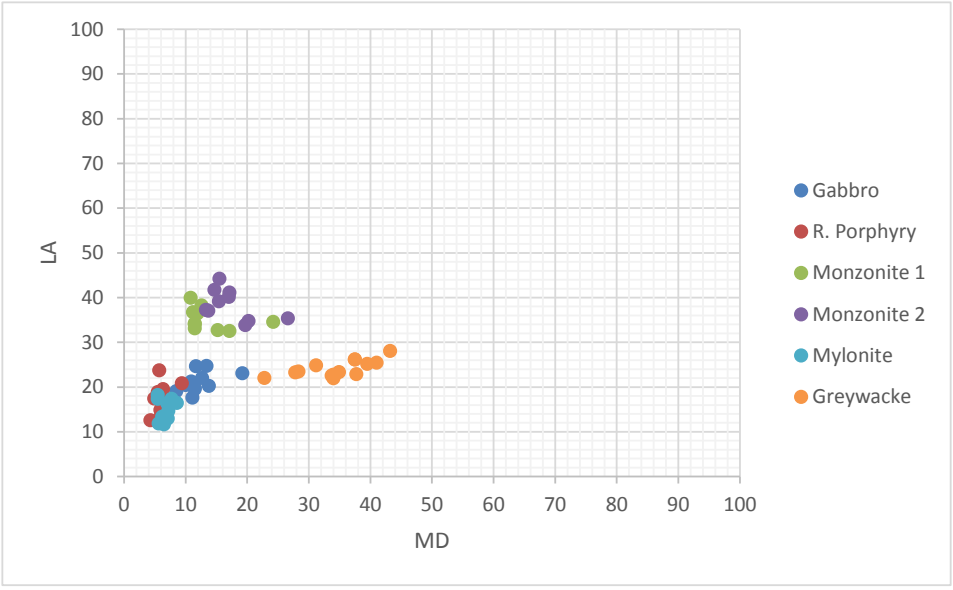

Figure 5.1: 69 LA versus 69 MD values influenced by varying FI and particle size.

5.2.1 Discussion of LA versus MD and Thin Section Analysis

Figure 5.1 gives a good overview of each rock type's mechanical properties. The results show how different rock types group together. When the results are compared to the thin section analysis, correlation can be seen between mineral grain size and LA value. Mylonite, r. porphyry, gabbro and greywacke have fine- to medium- and medium sized mineral grains and have the lowest LA values. The two monzonites have larger mineral grain sizes and have much higher LA values compared to the other rock types. Monzonite 2 has larger mineral grain sizes compared to monzonite 1 and has overall higher LA and MD values. The MD value seems to be less affected by mineral grain size and more affected by rock hardness. Correlations is observed between relative rock hardness (Mohs hardness test) and MD value. Resistance to abrasion is seen to decrease with increased content of

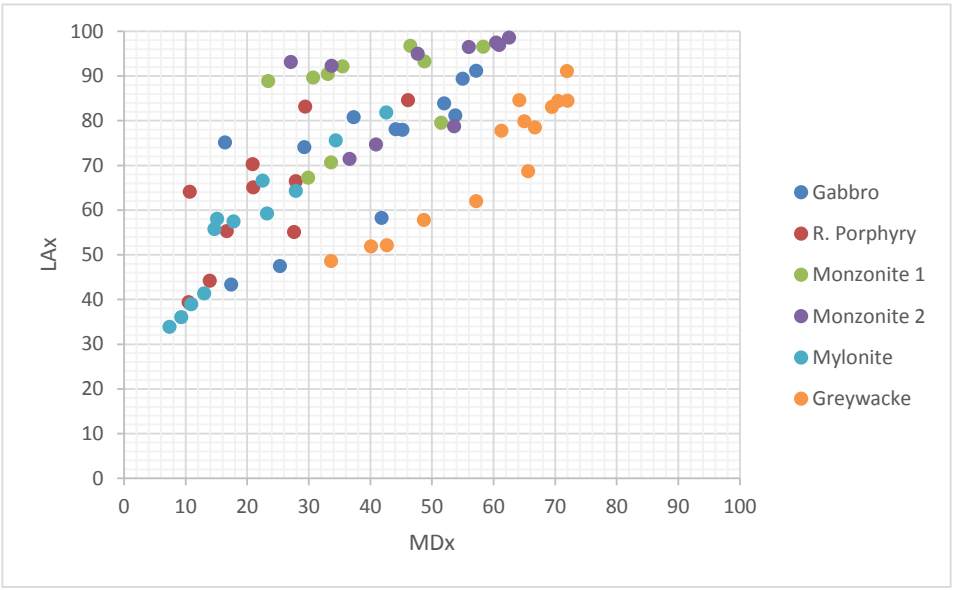

Figure 5.2: 69 LAx versus 69 MDx values influenced by varying FI and particle size.

soft minerals. Greywacke shows this clearly, it has the lowest rock hardness due to high amounts of calcite and high MD values. Figure 5.2 shows that the LAx and MDx values spread out much more when influenced by varying particle size and shape compared to the standard test method LA and MD that pack closely together. The figure therefore clearly shows that the LAx and MDx values are more sensitive to changes in particle size and shape compared to the standard LA and MD values.

5.3 Flakiness Index (FI) Versus Particle Size Fraction

Figure 5.3 shows FI plotted against each particle size fraction. Large variations are observed between rock types and FI. Rhomb porphyry, monzonite 1, monzonite 2 and mylonite all show a general increase in FI as the particle size decreases. Gabbro and greywacke show less clear trend between FI and particle size fraction. Regardless of rock type the highest FI is always observed in the 4/8 mm particle size fraction.

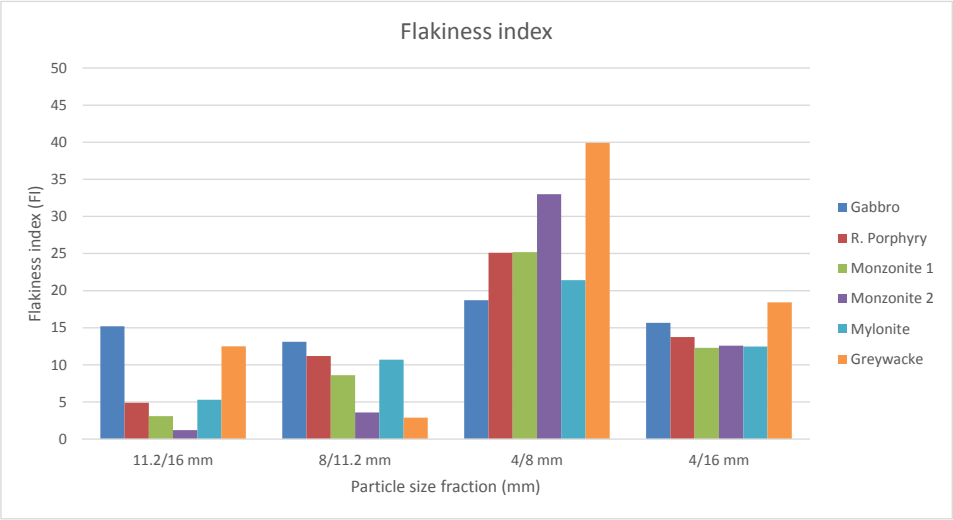

Figure 5.3: Flakiness index versus particle size fraction.

5.3.1 Discussion of FI Versus Particle Size Fraction

5.3 shows that fine- to medium-grained rock types are observed to have generally higher FI than coarse-grained rock types for size fractions 11.2/16 mm and 8/11.2 mm. this trend is not seen in size fraction 4/8 mm, production factors probably play a larger role here then the geology, the rock types have not gone through identical crushers and crushing stages.

When FI for a wide particle range (4/16 mm) is calculated, see figure 5.3, large variations observed between rock types and FI disappear. The FI for a wide particle range is calculated as an average of FI for each particle size fraction. It is therefore possible that low and high FI values for each size fraction are averaging each-other out. The results are similar to Erichsen et al. (2010) which suggests revision of today's requirements', a FI requirement for each particle size fraction, not average FI of all size fractions in a size range, for example 4/16 mm.

5.4 LA and LAx Versus Flakiness Index (FI)

All figures show normal procedure LA values marked as triangles in the graphs. Artificially mixed LA values are marked as dots on the graphs. trend lines are marked as dotted lines on the graphs. Detailed results are available in Appendix C. Tables B1, B2, B3, B4, B5 and B6 show the relationship equations and the coefficient of correlation, see Appendix B. Sensitivity to changes in LA and LAx in regard to changes in FI are determined by the slope of the trend line. Larger the slope angle, the more sensitive the LA or LAx values are to changes in the FI.

Figures 5.4 and 5.5 show LA and LA11 versus FI for each rock type, for **size fraction 11.2/16 mm**: all rock types show increase in both the LA and LA11 with increasing FI. The order from the overall highest to the lowest LA value is as follows: monzonite 2, monzonite 1, greywacke, gabbro, r. porphyry and mylonite. The order from most sensitive rock type to changes in the FI to the least according to the LA value is as follows: r. porphyry, gabbro, monzonite 1, monzonite 2, greywacke and mylonite. When these results are compared to the LA11 value the order stays the same for the overall highest to the lowest LA11 value. The order is, however, different from most sensitive rock type to changes in FI to the least, the order for the LA11 value is as follows: r. porphyry, mylonite, gabbro, greywacke, monzonite 1 and monzonite 2.

Figures 5.6 and 5.7 show LA and LA8 versus FI for each rock type, for **size fraction 8/11.2 mm**: all rock types show increase in both the LA and LA8 with increasing FI. The order from the overall highest to the lowest LA value is as follows: monzonite 2, monzonite 1, greywacke, gabbro, r. porphyry and mylonite. The order from most sensitive rock type to changes in the FI to the least according to the LA value is as follows: r. porphyry, gabbro, mylonite, monzonite 1, monzonite 2 and greywacke. When these results are compared to the LA8 value the order stays the same, except gabbro and greywacke switch places, gabbro has a higher percentage of material passing the uppermost sieve compared to greywacke. The order is also different for most sensitive rock type to changes in FI to the least, the order for the LA8 value is as follows: r. porphyry, mylonite, gabbro, greywacke, monzonite 1 and monzonite 2.

Figures 5.8 and 5.9 show LA and LA4 versus FI for each rock type, for **size fraction 4/8 mm**: all rock types show increase in both the LA and LA4 with increasing FI. The order from the overall highest to the lowest LA value is as follows: monzonite 2, monzonite 1, greywacke, gabbro, R. porphyry and mylonite. The order from most sensitive rock type to changes in the FI to the least according to the LA value is as follows: greywacke, gabbro, r. porphyry, mylonite, monzonite 1 and monzonite 2. When these results are compared to the LA4 value the order stays the same for the overall highest to the lowest LA4 value. The order is different from most sensitive rock type to changes in the FI to the least, the order for the LA4 value is as follows: rhomb porphyry, gabbro, monzonite 1, greywacke, monzonite 2 and mylonite.

Gabbro: Figure 5.10 shows the influence of FI and particle size on both LA and LAx, for gabbro. Gabbro has similar LA values for all size fractions. LA4 is observed to have less breakdown compared to LA8 and LA11. LA4 is also observed to be most sensitive to changes in the FI.

Rhomb porphyry: Figure 5.11 shows the influence of FI and particle size on both LA and LAx, for r. porphyry. R. porphyry has generally low LA values for all size fractions. LA4 is observed to have less breakdown compared to LA8 and LA11. LA11 is observed to be most sensitive to changes in FI.

Monzonite 1: Figure 5.12 shows the influence of FI and particle size on both the LA and LAx, for monzonite 1. Monzonite 1 has overall high LA values for all size fractions. LA4 is observed to have less breakdown compared to LA8 and LA11. LA4 is also observed to be most sensitive to changes in the FI.

Monzonite 2: Figure 5.13 shows the influence of FI and particle size on both LA and LAx, for monzonite 2. Monzonite 2 behaves in the same way as monzonite 1 but has generally higher LA and LAx values.

Mylonite: Figure 5.14 shows the influence of FI and particle size on both LA and LAx, for mylonite. Mylonite has generally low LA and LAx values and a trend of increasing sensitivity with increasing aggregate particle size. LA4 is observed to have less breakdown compared to LA8 and LA11.

Greywacke: Figure 5.15 shows the influence of FI and particle size on both LA and LAx, for greywacke. Greywacke shows similar LA values for all size fractions. LA4 is observed to have less breakdown compared to LA8 and LA11. LA4 is also observed to be most sensitive to changes in the FI.

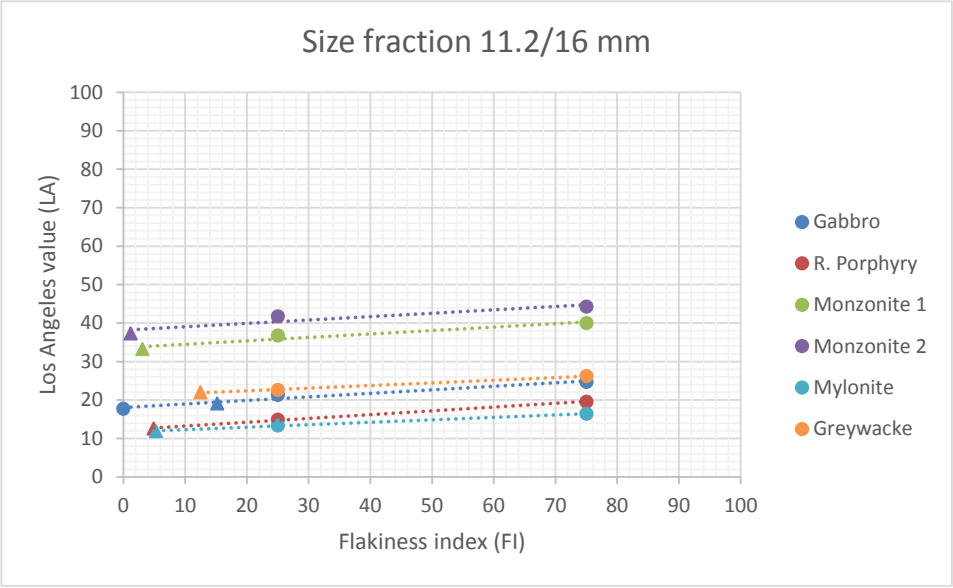

Figure 5.4: Los Angeles value (LA) versus flakiness index (FI).

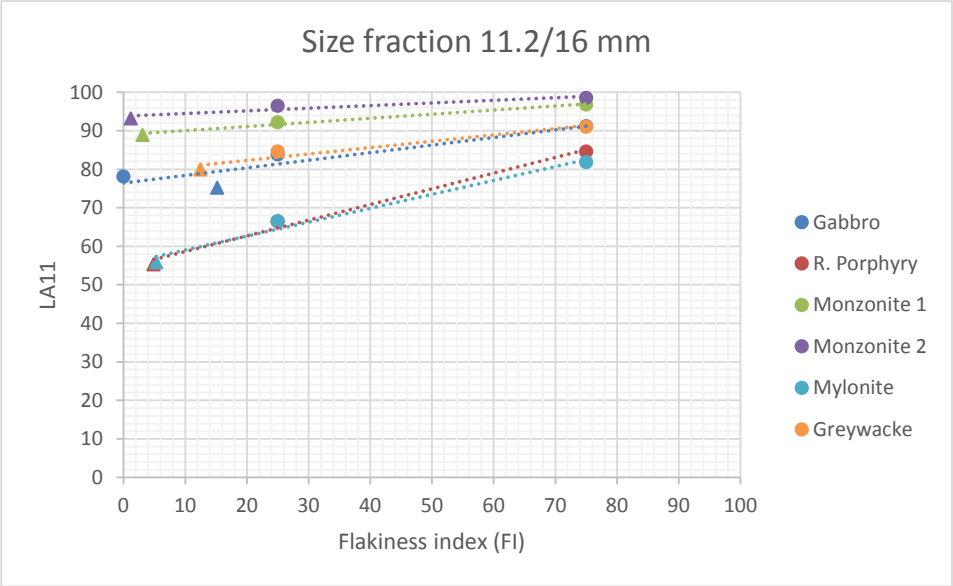

Figure 5.5: LA11 versus flakiness index (FI).

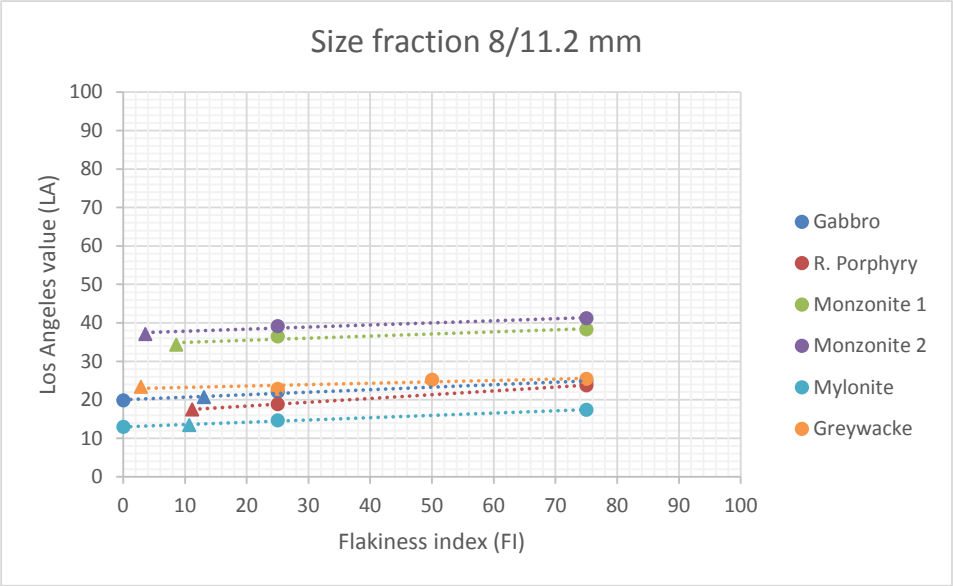

Figure 5.6: Los Angeles value (LA) versus flakiness index (FI).

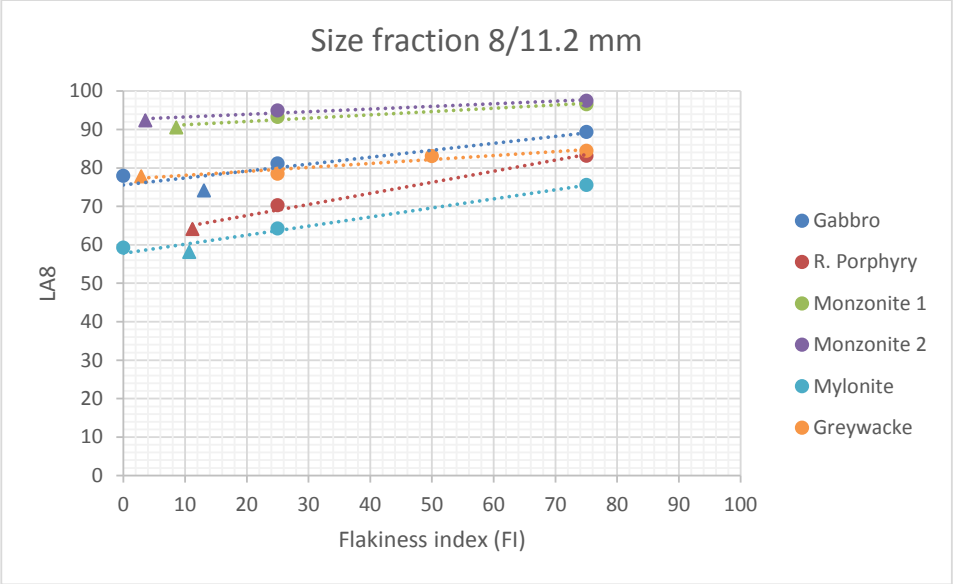

Figure 5.7: LA8 versus flakiness index (FI).

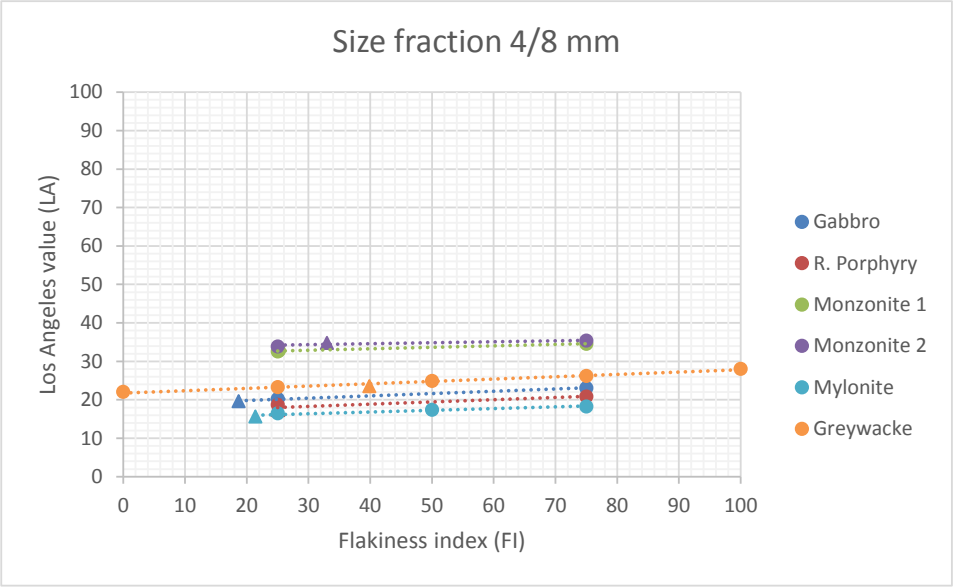

Figure 5.8: Los Angeles value (LA) versus flakiness index (FI).

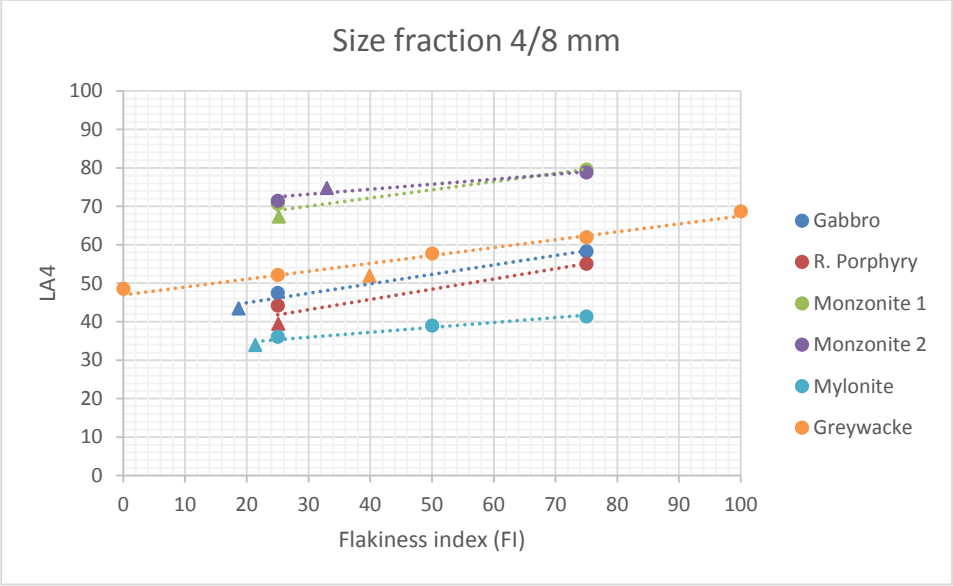

Figure 5.9: LA4 versus flakiness index (FI).

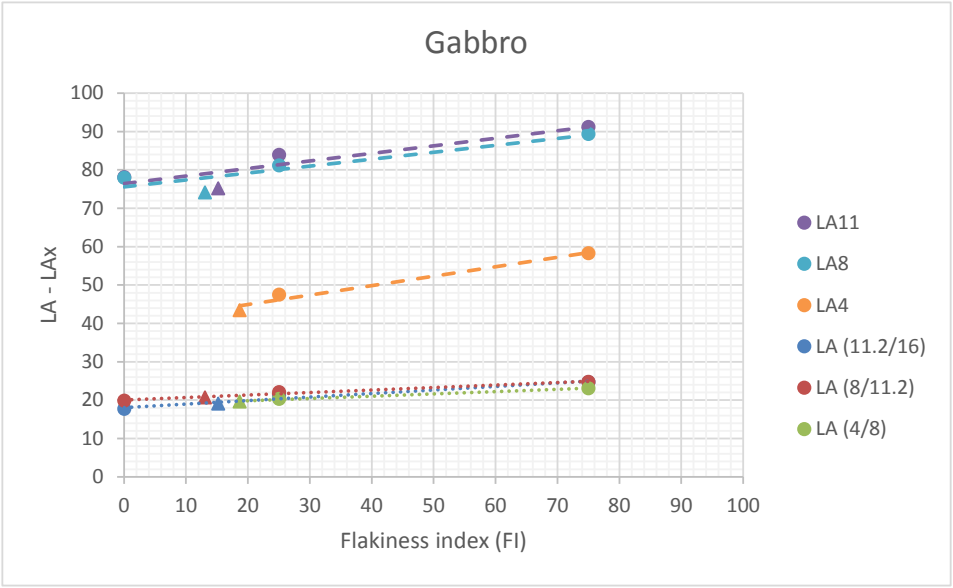

Figure 5.10: LA and LAx versus flakiness index (FI).

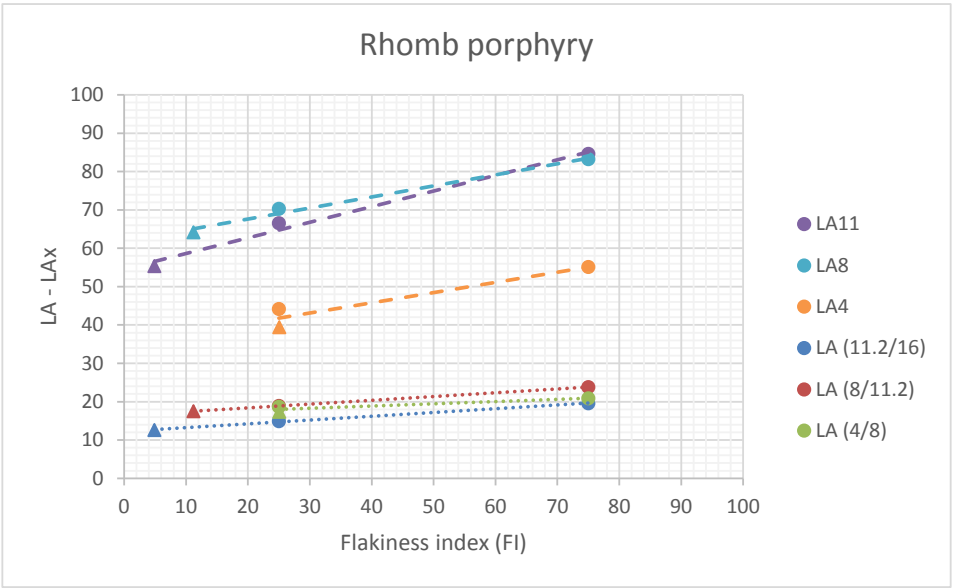

Figure 5.11: LA and LAx versus flakiness index (FI).

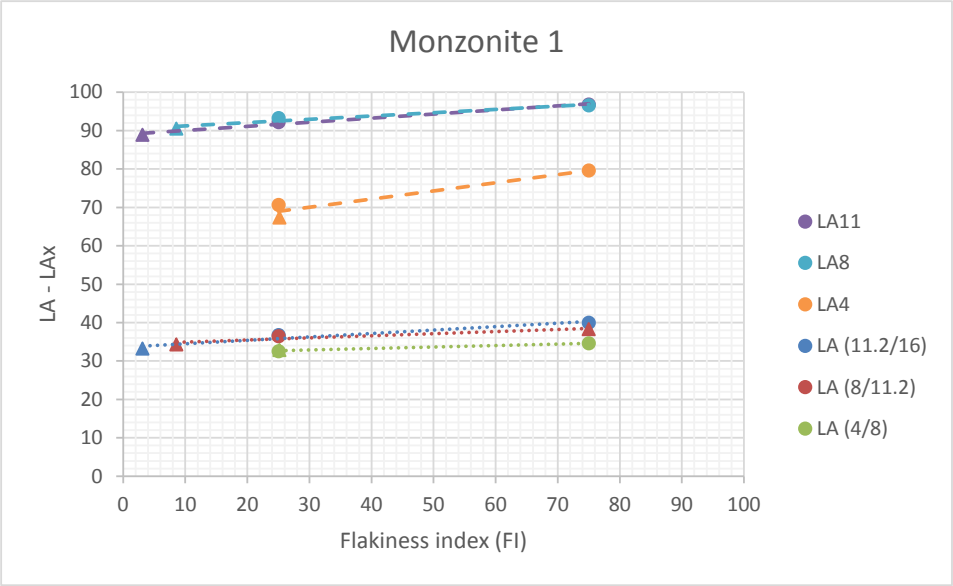

Figure 5.12: LA and LAx versus flakiness index (FI).

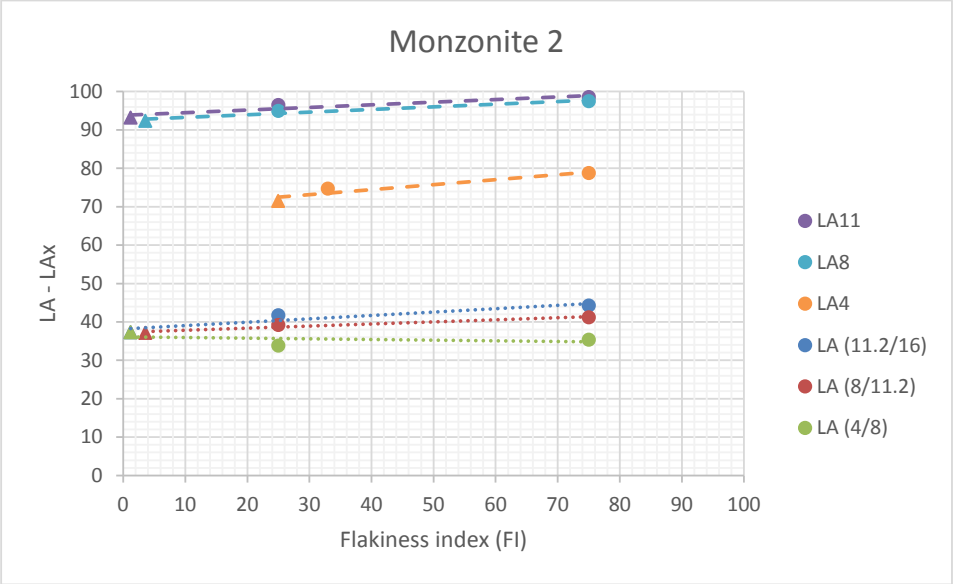

Figure 5.13: LA and LAx versus flakiness index (FI).

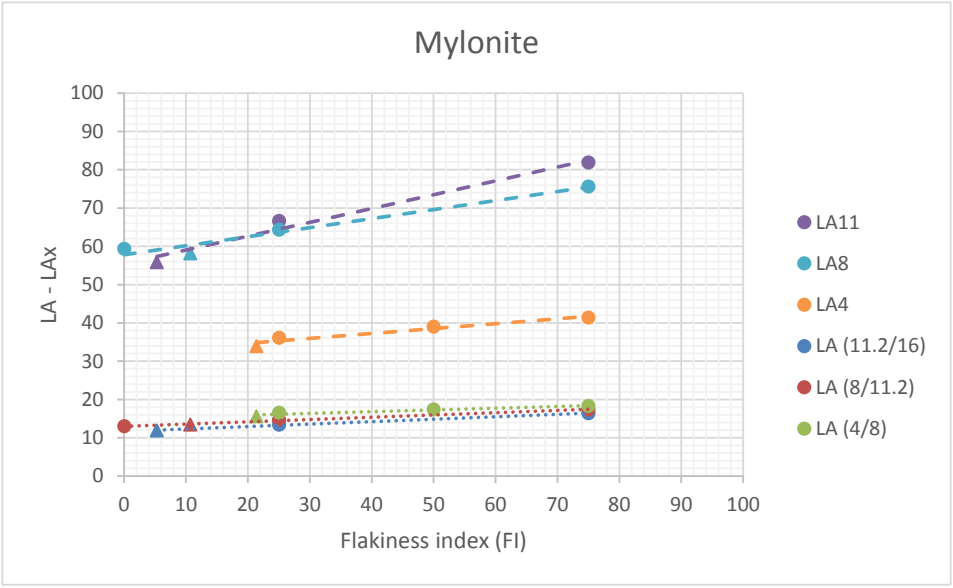

Figure 5.14: LA and LAx versus flakiness index (FI).

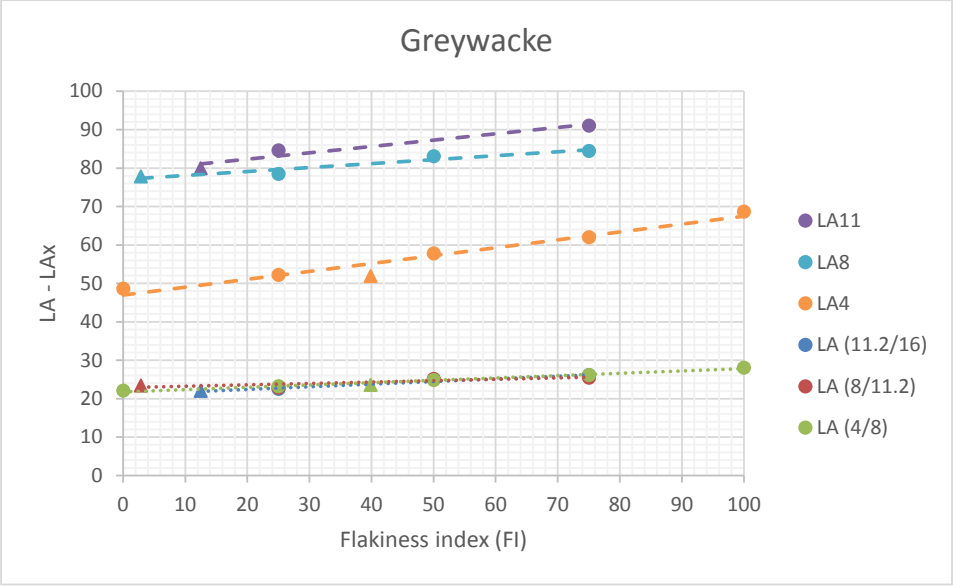

Figure 5.15: LA and LAx versus flakiness index (FI).

5.4.1 Discussion of LA and LAx Versus FI

Overall the Los Angeles value (LA) and LAx increase with increasing aggregate flakiness index (FI) - regardless of rock type - for all aggregate size fractions. The increase in the LA value is, however, small. The LAx value is seen to have much steeper lines, compared to the standard LA value. When slope angles, taken from the relationship equations between LA, LAx and flakiness index are compared, see table 5.3. LA11, LA8 and LA4 are seen to have much larger slope angles compared to the standard LA value. A higher slope angle number indicates that the value is more sensitive to changes in FI. The LAx have overall higher numbers compared to standard LA values indicating that the LAx value is much more sensitive to changes in FI than the standard LA value. The Los Angeles standard test method is therefore not sensitive to changes in particle shape.

It can also be seen in table 5.3 that the rock types with the lowest LA and LAx values are generally the ones that are most sensitive to changes in FI. The table is designed to list the rock types with the lowest LA values first. Mylonite, which has generally the lowest LA and LAx values, shows some inconsistency in this regard and is for example the least sensitive rock type for the LA4 value. Rock types with large mineral grain sizes (monzonite 1 and monzonite 2) are also seen to have the highest LA and LAx values but are least sensitive to changes in FI.

Table 5.3: Slope from the relationship equations between LA, LAx values and FI. The higher the number, the more sensitive the value is to changes in FI.

Rock types	LA (11.2/16)	LA11	LA (8/11.2)	LA8	LA (4/8)	LA4
Mylonite	0,1	0,4	0,1	0,2	0,0	0,1
R. porphyry	0,1	0,4	0,1	0,3	0,1	0,3
Gabbro	0,1	0,2	0,1	0,2	0,1	0,2
Greywacke	0,1	0,2	0,0	0,1	0,1	0,2
Monzonite 1	0,1	0,1	0,1	0,1	0,0	0,2
Monzonite 2	0,1	0,1	0,1	0,1	0,0	0,1

It must be said that results with much higher LA values were expected due to extreme values in the flakiness index. The LA value is, however, generally not sensitive to variations in FI. The reason for this could be related to how the LA value is calculated, the LA value takes no account of the coarser products produced by breakdown of material above 1.6 mm. The LA value is only influenced by material passing 1.6 mm sieve size, also called production of fines ($<$1.6 mm).

Sieve analysis (Appendix D) reveals how the test fractions breakdown into smaller particle size fractions with increasing FI. Increase in aggregate FI noticeably increases breakdown and fragmentation into smaller particle size fractions. The production of fines (<1.6 mm) does not dramatically increase with increasing FI. Figure 5.16 shows it very clearly how the mylonite test fraction 11/16 mm is breaking down into smaller particle size fractions. Production of fines (<1.6 mm) is barely increasing, resulting in small variations between LA values with increasing FI. Figure 5.16 also shows the reason behind the LAx value being more sensitive to changes in FI, compared to the LA value. Much more material is seen passing the 11.2 mm sieve size with increasing FI, resulting in large variations in the LA11 value.

The LAx value is therefore more sensitive indicator of aggregate breakdown when evaluating the effects of particle shape on mechanical properties of aggregates, compared to the standard LA value. This discovery is similar to the findings of Ramsay et al. (1974, 1977), Spence et al. (1974) and Dhir et al. (1971) who all demonstrated that the residual values AIVR and ACVR are more sensitive to changes in the particle shape compared to normal AIV and ACV.

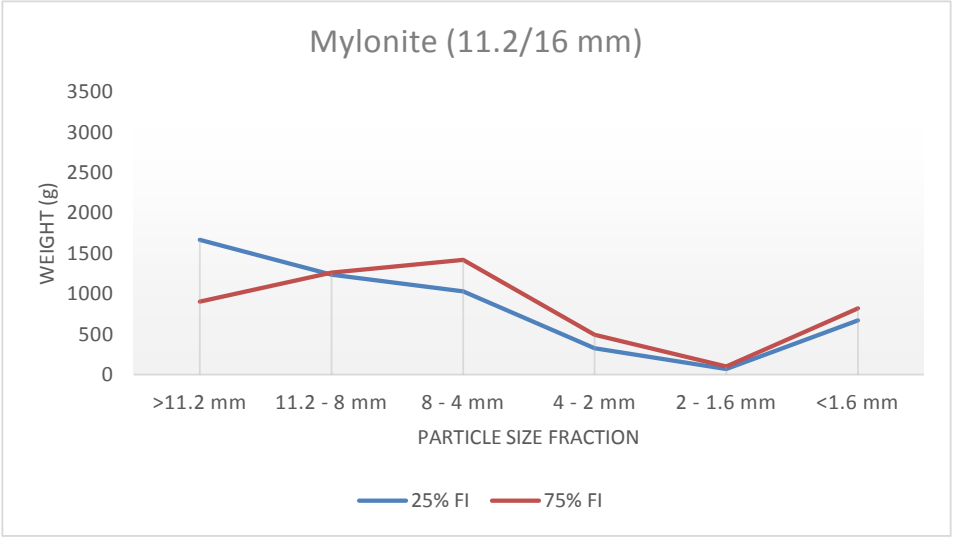

Figure 5.16: Mylonite size fraction 11.2/16 mm, sieve analysis of the Los Angeles test.

Different particle size fractions for each rock type show similar Los Angeles values (LA). Rock types that show general increase in the LA value with decrease in particle size fractions are: r. porphyry and mylonite. Rock types that show general decrease in the LA value with decrease in particle size fractions are: monzonite 1 and monzonite 2. Rock types that show little to no change in the LA value between particle size fractions are gabbro and greywacke. According to the LA value, size fraction 11.2/16 mm is the most sensitive to changes in FI, regardless of rock type.

Variations in LA value between size fractions is probably due to the LA test method not using the same number of steel balls inside the drum during testing for each particle size fraction. The size and weight of each steel ball is the same, smaller size particles are therefore loaded with larger force per area, when impacted by the steel balls, compared to larger sized particles. This could be the reason for variations in the LA value between different particle size fractions.

The LAx results show that the LAx value decreases as particle size fraction decreases, regardless of rock type. According to the LAx value, size fractions 4/8 mm (gabbro, monzonite 1, monzonite 2 and greywacke) and 11.2 mm (mylonite and r. porphyry) are the most sensitive to changes in FI.

The 4/8 mm (LA4) particle size fraction shows much less breakdown of material compared to size fractions 8/11.2 mm (LA8) and 11.2/16 mm (LA11), which show similar amount of material passing the uppermost sieve. This is surprising because smaller sized (4/8 mm) particles are impacted by steel balls of the same size and weight as the larger size particles (8/11.2 mm and 11.2/16 mm). Test fraction (4/8 mm) is although run with fewer steel balls. This does, however, not change the fact that the 4/8 mm particles are experiencing larger force per area compared to 8/11.2 mm and 11.2/16 mm particles. This higher breakdown of larger particles could be explained by the theory of statistical distribution of flaws. The larger the particle size, the more likely you have critical flaw occurring in the rock particle (Smith and Collis, 1993).

5.5 Norwegian Impact Value Versus Flakiness Index (FI)

Figures 5.17, 5.18 5.19 and 5.20 show the influence of varying flakiness index (FI), for each rock type, on both the S2, Sx, LA and LAx. LA values are marked as dots and S values are marked as rectangles. Trend line is marked as a dotted line on the graphs. The results are from NGU hard rock database (Tangstad and Vongraven, 2015), which uses the same sampled aggregate material as this study.

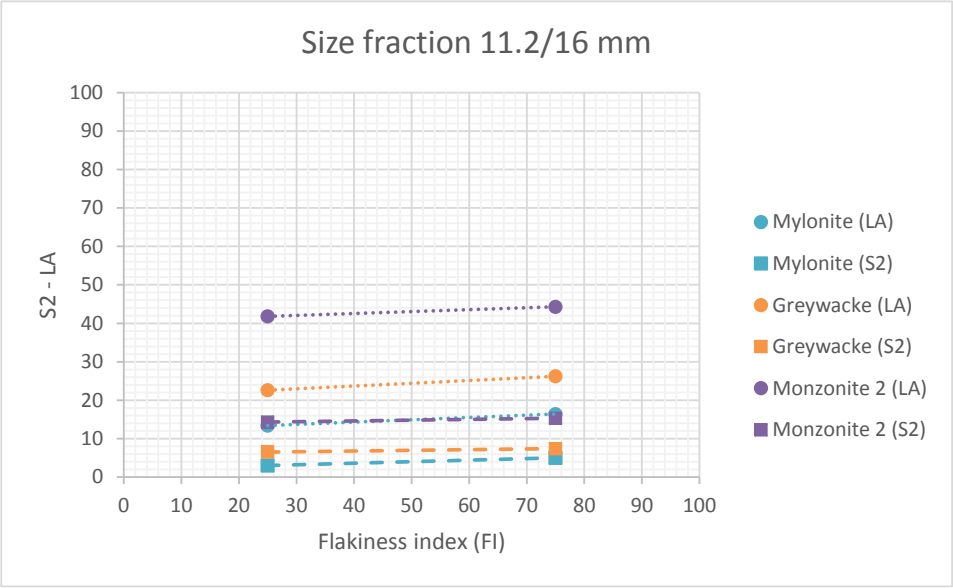

Figure 5.17: S2 and LA versus the flakiness index (FI).

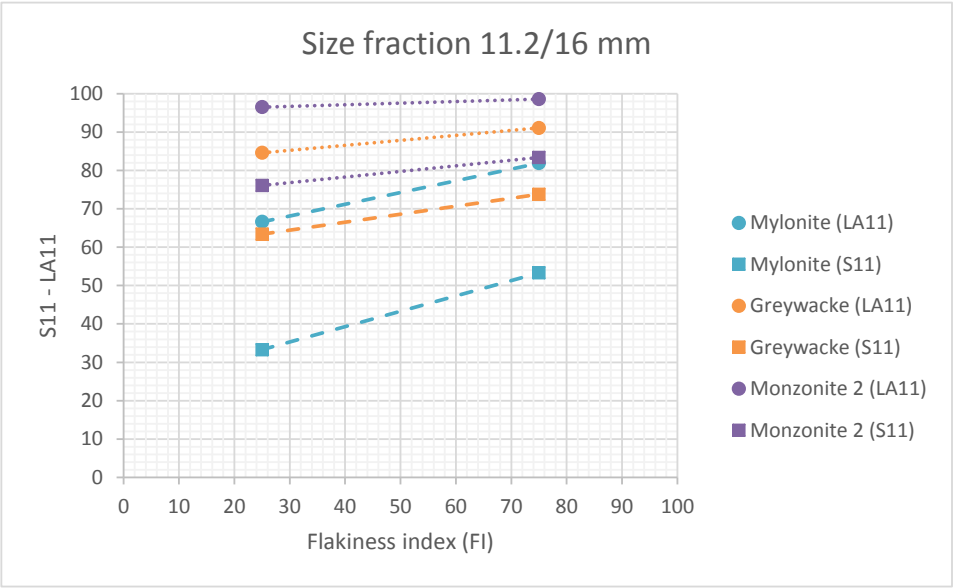

Figure 5.18: S11 and LA11 versus the flakiness index (FI).

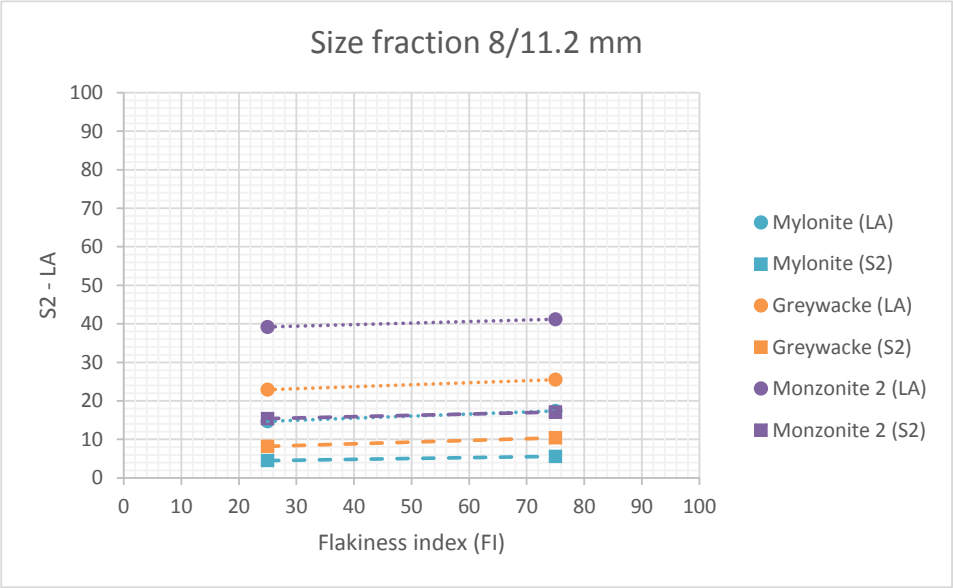

Figure 5.19: S2 and LA versus the flakiness index (FI).

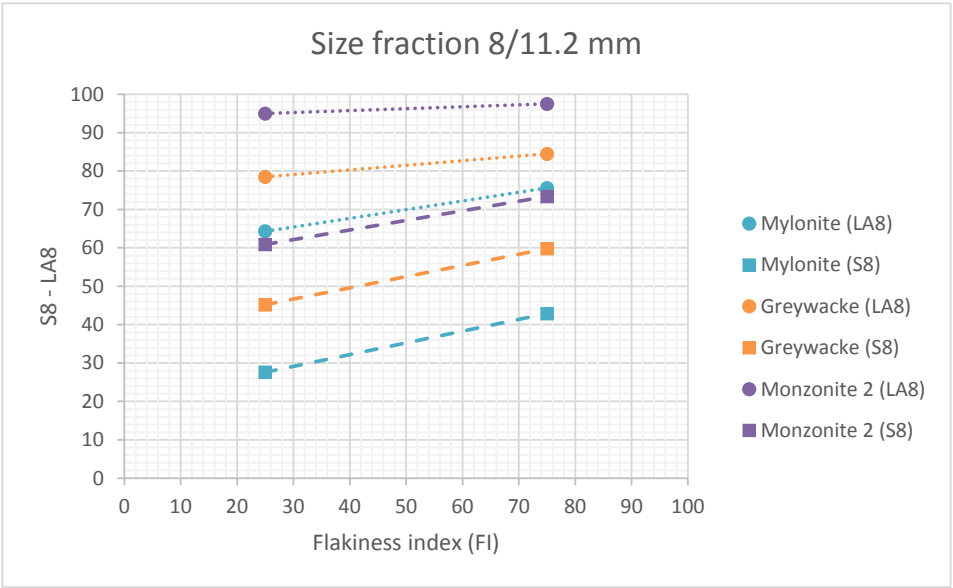

Figure 5.20: S8 and LA8 versus the flakiness index (FI).

5.5.1 Discussion of Norwegian Impact Value

Overall the Norwegian impact values S2, S8 and S11 increase with increasing aggregate flakiness index (FI) - regardless of rock type - for aggregate size fractions 8/11.2 mm and 11.2/16 mm. The increase in the S2 value is, however, small. When the S2 value (percent mass passing 2 mm sieve) are compared to the standard Los Angeles value (LA) (percent mass passing 1.6 mm sieve) both lines show low slope angles and are therefore not sensitive to changes in the FI. S11 and S8 values are, however, seen to be much more sensitive to changes in FI, compared to the S2 and LA values, see table 5.4. This fits well with Selmer-Olsen (1980) research which stated that the Los Angeles test method is not as sensitive to changes in particle shape, compared to the Norwegian impact test method (S11 and S8).

The S8 value shows more consistent slope angles between rock types compared to the LA8 value. The reason for this inconsistency in LA8, between rock types, could be the abrasion effect. The Norwegian impact test breaks down the rock by shattering it with pure impact, while the Los Angeles test breaks down the rock by shattering it with impact and wearing it down by abrasion. Other possibilities are that as the rock gets more coarse grained it is less influenced by aggregate flakiness in the Los Angeles test. The Los Angeles test and the impact test, however, categorize the material in the same way between good and poor mechanical properties of rock, they both give high and low values to the same rock types.

This comparison between two impact test methods, the Los Angeles test and Norwegian impact test, shows that measuring production of fines ($<$1.6 mm and $<$2 mm) is not a sensitive method to judge aggregate breakdown due to increase in the flakiness index (FI). Both test methods show that measuring percentage of mass passing a sieve size with same aperture size as the lower fraction of the size range (Sx and LAx) give better indication of aggregate breakdown due to increase in FI.

Table 5.4: Slope from the relationship equations between LA, LAx, S2, Sx and FI. The higher the number, the more sensitive the value is to changes in FI.

	Norwegian impact test					Los Angeles test			
Rock types	**S2 (11.2/16)**	**S11**	**S2 (8/11.2)**	**S8**		**LA (11.2/16)**	**LA11**	**LA (8/11.2)**	**LA8**
Mylonite	0,0	0,4	0,0	0,3		0,1	0,3	0,1	0,2
Greywacke	0,0	0,2	0,0	0,3		0,1	0,1	0,1	0,1
Monzonite 2	0,0	0,1	0,0	0,3		0,1	0,0	0,0	0,1

5.6 MD and MDx Versus Flakiness Index (FI)

All figures show normal procedure MD values marked as triangles in the graphs. Artificially mixed MD values are marked as dots on the graphs. Trend lines are marked as dotted lines on the graphs Detailed results are available in Appendix C. Tables B7, B8, B9, B10, B11 and B12 show the relationship equations and the coefficient of correlation, see Appendix B. Sensitivity to changes in MD and MDx in regard to changes in FI are determined by the slope of the trend line. Larger the slope angle, the more sensitive the MD or MDx values are to changes in the FI.

Figures 5.21 and 5.22 show MD and MD11 versus FI for each rock type, for **size fraction 11.2/16 mm**: all rock types, except for monzonite 1, show increase in MD with increasing FI, monzonite 1 shows a decrease with a very small negative slope. All rock types, however, show increase in MD11 with increasing FI. The order from the overall highest to the lowest MD value is as follows: greywacke, monzonite 2, monzonite 1, gabbro, r. porphyry and mylonite. The order from most sensitive rock type to changes in FI to the least, according to the MD value is as follows: greywacke, monzonite 2, r. porphyry, gabbro, mylonite and monzonite 2. When these results are compared to the MD11 the order changes slightly and is as follows: greywacke, monzonite 2, gabbro, monzonite 1, r. porphyry and mylonite. The most sensitive rock type to changes in the FI to the least, according to the MD11 value is as follows: monzonite 2, r. porphyry, mylonite, gabbro, monzonite 1 and greywacke.

Figures 5.23 and 5.24 show MD and MD8 versus FI for each rock type, for **size fraction 8/11.2 mm**: all rock types show increase in both MD and MD8 with increasing FI. The order from the overall highest to the lowest MD value is as follows: greywacke, monzonite 2, gabbro, monzonite 1, mylonite and r. porphyry. The order from most sensitive rock type to changes in FI to the least, according to the MD value is as follows: greywacke, monzonite 2, gabbro, monzonite 1, mylonite and r. porphyry. When these results are compared to MD8 the order changes and is as follows: greywacke, gabbro, monzonite 1, monzonite 2, mylonite and r. porphyry. The most sensitive rock type to changes in the FI to the least, according to the MD8 value is as follows: monzonite 2, monzonite 1, r. porphyry, gabbro, mylonite and greywacke.

Figures 5.25 and 5.26 show MD and MD4 versus FI for each rock type, for **size fraction 4/8 mm**: all rock types show increase in both the MD and MD4 with increasing FI. The order from the overall highest to the lowest MD value is as follows: greywacke, monzonite 2, monzonite 1, gabbro, mylonite and r. porphyry. The order from most sensitive rock type to changes in FI to the least, according to the MD value is as follows: greywacke, monzonite 1, monzonite 2, gabbro, r. porphyry and mylonite. When these results are compared to MD4 the order changes and is as follows: greywacke, monzonite 2, monzonite 1, gabbro, r. porphyry and mylonite. The most sensitive rock type to changes in the FI to the least, according to the MD4 value is as follows: monzonite 1, gabbro, monzonite 2, greywacke, r. porphyry and mylonite.

Gabbro: Figure 5.27 shows the influence of FI and particle size on both MD and MDx, for gabbro. Gabbro shows similar MD values for size fractions 11.2/16 mm and 8/11.2 mm. 4/8 mm has both higher MD values and is more sensitive to changes in the FI. MD4 is observed to have less breakdown compared to MD8 and MD11. MD4 is observed to be most sensitive to changes in the FI.

Rhomb porphyry: Figure 5.28 shows the influence of FI and particle size on both MD and MDx, for r. porphyry. R. porphyry shows similar MD values for all size fractions. MD4 is observed to have less breakdown compared to MD8 and MD11. MD11 is observed to be the most sensitive to changes in FI.

Monzonite 1: Figure 5.29 shows the influence of FI and particle size on both MD and MDx, for monzonite 1. Monzonite 1 shows similar MD values for size fractions 11.2/16 mm and 8/11.2 mm. 4/8 mm has both higher MD values and is more sensitive to changes in FI. MD4 is observed to have less breakdown compared to MD8 and MD11. MD4 is observed to be most sensitive to changes in the FI.

Monzonite 2: Figure 5.30 shows the influence of FI and particle size on both the both MD and MDx, for monzonite 2. Monzonite 2 is observed to have similar MD and MDx values compared to monzonite 1 but has generally higher values.

Mylonite: Figure 5.31 shows the influence of FI and particle size on both MD and MDx, for mylonite. Mylonite shows similar values for all size fraction. MD4 is observed to have less breakdown compared to MD8 and MD11. MD11 is observed to be most sensitive to changes in FI.

Greywacke: Figure 5.32 shows the influence of FI and particle size on both MD and MDx, for greywacke. Greywacke has generally very high MD. Size fraction 8/11.2 mm has the highest values but 4/8 mm is most sensitive to changes in FI. MD4 is observed to have less breakdown compared to MD8 and MD11.

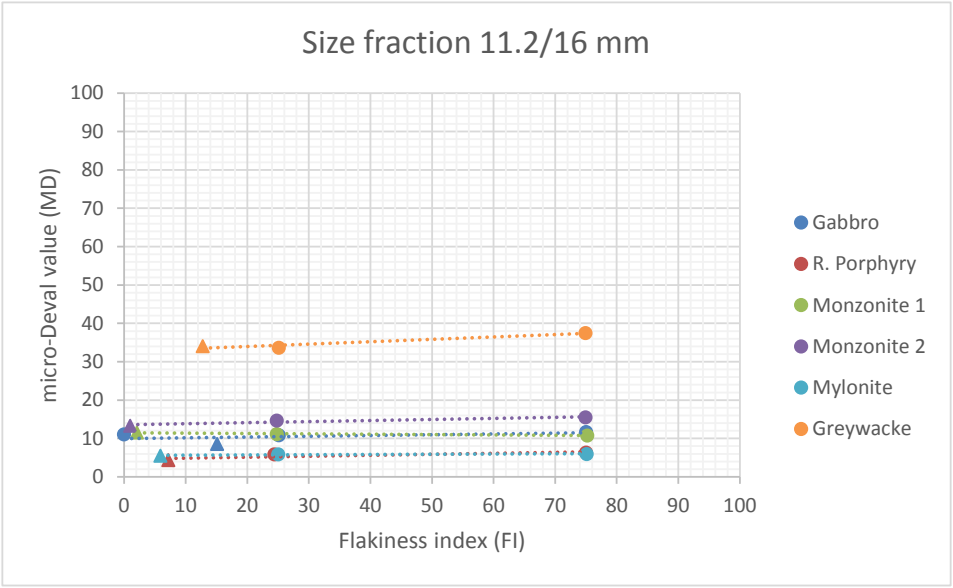

Figure 5.21: Micro-Deval value (MD) versus flakiness index (FI).

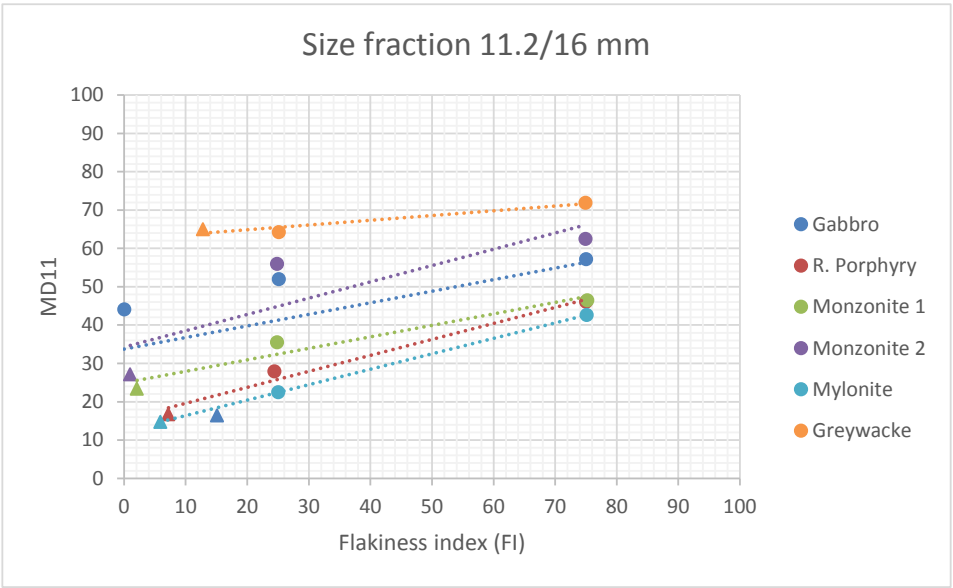

Figure 5.22: MD11 versus flakiness index (FI).

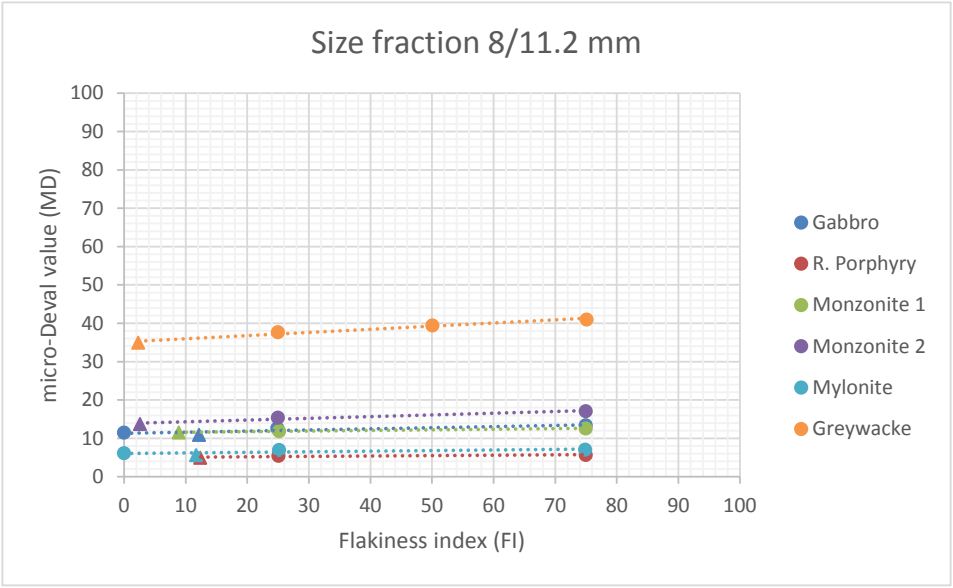

Figure 5.23: Micro-Deval value (MD) versus flakiness index (FI).

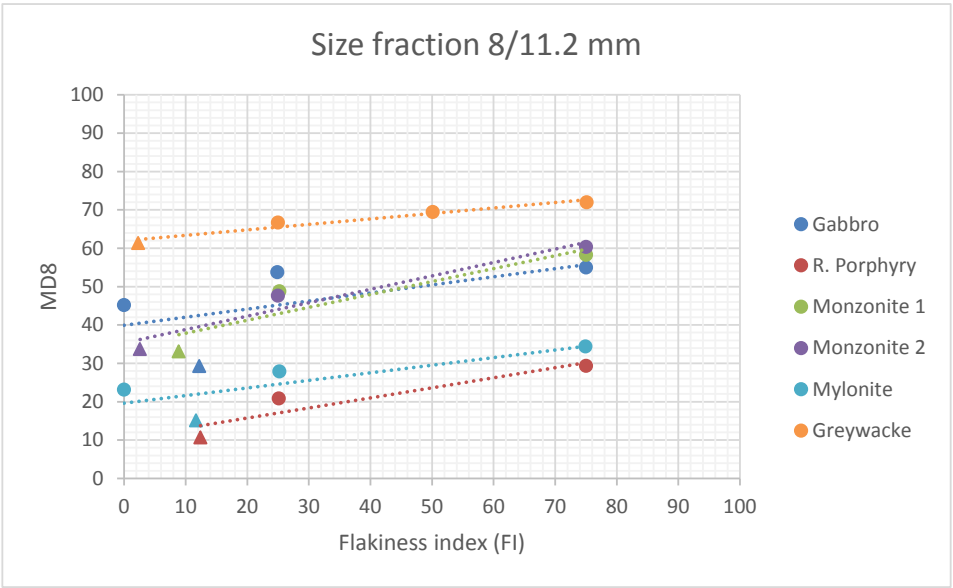

Figure 5.24: MD8 versus flakiness index (FI).

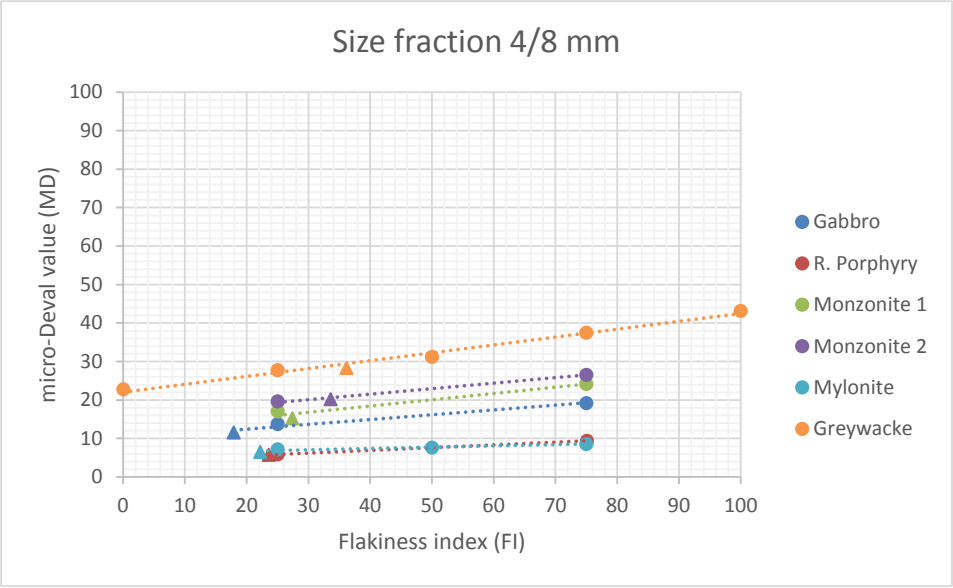

Figure 5.25: Micro-Deval value (MD) versus flakiness index (FI).

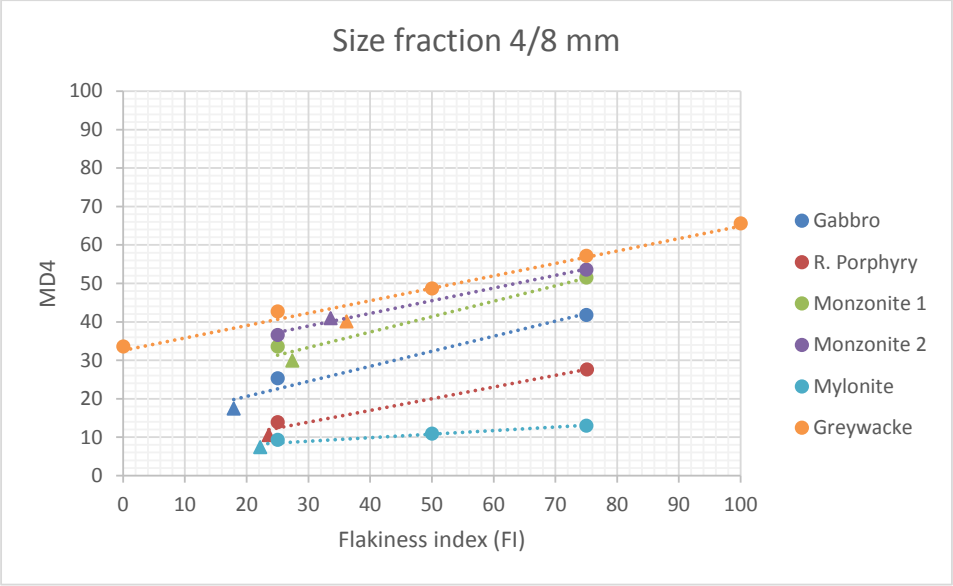

Figure 5.26: MD4 versus flakiness index (FI).

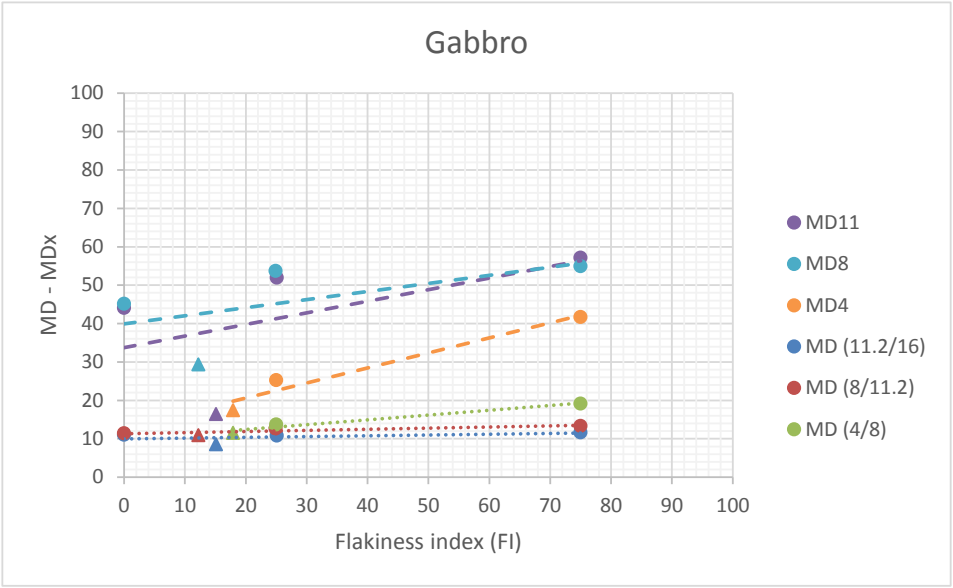

Figure 5.27: MD and MDx versus flakiness index (FI).

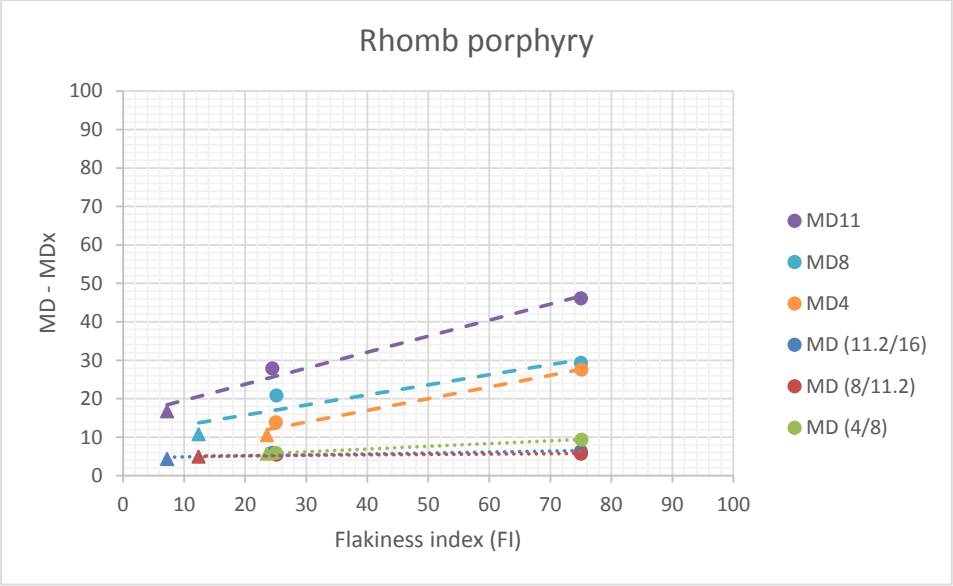

Figure 5.28: MD and MDx versus flakiness index (FI).

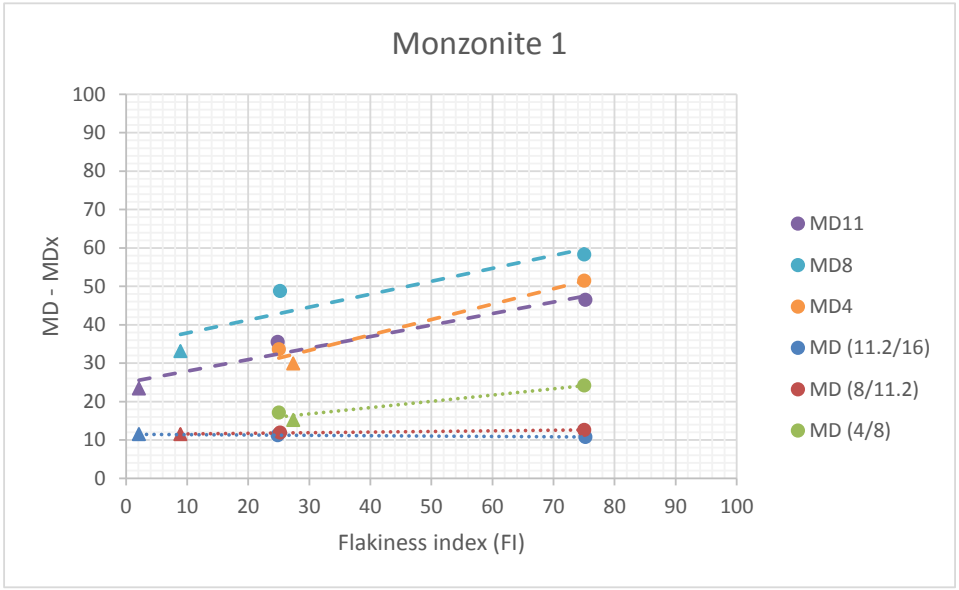

Figure 5.29: MD and MDx versus flakiness index (FI).

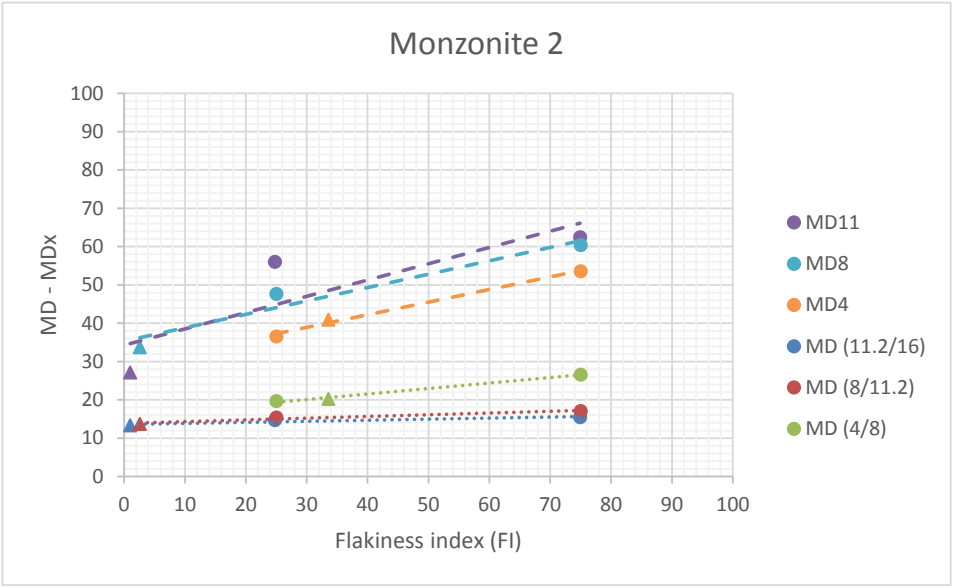

Figure 5.30: MD and MDx versus flakiness index (FI).

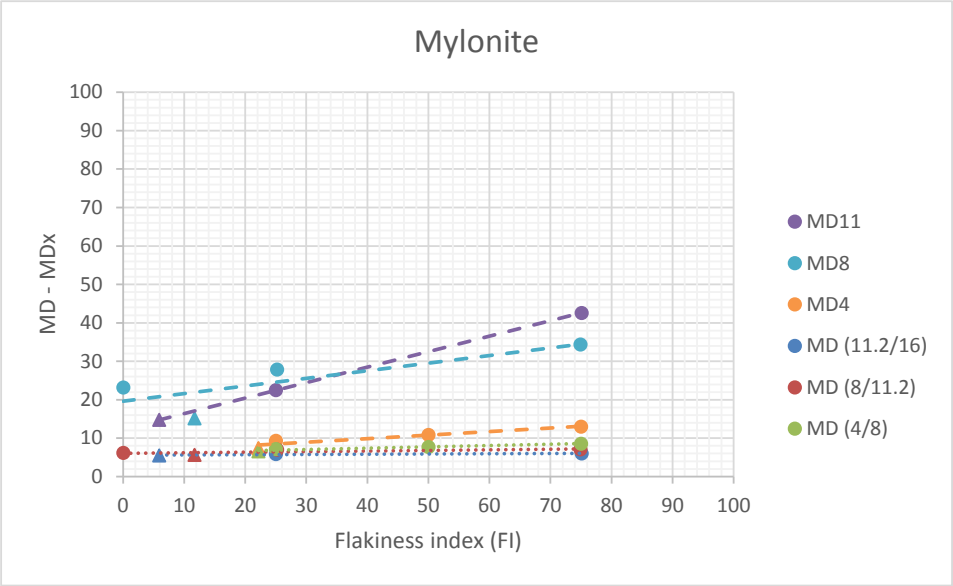

Figure 5.31: MD and MDx versus flakiness index (FI).

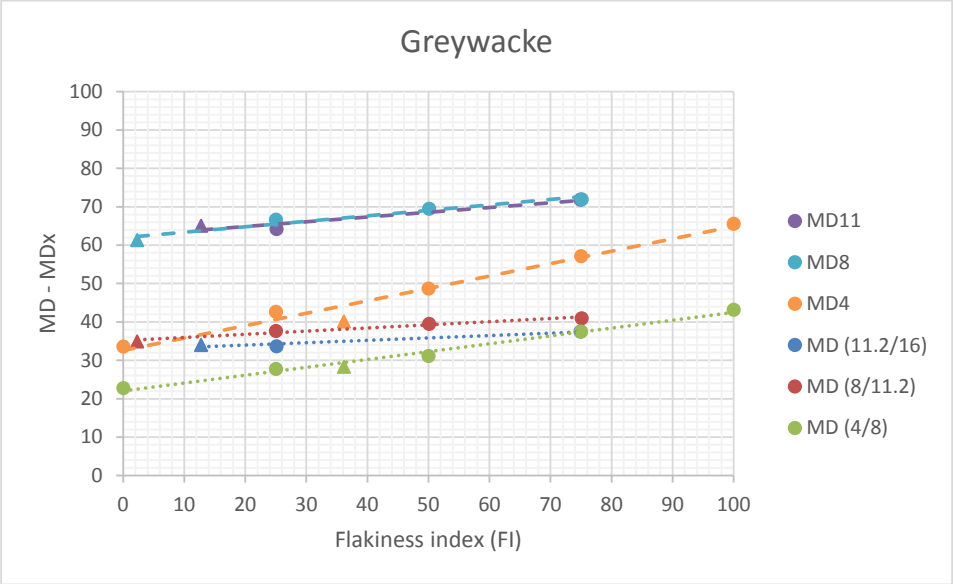

Figure 5.32: MD and MDx versus flakiness index (FI).

5.6.1 Discussion of MD and MDx Versus FI

Overall the micro-Deval value (MD) and MDx increase with increasing aggregate flakiness index (FI) - regardless of rock type - for aggregate size fractions 4/8 mm, 8/11.2 mm and 11.2/16 mm. The increase in the MD value is, however, small. The MDx value is observed to have much steeper lines, compared to the standard MD value. When slope angles, taken from the relationship equations between MD, MDx and flakiness index are compared, see table 5.5, MD11, MD8 and MD4 are observed to have much larger slope angles compared to the standard MD value. A higher slope angle number indicates that the value is more sensitive to changes in FI. The MDx have overall higher numbers compared to standard MD values indicating that the MDx value is much more sensitive to changes in particle shape than the standard MD value. The micro-Deval standard test methods is therefore not sensitive to changes in particle shape.

It can also be seen in table 5.5 that no clear distinction can be made if rock types with low MD and MDx values are the most sensitive to changes in FI like the results from the Los Angeles test revealed. The MD test results are overall harder to interpret compared to the Los Angeles test results. The micro-Deval test has more complex breakdown tied to the mineralogical composition. When MD and MDx are compared to relative hardness calculated from the mineralogical composition, see figure 5.1, good correlation is observed between the two. The higher the MD and MDx are, the lower rock relative hardness is.

Table 5.5: Slope from the relationship equations between MD, MDx values and FI. The higher the number, the more sensitive the value is to changes in FI.

Rock types	MD (11.2/16)	MD11	MD (8/11.2)	MD8	MD (4/8)	MD4
Mylonite	0,0	0,4	0,0	0,2	0,0	0,1
R. porphyry	0,0	0,4	0,0	0,3	0,1	0,3
Gabbro	0,0	0,3	0,0	0,2	0,1	0,4
Greywacke	0,1	0,1	0,1	0,1	0,2	0,3
Monzonite 1	0,0	0,3	0,0	0,3	0,2	0,4
Monzonite 2	0,0	0,4	0,0	0,3	0,1	0,3

It must also be said that results with much higher MD values were expected due to extreme values in FI. The MD value is, however, generally not sensitive to variations in FI. The reason for this could be the same as for the LA value. The MD test value takes no account of the coarser products produced by breakdown of material above 1.6 mm. The MD value is only influenced by material passing 1.6 mm sieve size.

Sieve analysis (Appendix D) reveals how the test fractions break down into smaller particle size fractions with increasing FI. Increase in FI noticeably increases breakdown and fragmentation into smaller particle size fractions. The production of fines (<1.6 mm) does not dramatically increase with increasing FI. Figure 5.33 shows it very clearly how the r. porphyry test fraction 11/16 mm is breaking down into smaller particle. Production of fines (<1.6 mm) is barely increasing, resulting in very small variations between MD values with increasing FI. Figure 5.33 also shows the reason behind the MDx value being more sensitive to changes in FI, compared to the MD value. Much more material is seen passing the 11.2 mm sieve size with increasing FI, resulting in large variations in the MD11 value.

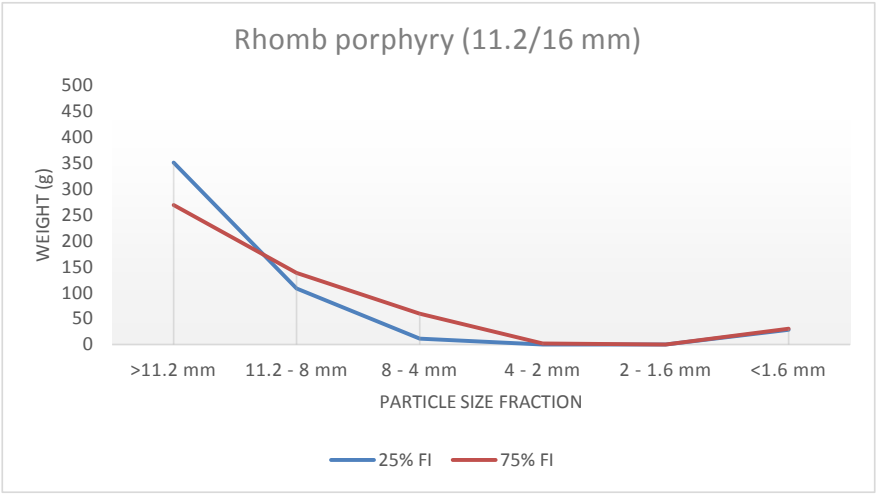

Figure 5.33: R. porphyry size fraction 11.2/16 mm, sieve analysis of the micro-Deval test.

The MDx value is therefore more sensitive indicator of aggregate breakdown when evaluating the effects of particle shape on mechanical properties of aggregates, compared to the standard MD value. Sieve analysis of the micro-Deval test for mylonite (4/8 mm) shows hardly any increase in aggregate breakdown due to increase in FI, see figure 5.34. This may be caused by high amounts of quartz in mylonite resulting in high relative hardness (Mohs scale). Figure 5.35 shows sieve analyses of micro-Deval test for greywacke (4/8 mm) which shows high amounts of breakdown and production of fines with increase in FI. This may be caused by high amounts of soft minerals in greywacke resulting in low rock hardness. Rock hardness might therefore play a larger role than particle shape when it comes to breakdown inside the micro-Deval test drum.

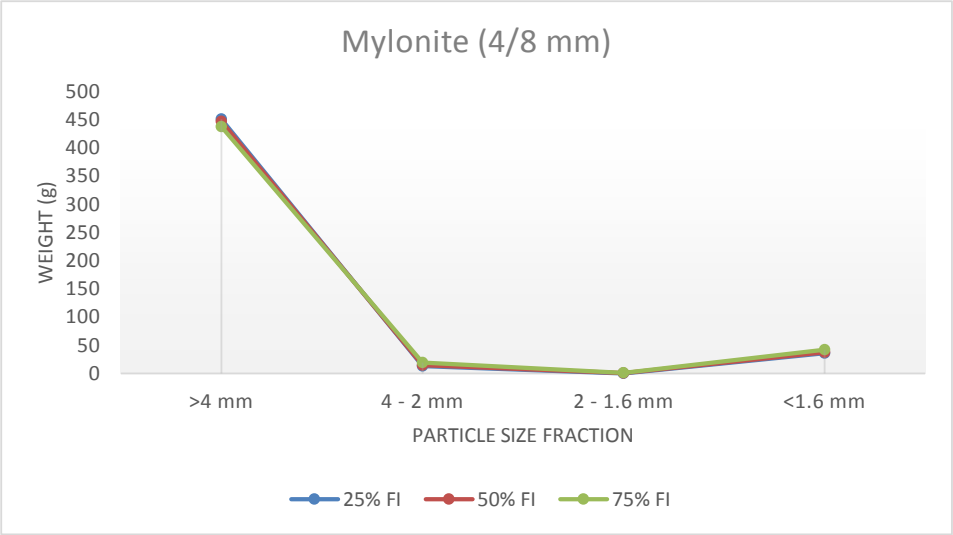

Figure 5.34: Mylonite size fraction 4/8 mm, sieve analysis of the micro-Deval test.

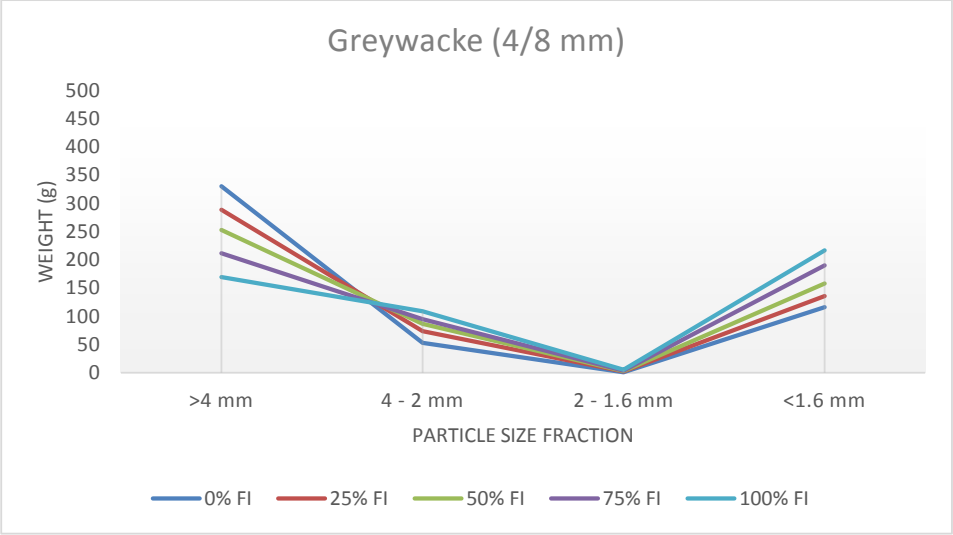

Figure 5.35: Greywacke size fraction 4/8 mm, sieve analysis of the micro-Deval test.

Different particle size fractions for each rock type show similar MD values. Rock types that show general increase in the MD value with decrease in particle size fractions are: monzonite 1, monzonite 2 and gabbro. Rock types that show little to no change in the MD value between particle size fractions are r. porphyry and mylonite. Finally greywacke shows no clear trend. According to the MD value, size fraction 4/8 mm is the most sensitive size fraction to changes in the flakiness index, regardless of rock type.

Variations in the MD value between size fractions is probably due to the same reason as in the Los Angeles test. The micro-Deval test method does not use the same amount of steel balls for each fraction, fewer steel balls are used for the smaller size fractions. The steel balls are, however, larger in comparison to the smaller particle fraction compared to the larger particle fraction. Smaller particle size fractions are therefore possibly loaded with larger force per area compared to larger particle sizes. This could be the reason for variations in the MD value between different particle size fractions.

The results show that the MDx value decreases as particle size fraction decreases, regardless of rock type. According to the MDx value, size fractions 4/8 mm (gabbro, monzonite 1 and greywacke) and 11.2 mm (monzonite 2, r. porphyry and mylonite) are the most sensitive to changes in the flakiness index.

Similarly to the LA4 results, the 4/8 mm (MD4) particle size fraction shows generally less breakdown of material compared to size fractions 8/11.2 mm (MD8) and 11.2/16 mm (MD11), which show similar amount of material passing the uppermost sieve. This is as surprising as for the Los Angeles test due to the fact that the smaller sized particles (4/8 mm) are being worn down by steel balls of the same size and weight as the larger size particles (8/11.2 mm and 11.2/16 mm). Test fraction (4/8 mm) is although run with fewer steel balls. This does, however, not change the fact that the 4/8 mm particles are experiencing larger force per area compared to 8/11.2 mm and 11.2/16 mm particles. This higher breakdown of the larger particles compared to the smallest particle size fraction could be explained by the theory of statistical distribution of flaws. The larger the particle size, the more likely you have a critical flaw occurring in the rock particle (Smith and Collis, 1993).

Chapter 6

Conclusions and Recommendations

All in all 138 tests were conducted for this study, 69 Los Angeles and 69 micro-Deval tests. That amounts to 414 kilograms of aggregate material tested in total. In order to assess the influence of flakiness index on mechanical properties, the proportion of flaky and cubic particles was artificially varied from 0 to 100 percent in a series of tests for each rock type.

The main findings are that the standard Los Angeles and micro-Deval test methods which measure the amounts of fines ($<$1.6 mm) produced by impact and/or wear are generally not sensitive to variations in the flakiness index. The LAx and MDx values, which are measured by the amounts of material passing the lower fraction of the size range, are more sensitive to variations in the flakiness index. The LAx and MDx values are therefore more sensitive indicators of aggregate breakdown when evaluating the effects of particle shape on mechanical properties of aggregates, compared to the standard LA and MD values.

Sieve analysis also shows that the standard LA and MD method of measuring production of fines is not always a good indicator of aggregate breakdown and may in some cases ignore increased breakdown of the aggregate coarser than 1.6 mm. The LAx and MDx values better demonstrate the behavior of the aggregate coarser than 1.6 mm and give better information about the extent of aggregate breakdown after the test. It is therefore recommended that these values, that can be determined with little extra work, be implemented as additional values in aggregate analysis.

Conclusions that can be drawn from this research are:

- The Los Angeles value (LA) increases with increasing aggregate flakiness index (FI) - regardless of rock type - for aggregate size fractions 4/8 mm, 8/11.2 mm and 11.2/16 mm. The increase in the LA value is, however, small.
- LAx increases with increasing aggregate flakiness index (FI) - regardless of rock type - for aggregate size fractions 4/8 mm, 8/11.2 mm and 11.2/16 mm. It is also found to be more sensitive to changes in FI, compared to the standard Los Angeles value (LA).
- The micro-Deval value (MD) increases with increasing aggregate flakiness index (FI) - regardless of rock type - for aggregate size fractions 4/8 mm, 8/11.2 mm and 11.2/16 mm. The increase in the MD value is, however, small.
- MDx increases with increasing aggregate flakiness index (FI) - regardless of rock type - for aggregate size fractions 4/8 mm, 8/11.2 mm and 11.2/16 mm. It is also found to be more sensitive to changes in FI, compared to the standard micro-Deval value (MD).
- Rock types (gabbro, rhomb porphyry and mylonite) with good mechanical properties, measured by the Los Angeles test are more sensitive to changes in the flakiness index (FI) then rock types with poorer mechanical properties (monzonite 1, monzonite 2 and greywacke).
- Flakiness index calculated for each particle size fraction (11.2/16 mm, 8/11.2 mm 4/8 mm) gives more detailed information about the flakiness of a rock type compared to flakiness index calculated for a wide particle range (4/16 mm). Requirement for each size fractions, not wide particle range is therefore recommended.
- Correlation was observed between MD, MDx and amount of soft mineral content. Resistance to abrasion decreases (high MD and MDx) with increased content of soft minerals.
- Correlation was observed between LA, LAx and mineral grain size. Resistance to impact and abrasion generally decreases (high LA and LAx) as mineral grain size increases.

Bibliography

Akbulut, H., Gürer, C., 2007. Use of aggregates produced from marble quarry waste in asphalt pavements. Building and Environment 42 (5), 1921–1930.

Aksnes, J., Evensen, R., 2009. Environmentally friendly pavemetns, final report. Statens vegvesen (2578).

Barksdale, R. D., 1991. The Aggegate Handbook. National Stone Association, Washington, DC.

Bouquety, M. N., Descantes, Y., Barcelo, L., de Larrard, F., Clavaud, B., 2007. Experimental study of crushed aggregate shape. Construction and Building Materials 21 (4), 865–872.

Brattli, B., 1992. The influence of geological factors on the mechanical properties of igneous rocks used as road surface aggregates. Engineering Geology 33, 31–44.

British Standards Institution, 1989. Testing aggregates. Methods for determination of particle shape. Flakiness index (BS 812:1989).

British Standards Institution, 1990a. Testing aggregates. Method for determination of aggregate crushing value (BS 812-110:1990).

British Standards Institution, 1990b. Testing aggregates. Method for determination of aggregate impact value (BS 812-112:1990).

Brown, E. R., McRae, J. L., Crawley, A. B., 1989. Effect of aggregates on performance of bituminous concrete. American Society for Testing and Materials ASTM STP 1016, 34–63.

Czarnecka, E., Gillott, J., 1982. Effect of different types of crushers on shape and roughness of aggregates. Cement, Concrete Aggregates, CCAGDP 4 (1), 6–33.

Dahl, F., Bruland, A., Jakobsen, P. D., Nilsen, B., Grv, E., 2012. Classifications of properties influencing the drillability of rocks, based on the ntnu/sintef test method. Tunnelling and Underground Space Technology 28 (0), 150–158.

Deere, D. U., Miller, R. P., 1966. Engineering classification and index properties for intact rock. Technical Report AFWL-TR-65-116 Air Force Weapons Laboratory, Kirtland.

Dhir, R. K., Ramsey, D. M., Balfour, N., 1971. A study of the aggregate impact and crushing value tests. Journal of the Institute of Highway Engineers 18, 17–27.

Dunlevey, J. N., Stephens, D. J., 1998. The coarse aggregate resources of south africa. Aggregate Resources: A Global Perspective, 131–145.

Erichsen, E., 2013. Vurdering av testmetoder for tilslagsmaterialer. NGU (No. 121), 0–35.

Erichsen, E., 2014. Plotting aggregate degradation results from the los angeles test on a triangular diagram: proposal of a new quality ranking for aggregates. Bulletin of Engineering Geology and the Environment, 1–5.

Erichsen, E., Ulvik, A., Vongraven, H., Tangstad, R., Fossan, B., 2010. Miljøvennlige vegdekker - materialtekniske egenskaper for ulike testfraksjoner. Norges geologiske undersøkelse 2010.065 (3317), 4–23.

European standard, 2003. Tests for geometrical properties of aggregates - Part 3: Determination of particle shape - Flakiness index (EN 933-3:1997+A1).

European standard, 2010. Tests for mechanical and physical properties of aggregates - Part 2: Methods for the determination of resistance to fragmentation (EN 1097-2:2010).

European standard, 2011. Tests for mechanical and physical properties of aggregates - Part 1: Determination of the resistance to wear (micro-Deval)(EN 1097-:2011).

Fernlund, J. M. R., 2005. 3-d image analysis size and shape method applied to the evaluation of the los angeles test. Engineering Geology 77 (1-2), 57–67.

Haraldsson, H., 1984. Relation between petropraphy and the aggregate properties of icelandic rocks. Bulletin of the International Association of Engineering Geology, 73–76.

Kandhal, P. S., Khatri, M. A., Motter, J. B., 1992. Evaluation of particle shape and texture of mineral aggregates and their blends. Journal of Association of Asphalt Paving Technologists, 217–328.

Kim, Y. R., Kim, N., Khosha, N. P., 1992. Effects of aggregate type and gradation on fatigue and permanent deformation of asphalt concrete. American Society for Testing and Materials ASTM STP 1147, 310–328.

Liu, H., Kou, S., Lindqvist, P.-A., Lindqvist, J. E., Åkesson, U., 2005. Microscope rock texture characterization and simulation of rock aggregate properties. Geological Survey of Sweden (SGU) (SGU project 60-1362/2004).

Marker, M., 2005. Geologisk undersøkelse av øvre brudd og nytt tilleggsområde. Norges geologiske undersøkelse (NGU) 263324 (2005.077), 2–16.

Meininger, R. C., 1994. Degradation resistance, strength, and related properties. proceedings of a conference on significance of tests and properties of concrete and concrete making materials. American society for Testing and Materials, Special Pubication STP 169C, 388–400.

Nålsund, R., 2014. Railway Ballast Characteristics, Selection Criteria and Performance. Norwegian university of science and technology, Faculty of engineering science and technology, Department of civil and transport engineering.

Nålsund, R., Jensen, V., 2013. Infuence of mineral grain size, grain size distribution and micro-cracks on rocks mechanical strength. 14th Euro-seminar on Microscopy Applied to Building Materials, 1–12.

NGU, 2014. Mineral resources in norway 2013. production data and annual report. Geological Survey of Norway (NGU) (2), 7–36.

Prowell, B. D., Zhang, J., Brown, E. R., 2005. Aggregate properties and the performance of superpave-designed hot mix asphalt. Washington, D.C : Transportation Research Board.

Ramsay, D. M., Dhir, R. K., Spence, I. M., 1974. The role of rock and clast fabric in the physical performance of crushed-rock aggregate. Engineering Geology 8, 267–285.

Ramsay, D. M., Dhir, R. K., Spence, I. M., 1977. The practical and theoretical merits of the aggregate impact value in the study of crushed rock aggregate. Rock Engineering, Ed. P B Attewell, British Geotechnical Society, 1–10.

Rigopoulos, I., Tsikouras, B., Pomonis, P., Hatzipanagiotou, K., 2013. Determination of the interrelations between the engineering parameters of construction aggregates from ophiolite complexes of greece using factor analysis. Construction and Building Materials 49 (0), 747–757.

Röthlisberger, F., Däppen, J., Kurzen, E., Würsch, E., 2005. Los angeles prüfung für gleisschotter aussgekraft und folgerung. Eisenbahntechnische Rundschau, 355–361.

Selmer-Olsen, R., 1949. Prøving av steinmaterialer til vegdekker. Meddelelser fra Vegdirektøren 12, 187–194.

Selmer-Olsen, R., 1980. Ingeniørgeologi. 1: Generell geologi. Tapir.

Senior, S. A., Rogers, C. A., 1991. Laboratory tests for predicting coarse aggregate performance in ontario. Transportation Research Record 1301, Transportation Research Board, National Research Council, Washington, DC, 97–106.

Smith, M., Collis, L., 1993. Aggregates: Sand, Gravel and Crushed Rock Aggregates for Construction Purposes. Geological Society.

Spence, I. M., Ramsay, D. M., Dhir, R. K., 1974. A conspectus of aggregate strength and the relevance of this factor as the basis for a physical classification of crushed rock aggregate. Int. Cong. Rock. Mechs 2A, 79–84.

Statens vegvesen, 1997. Håndbok 014 - Laboratorieundersøkelser, kapittel 14.451 Flisighet og sprøhet.

Statens vegvesen, 2014. Håndbok N200 Vegbygging. Oslo, Norway.

Tangstad, R., Vongraven, H., 2015. Results from the norwegian geological survey hard rock database (ngu).

Wieden, P., Augustin, H., 1977. Versuche zur verbesserung des los angeles tests. Bundesministerium für Bauten und Technik.

Wigum, B. J. (Ed.), 2014. Lecture 5 (Crushing). Aggregate Production (TGB4250) at Norwegian University of Science and Technology (NTNU).

Appendices

Appendix A: Thin Section Photographs

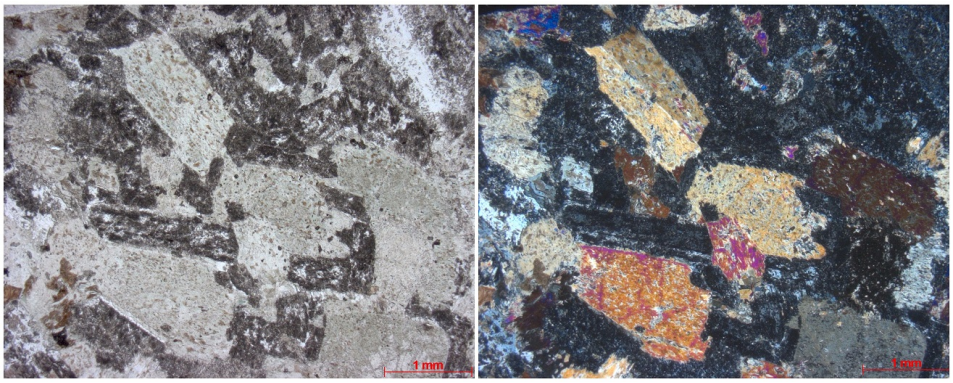

Figure A1: Gabbro, thin section photographs.

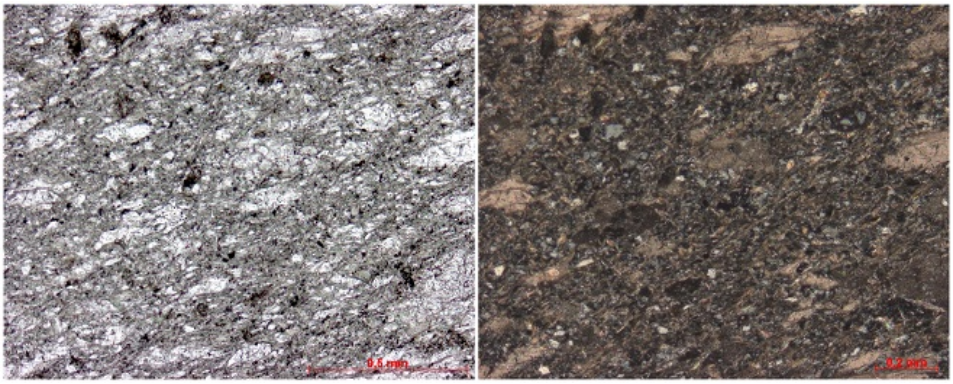

Figure A2: Greywacke, thin section photographs.

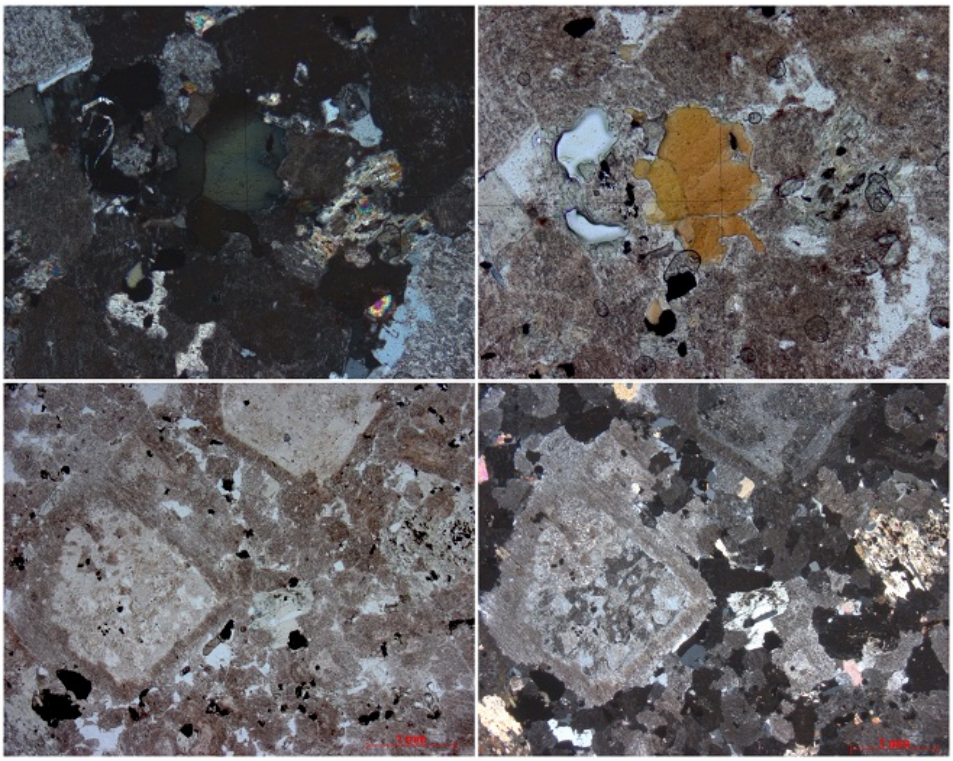

Figure A3: Rhomb porphyry, thin section photographs.

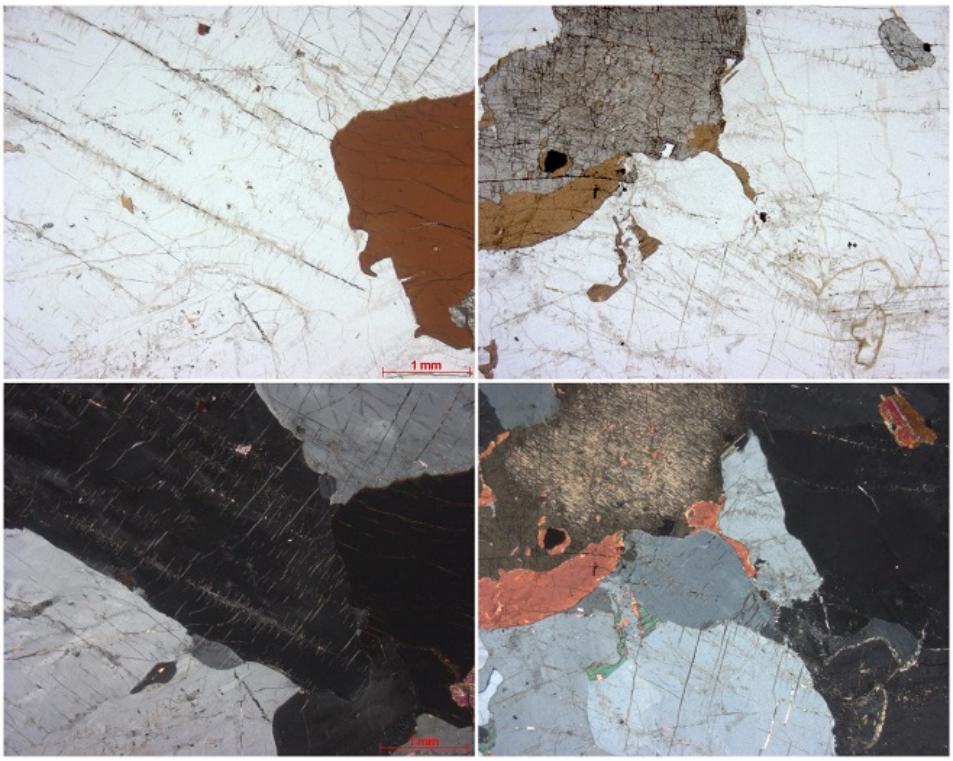

Figure A4: Monzonite 1, thin section photographs.

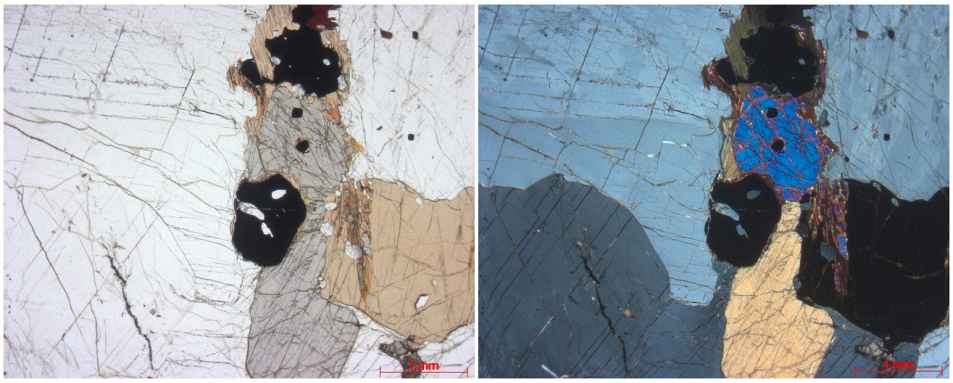

Figure A5: Monzonite 2, thin section photographs.

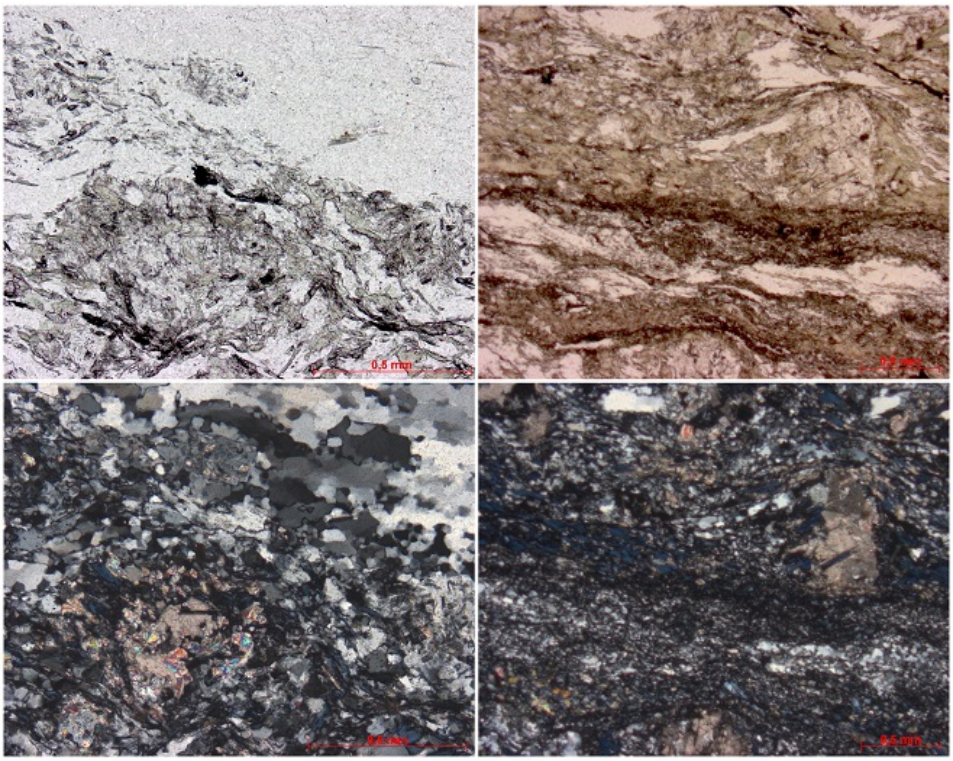

Figure A6: Mylonite, thin section photographs.

Appendix B: Relationship Equations and the Coefficient of Correlation

Table B1: LA and FI relationship, size fraction 11.2/16 mm.

LA (11.2/16 mm)		
Rock type	**LA and Flakiness Index Relationship**	**Coefficient of Correlation**
Gabbro	LA = 0,0919 FI + 18,054	r = 0,9781
Rhomb porphyry	LA = 0,0987 FI + 12,247	r = 0,9989
Monzonite 1	LA = 0,0893 FI + 33,598	r = 0,9674
Monzonite 2	LA = 0,0879 FI + 38,167	r = 0,9339
Mylonite	LA = 0,0637 FI + 11,665	r = 0,9984
Greywacke	LA = 0,0686 FI + 21,029	r = 0,9983

Table B2: LA and FI relationship, size fraction 8/11.2 mm.

LA (8/11.2 mm)		
Rock type	**LA and Flakiness Index Relationship**	**Coefficient of Correlation**
Gabbro	LA = 0,065 FI + 20,0370	r = 0,9907
Rhomb porphyry	LA = 0,0985 FI + 16,414	r = 1,0000
Monzonite 1	LA = 0,0546 FI + 34,391	r = 0,9421
Monzonite 2	LA = 0,0543 FI + 37,290	r = 0,9710
Mylonite	LA = 0,0596 FI + 12,974	r = 0,9956
Greywacke	LA = 0,036 FI + 22,8720	r = 0,8693

Table B3: LA and FI relationship, size fraction 4/8 mm.

LA (4/8 mm)		
Rock type	**LA and Flakiness Index Relationship**	**Coefficient of Correlation**
Gabbro	LA = 0,0598 FI + 18,634	r = 0,9961
Rhomb porphyry	LA = 0,058 FI + 16,5470	r = 0,9220
Monzonite 1	LA = 0,0381 FI + 31,744	r = 0,9962
Monzonite 2	LA = 0,0248 FI + 33,600	r = 0,8828
Mylonite	LA = 0,0449 FI + 15,027	r = 0,9624
Greywacke	LA = 0,0607 FI + 21,751	r = 0,9858

Table B4: LA11 and FI relationship.

LA11		
Rock type	**LA and Flakiness Index Relationship**	**Coefficient of Correlation**
Gabbro	LA11 = 0,1968 FI + 76,431	r = 0,9049
Rhomb porphyry	LA11 = 0,4073 FI + 54,559	r = 0,9943
Monzonite 1	LA11 = 0,1068 FI + 88,963	r = 0,9919
Monzonite 2	LA11 = 0,0684 FI + 93,794	r = 0,9461
Mylonite	LA11 = 0,3611 FI + 55,426	r = 0,9892
Greywacke	LA11 = 0,1651 FI + 79,007	r = 0,9711

Table B5: LA8 and FI relationship.

LA8		
Rock type	**LA and Flakiness Index Relationship**	**Coefficient of Correlation**
Gabbro	LA8 = 0,1803 FI + 75,576	r = 0,9093
Rhomb porphyry	LA8 = 0,2883 FI + 61,847	r = 0,9932
Monzonite 1	LA8 = 0,0858 FI + 90,360	r = 0,9721
Monzonite 2	LA8 = 0,0688 FI + 92,558	r = 0,9690
Mylonite	LA8 = 0,2358 FI + 57,799	r = 0,9800
Greywacke	LA8 = 0,1028 FI + 77,045	r = 0,9638

Table B6: LA4 and FI relationship.

LA4		
Rock type	**LA and Flakiness Index Relationship**	**Coefficient of Correlation**
Gabbro	LA4 = 0,246 FI + 39,999	r = 0,9861
Rhomb porphyry	LA4 = 0,2661 FI + 35,136	r = 0,9539
Monzonite 1	LA4 = 0,2122 FI + 63,677	r = 0,9626
Monzonite 2	LA4 = 0,13 FI + 69,2350	r = 0,9544
Mylonite	LA4 = 0,1279 FI + 32,12	r = 0,9708
Greywacke	LA4 = 0,2052 FI + 46,95	r = 0,9727

Table B7: MD and FI relationship, size fraction 11.2/16 mm.

MD (11.2/16 mm)		
Rock type	**MD and Flakiness Index Relationship**	**Coefficient of Correlation**
Gabbro	MD = 0,0202 FI + 9,9670	r = 0,4669
Rhomb porphyry	MD = 0,0251 FI + 4,6189	r = 0,8263
Monzonite 1	MD = -0,0093 FI + 11,483	r = 0,9912
Monzonite 2	MD = 0,0276 FI + 13,572	r = 0,9363
Mylonite	MD = 0,0062 FI + 5,5821	r = 0,8328
Greywacke	MD = 0,0621 FI + 32,732	r = 0,9666

Table B8: MD and FI relationship, size fraction 8/11.2 mm.

MD (8/11.2 mm)		
Rock type	**MD and Flakiness Index Relationship**	**Coefficient of Correlation**
Gabbro	MD = 0,0292 FI + 11,306	r = 0,8492
Rhomb porphyry	MD = 0,0103 FI + 4,9804	r = 0,8188
Monzonite 1	MD = 0,016 FI + 11,4170	r = 0,9918
Monzonite 2	MD = 0,0448 FI + 13,868	r = 0,9766
Mylonite	MD = 0,0153 FI + 6,0476	r = 0,7108
Greywacke	MD = 0,0822 FI + 35,140	r = 0,9855

Table B9: MD and FI relationship, size fraction 4/8 mm.

MD (4/8 mm)		
Rock type	**MD and Flakiness Index Relationship**	**Coefficient of Correlation**
Gabbro	MD = 0,1249 FI + 9,9232	r = 0,9837
Rhomb porphyry	MD = 0,0709 FI + 4,0763	r = 0,9997
Monzonite 1	MD = 0,1632 FI + 11,902	r = 0,9703
Monzonite 2	MD = 0,1433 FI + 15,787	r = 0,9953
Mylonite	MD = 0,0343 FI + 6,0224	r = 0,9598
Greywacke	MD = 0,2045 FI + 22,044	r = 0,9927

Table B10: MD11 and FI relationship.

MD11		
Rock type	**MD and Flakiness Index Relationship**	**Coefficient of Correlation**
Gabbro	MD11 = 0,3019 FI + 33,731	r = 0,5397
Rhomb porphyry	MD11 = 0,4169 FI + 15,421	r = 0,9902
Monzonite 1	MD11 = 0,2998 FI + 24,932	r = 0,9707
Monzonite 2	MD11 = 0,4251 FI + 34,263	r = 0,8510
Mylonite	MD11 = 0,4028 FI + 12,369	r = 1,0000
Greywacke	MD11 = 0,1236 FI + 62,385	r = 0,9603

Table B11: MD8 and FI relationship.

MD8		
Rock type	**MD and Flakiness Index Relationship**	**Coefficient of Correlation**
Gabbro	MD8 = 0,2107 FI + 39,921	r = 0,5853
Rhomb porphyry	MD8 = 0,2624 FI + 10,491	r = 0,9276
Monzonite 1	MD8 = 0,3366 FI + 34,493	r = 0,9107
Monzonite 2	MD8 = 0,3496 FI + 35,311	r = 0,9702
Mylonite	MD8 = 0,1979 FI + 19,619	r = 0,8027
Greywacke	MD8 = 0,1426 FI + 61,939	r = 0,9763

Table B12: MD4 and FI relationship.

MD4		
Rock type	**MD and Flakiness Index Relationship**	**Coefficient of Correlation**
Gabbro	MD4 = 0,3914 FI + 12,785	r = 0,9783
Rhomb porphyry	MD4 = 0,3044 FI + 4,7836	r = 0,9864
Monzonite 1	MD4 = 0,4012 FI + 21,296	r = 0,9794
Monzonite 2	MD4 = 0,3295 FI + 29,027	r = 0,9964
Mylonite	MD4 = 0,0923 FI + 6,1747	r = 0,9588
Greywacke	MD4 = 0,3232 FI + 32,567	r = 0,9831

Appendix C: Detailed Results

Table B1: LA, standard procedure test results.

Quarry	Los Angeles			
	11.2/16 mm	10/14 mm	8/11.2 mm	4/8 mm
Gabbro	19,1	20,5	20,7	19,6
R. Porphyry	12,6	13,7	17,5	17,3
Monzonite 1	33,2	34,1	34,3	32,8
Monzonite 2	37,3	40,2	37,1	34,8
Mylonite	11,9	11,7	13,4	15,6
Greywacke	22,0	22,8	23,4	23,5

Table B2: FI calculated in accordance to the LA standard procedure.

Quarry	Los Angeles - Flakiness index			
	11,2/16 mm	10/14 mm	8/11,2 mm	4/8 mm
Gabbro	15,2	17,5	13,1	18,7
R. porphyry	4,9	6,6	11,2	25,1
Monzonite 1	3,1	3,5	8,6	25,2
Monzonite 2	1,2	8,9	3,6	33,0
Mylonite	5,3	4,9	10,7	21,4
Greywacke	12,5	12,9	2,9	39,9

Table B3: MD, standard procedure test results.

Quarry	micro-Deval			
	11.2/16 mm	10/14 mm	8/11.2 mm	4/8 mm
Gabbro	8,5	10,0	10,9	11,5
R. porphyry	4,3	6,0	4,9	5,7
Monzonite 1	11,5	11,5	11,5	15,2
Monzonite 2	13,3	17,0	13,7	20,2
Mylonite	5,5	5,5	5,6	6,5
Greywacke	34,0	34,0	34,9	28,3

Table B4: FI calculated in accordance to the MD standard procedure.

Quarry	micro-Deval - Flakiness index			
	11,2/16 mm	10/14 mm	8/11,2 mm	4/8 mm
Gabbro	15,1	17,5	12,2	17,9
R. porphyry	7,2	6,7	12,4	23,6
Monzonite 1	2,1	2,1	8,9	27,4
Monzonite 2	1,0	8,6	2,6	33,6
Mylonite	5,9	7,5	11,7	22,2
Greywacke	12,8	10,8	2,3	36,2

Table B5: LA, size fraction 11.2/16 mm.

Quarry	LA value 11.2/16 mm				
	0% FI	25% FI	50% FI	75% FI	100% FI
Gabbro	17,7	21,3		24,7	
R. porphyry		14,9		19,6	
Monzonite 1		36,8		40,0	
Monzonite 2		41,8		44,3	
Mylonite		13,4		16,4	
Greywacke		22,6		26,2	

Table B6: LA, size fraction 8/11.2 mm.

Quarry	LA value 8/11.2 mm				
	0% FI	25% FI	50% FI	75% FI	100% FI
Gabbro	19,9	22,1		24,8	
R. porphyry		18,9		23,8	
Monzonite 1		36,5		38,3	
Monzonite 2		39,2		41,2	
Mylonite	13,0	14,7		17,4	
Greywacke		22,9	25,2	25,5	

Table B7: LA, size fraction 4/8 mm.

Quarry	LA value 4/8 mm				
	0% FI	25% FI	50% FI	75% FI	100% FI
Gabbro		20,3		23,1	
R. porphyry		18,7		20,9	
Monzonite 1		32,6		34,6	
Monzonite 2		33,9		35,4	
Mylonite		16,5	17,4	18,3	
Greywacke	22,1	23,3	24,9	26,2	28,1

Table B8: LA11, size fraction 11.2/16 mm.

Quarry	LA_{11}				
	0% FI	25% FI	50% FI	75% FI	100% FI
Gabbro	78,1	83,9		91,2	
R. porphyry		66,5		84,6	
Monzonite 1		92,2		96,8	
Monzonite 2		96,5		98,6	
Mylonite		66,6		81,9	
Greywacke		84,6		91,1	

Table B9: LA8, size fraction 8/11.2 mm.

Quarry	LA_8				
	0% FI	25% FI	50% FI	75% FI	100% FI
Gabbro	78,0	81,2		89,4	
R. porphyry		70,3		83,2	
Monzonite 1		93,3		96,6	
Monzonite 2		95,0		97,5	
Mylonite	59,3	64,3		75,6	
Greywacke		78,5	83,1	84,5	

Table B10: LA4, size fraction 4/8 mm.

Quarry	LA_4				
	0% FI	25% FI	50% FI	75% FI	100% FI
Gabbro		47,5		58,3	
R. porphyry		44,2		55,1	
Monzonite 1		70,7		79,6	
Monzonite 2		71,5		78,8	
Mylonite		36,1	39,0	41,4	
Greywacke	48,6	52,2	57,8	62,0	68,7

Table B11: MD, size fraction 11.2/16 mm.

Quarry	micro-Deval 11.2/16 mm				
	0% FI	25% FI	50% FI	75% FI	100% FI
Gabbro	11,1	10,9		11,7	
R. porphyry		5,9		6,3	
Monzonite 1		11,2		10,8	
Monzonite 2		14,7		15,5	
Mylonite		5,9		6,0	
Greywacke		33,7		37,5	

Table B12: MD, size fraction 8/11.2 mm.

Quarry	micro-Deval 8/11.2 mm				
	0% FI	25% FI	50% FI	75% FI	100% FI
Gabbro	11,5	12,7		13,4	
R. porphyry		5,5		5,7	
Monzonite 1		11,9		12,6	
Monzonite 2		15,4		17,1	
Mylonite	6,2	7,0		7,1	
Greywacke		37,7	39,5	41,0	

Table B13: MD, size fraction 4/8 mm.

Quarry	micro-Deval 4/8 mm				
	0% FI	25% FI	50% FI	75% FI	100% FI
Gabbro		13,8		19,2	
R. porphyry		5,9		9,4	
Monzonite 1		17,1		24,2	
Monzonite 2		19,7		26,6	
Mylonite		7,2	7,7	8,6	
Greywacke	22,8	27,8	31,2	37,5	43,2

Table B14: MD11, size fraction 11.2/16 mm.

Quarry	MD_{11}				
	0% FI	25% FI	50% FI	75% FI	100% FI
Gabbro	44,1	52,0		57,2	
R. porphyry		27,9		46,1	
Monzonite 1		35,5		46,5	
Monzonite 2		56,0		62,5	
Mylonite		22,5		42,6	
Greywacke		64,2		71,9	

Table B15: MD8, size fraction 8/11.2 mm.

Quarry	MD_{8}				
	0% FI	25% FI	50% FI	75% FI	100% FI
Gabbro	45,2	53,8		55,0	
R. porphyry		20,9		29,4	
Monzonite 1		48,8		58,3	
Monzonite 2		47,7		60,4	
Mylonite	23,2	27,9		34,4	
Greywacke		66,7	69,5	72,0	

Table B16: MD4, size fraction 4/8 mm.

Quarry	MD_4				
	0% FI	25% FI	50% FI	75% FI	100% FI
Gabbro		25,3		41,8	
R. porphyry		13,9		27,6	
Monzonite 1		33,6		51,5	
Monzonite 2		36,6		53,6	
Mylonite		9,3	10,9	13,0	
Greywacke	33,6	42,7	48,7	57,2	65,6

Table B17: S2, size fraction 11.2/16 mm.

Rock type	Impact test (S2) 11.2/16 mm				
	0% FI	25% FI	50% FI	75% FI	100% FI
Gabbro					
R. porphyry					
Monzonite 1					
Monzonite 2		14,3		15,3	
Mylonite		3,0		5,0	
Greywacke		6,5		7,4	

Table B18: S2, size fraction 8/11.2 mm.

Rock type	Impact test (S2) 8/11.2 mm				
	0% FI	25% FI	50% FI	75% FI	100% FI
Gabbro					
R. porphyry					
Monzonite 1					
Monzonite 2		15,4		17,1	
Mylonite		4,5		5,6	
Greywacke		8,2		10,4	

Table B19: S11, size fraction 11.2/16 mm.

Rock type	Impact test residue (S11) 11.2/16 mm				
	0% FI	25% FI	50% FI	75% FI	100% FI
Gabbro					
R. porphyry					
Monzonite 1					
Monzonite 2		76,1		83,4	
Mylonite		33,3		53,3	
Greywacke		63,4		73,8	

Table B20: S8, size fraction 8/11.2 mm.

Rock type	Impact test residue (S8) 8/11.2 mm				
	0% FI	25% FI	50% FI	75% FI	100% FI
Gabbro					
R. porphyry					
Monzonite 1					
Monzonite 2		60,9		73,4	
Mylonite		27,6		42,9	
Greywacke		45,2		59,8	

Appendix D: Sieve Analysis

Los Angeles Test: Sieve Analysis

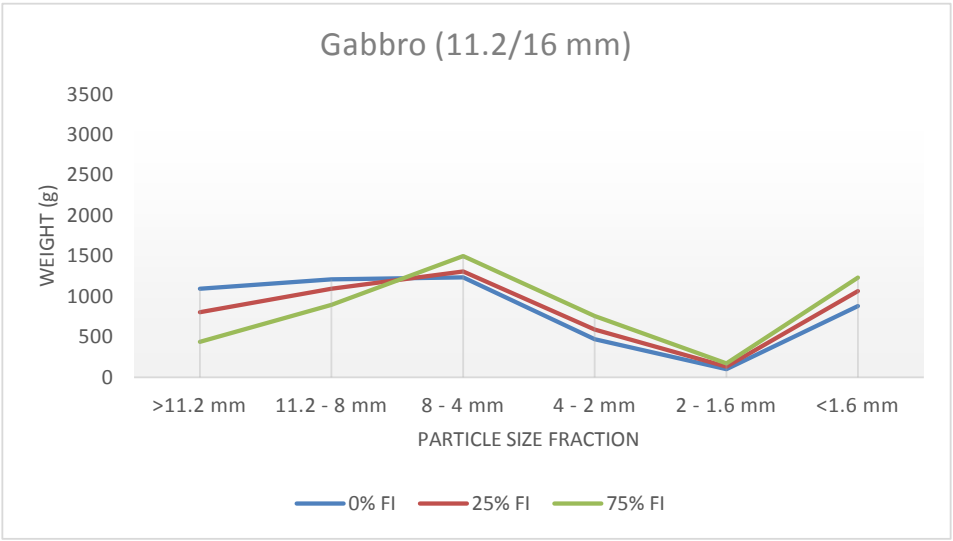

Figure D1: Gabbro size fraction 11.2/16 mm, sieve analysis of the Los Angeles test.

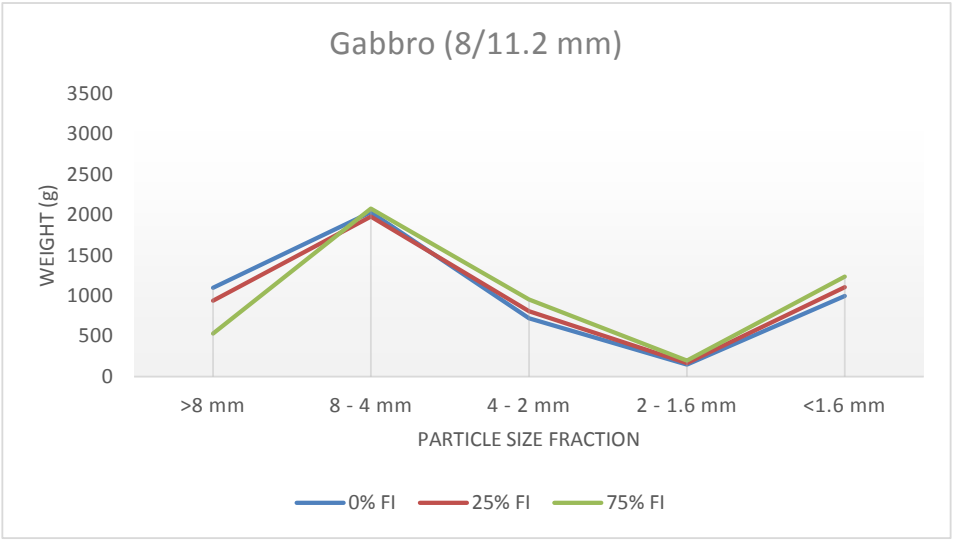

Figure D2: Gabbro size fraction 8/11.2 mm, sieve analysis of the Los Angeles test.

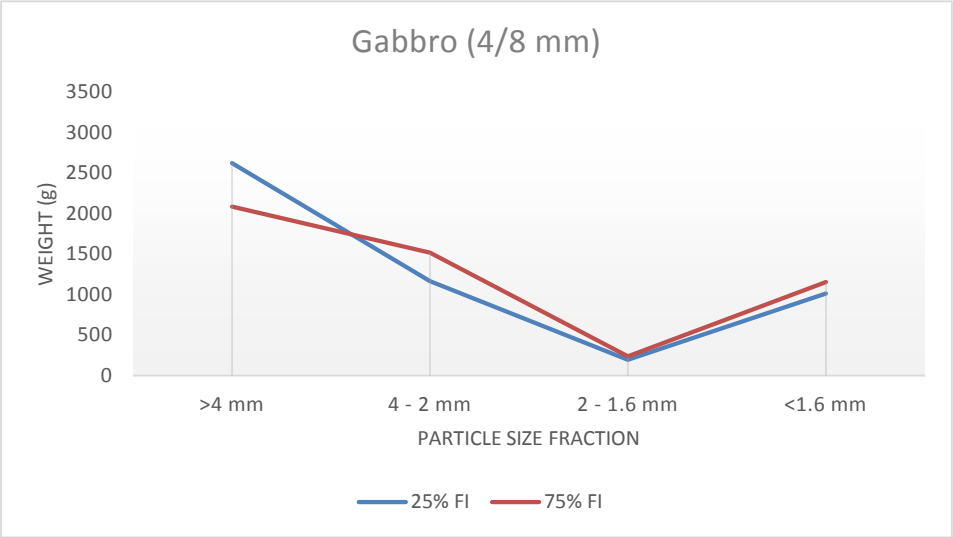

Figure D3: Gabbro size fraction 4/8 mm, sieve analysis of the Los Angeles test.

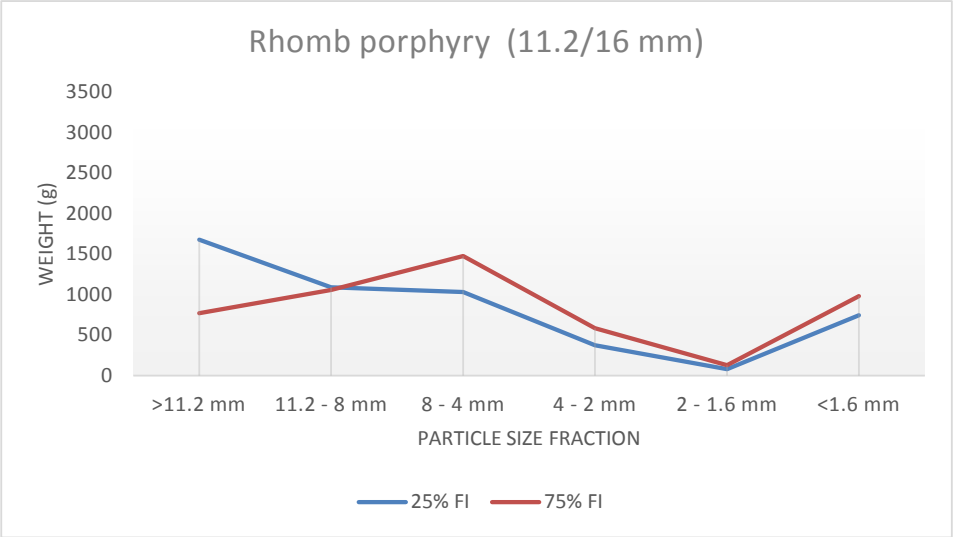

Figure D4: R. porphyry size fraction 11.2/16 mm, sieve analysis of the Los Angeles test.

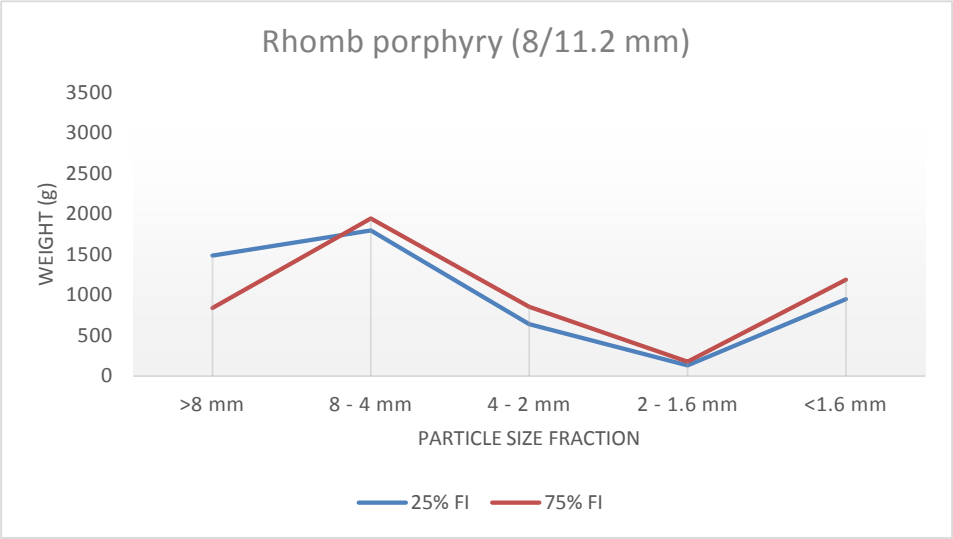

Figure D5: R. porphyry size fraction 8/11.2 mm, sieve analysis of the Los Angeles test.

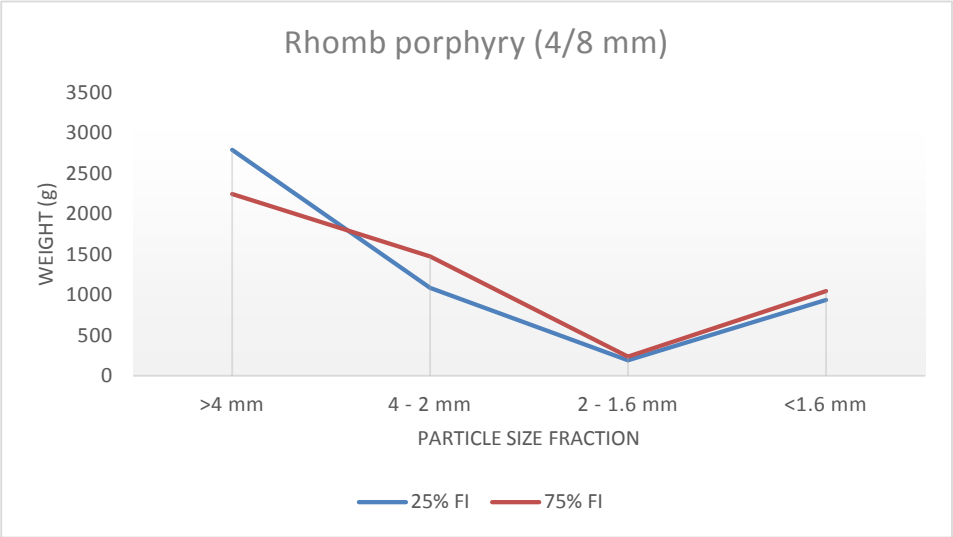

Figure D6: R. porphyry size fraction 4/8 mm, sieve analysis of the Los Angeles test.

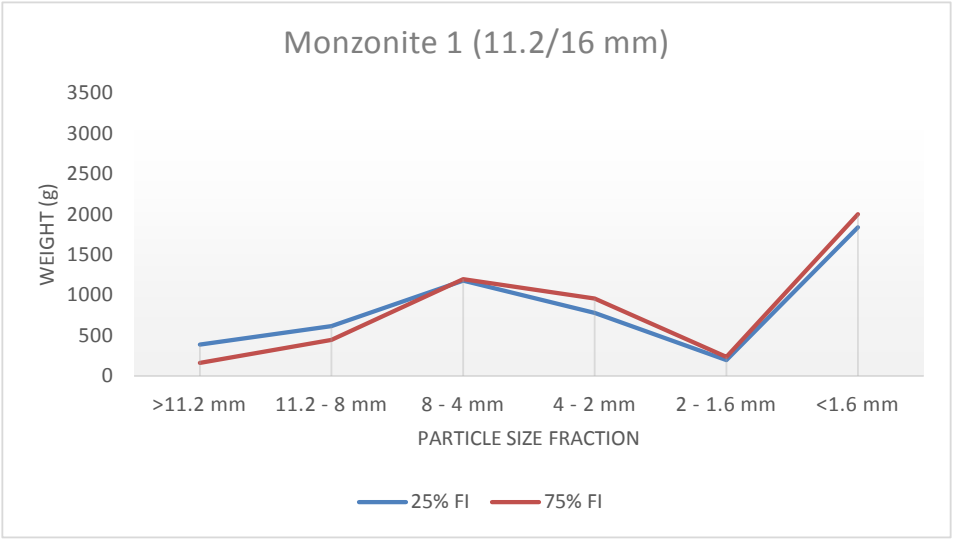

Figure D7: Monzonite 1 size fraction 11.2/16 mm, sieve analysis of the LA test.

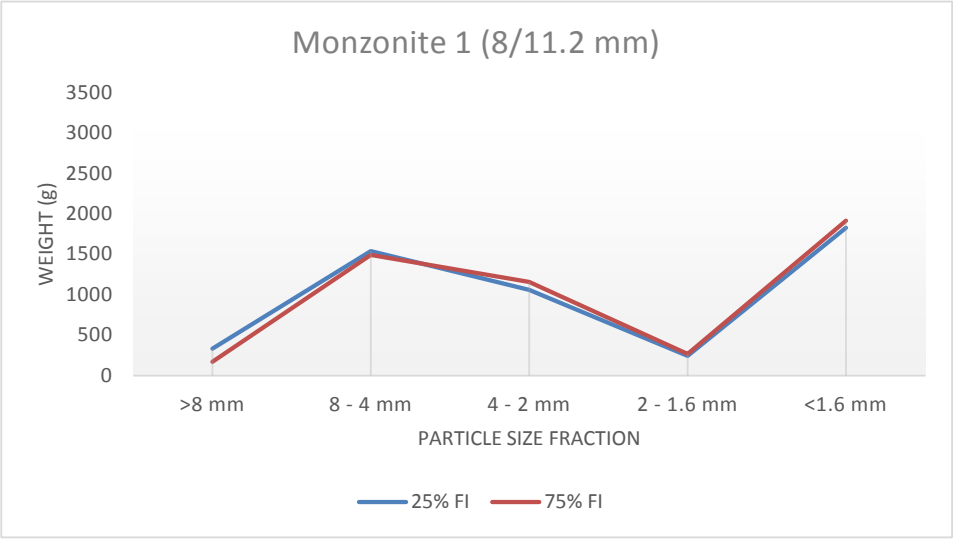

Figure D8: Monzonite 1 size fraction 8/11.2 mm, sieve analysis of the Los Angeles test.

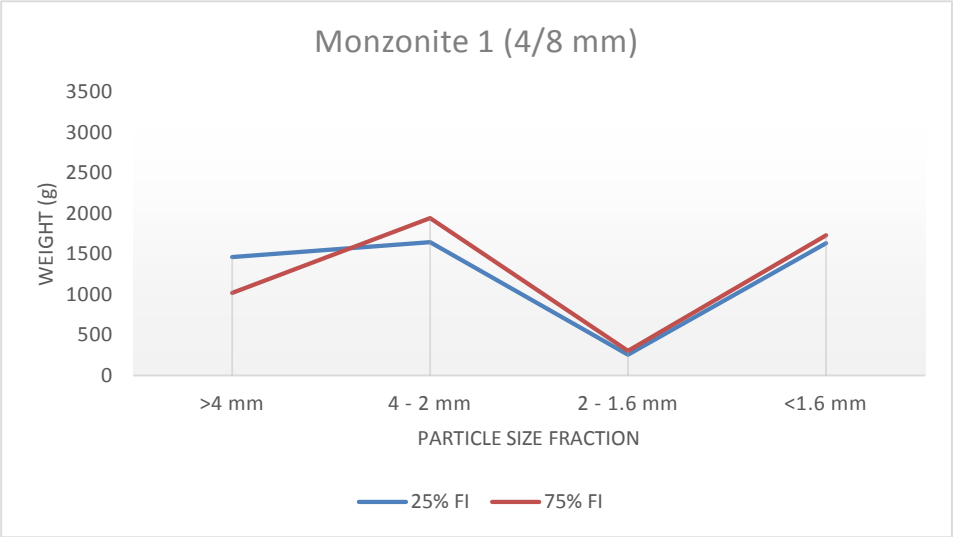

Figure D9: Monzonite 1 size fraction 4/8 mm, sieve analysis of the Los Angeles test.

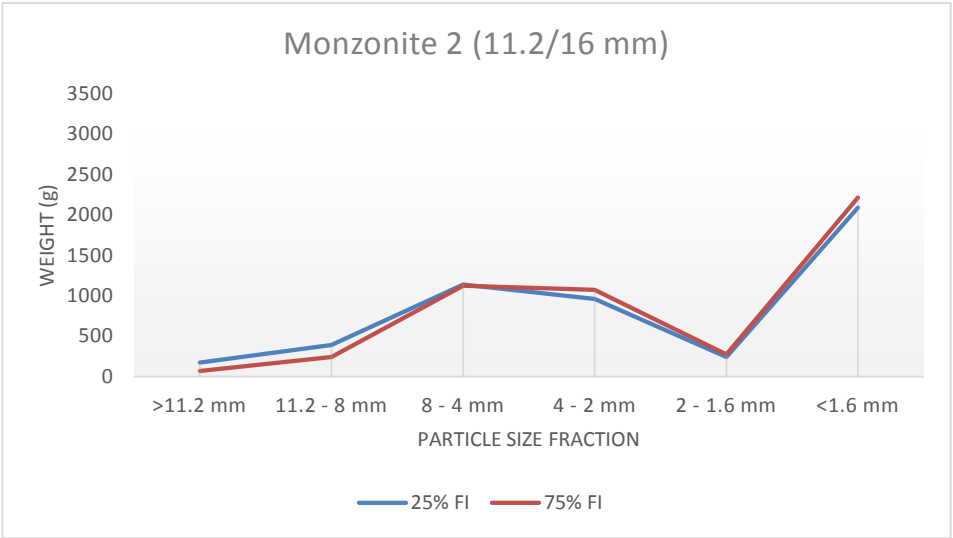

Figure D10: Monzonite 2 size fraction 11.2/16 mm, sieve analysis of the LA test.

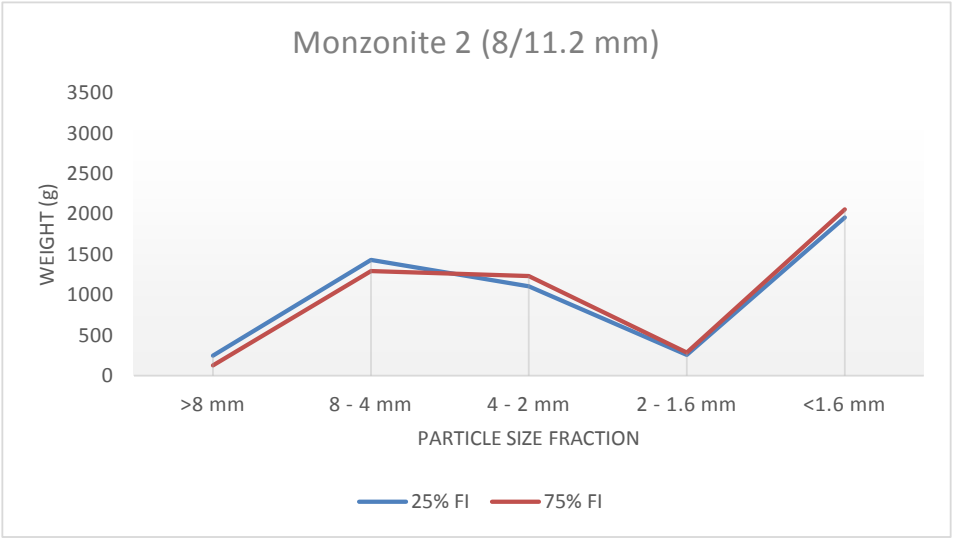

Figure D11: Monzonite 2 size fraction 8/11.2 mm, sieve analysis of the Los Angeles test.

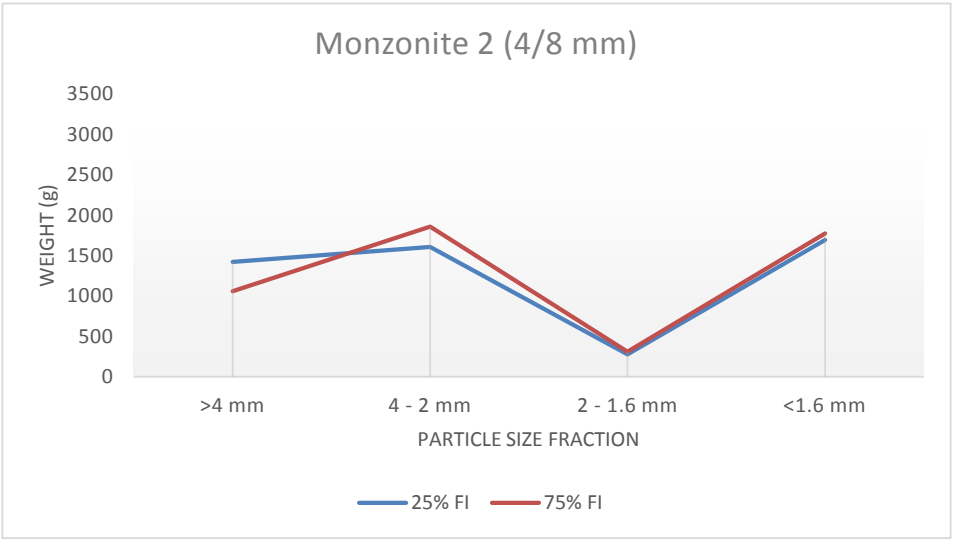

Figure D12: Monzonite 2 size fraction 4/8 mm, sieve analysis of the Los Angeles test.

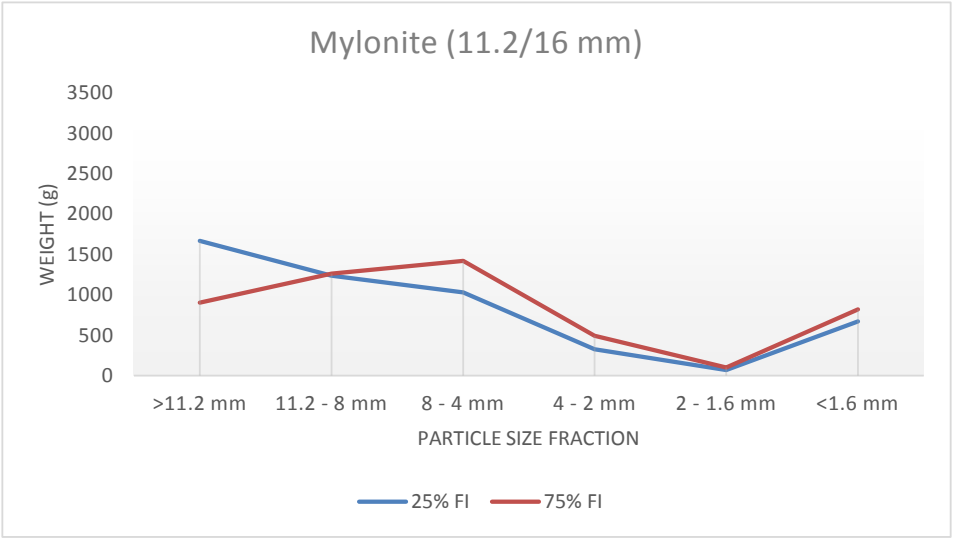

Figure D13: Mylonite size fraction 11.2/16 mm, sieve analysis of the Los Angeles test.

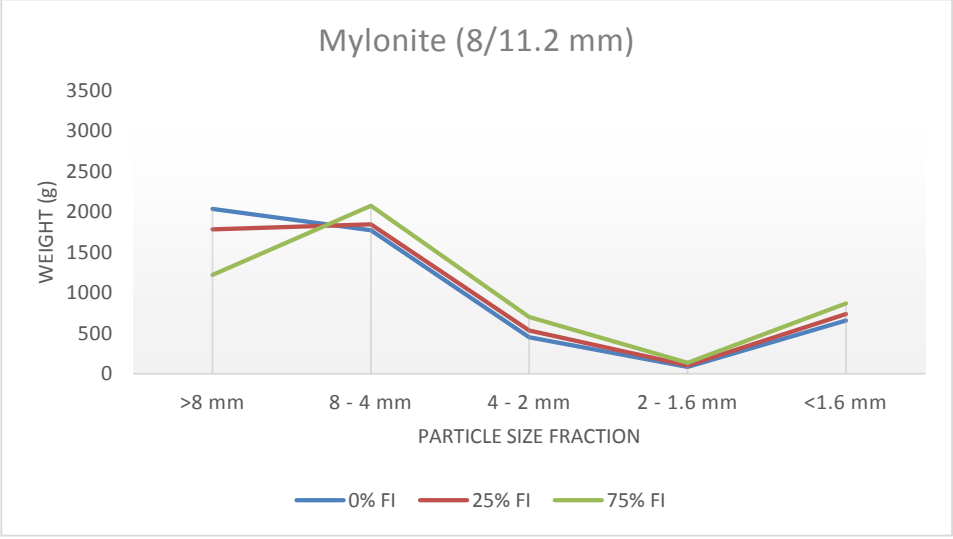

Figure D14: Mylonite size fraction 8/11.2 mm, sieve analysis of the Los Angeles test.

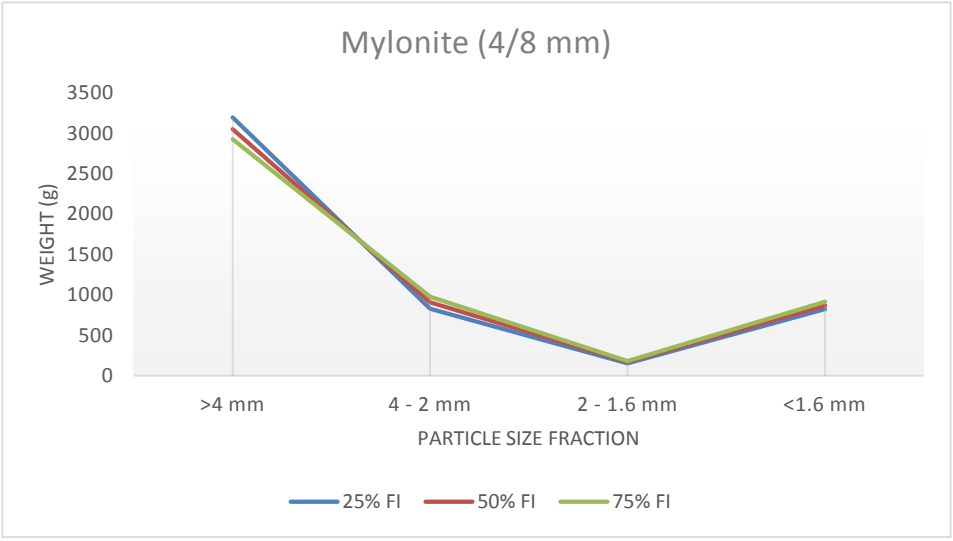

Figure D15: Mylonite size fraction 4/8 mm, sieve analysis of the Los Angeles test.

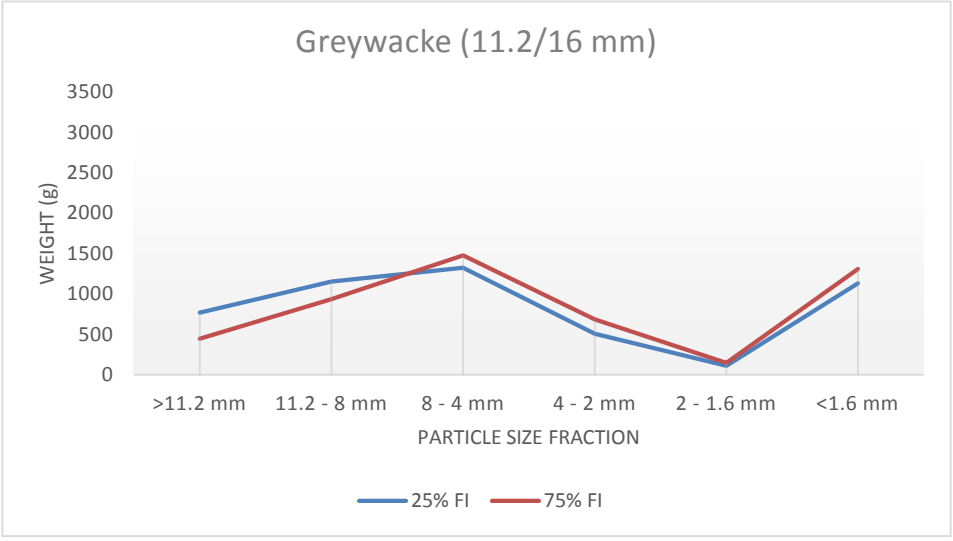

Figure D16: Greywacke size fraction 11.2/16 mm, sieve analysis of the Los Angeles test.

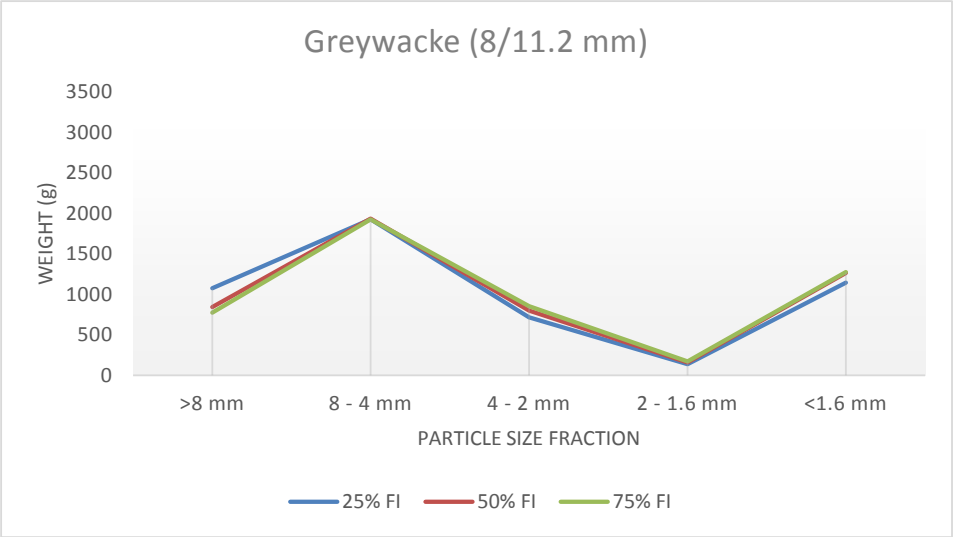

Figure D17: Greywacke size fraction 8/11.2 mm, sieve analysis of the Los Angeles test.

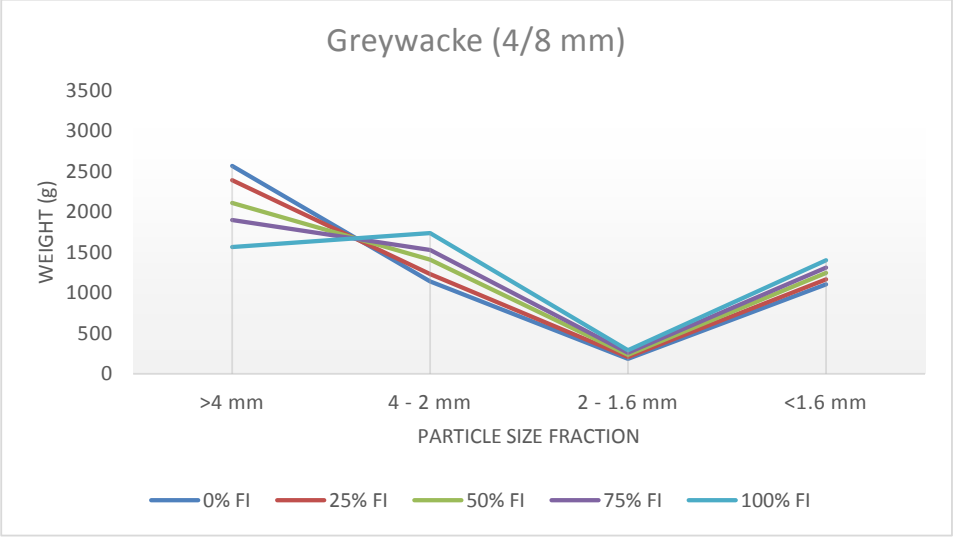

Figure D18: Greywacke size fraction 4/8 mm, sieve analysis of the Los Angeles test.

Micro-Deval Test: Sieve Analysis

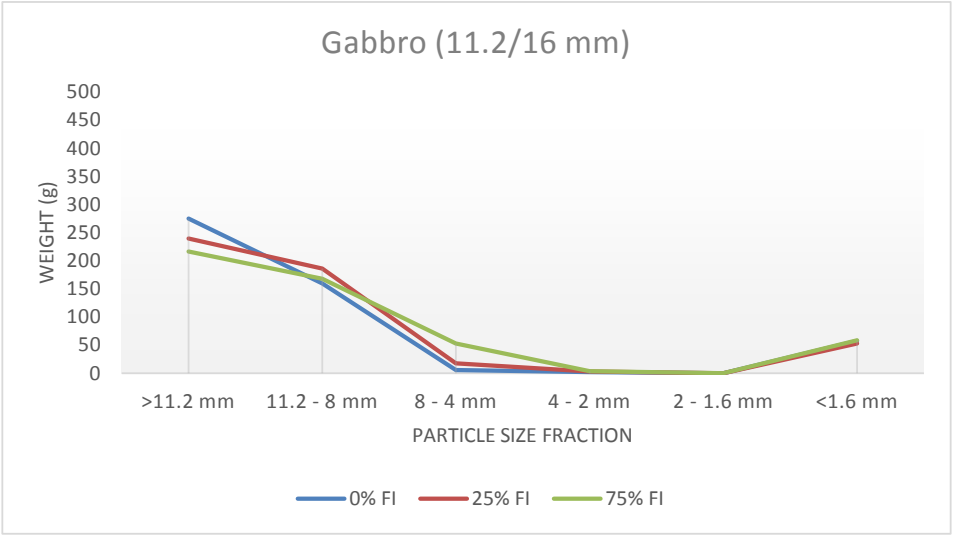

Figure D19: Gabbro size fraction 11.2/16 mm, sieve analysis of the micro-Deval test.

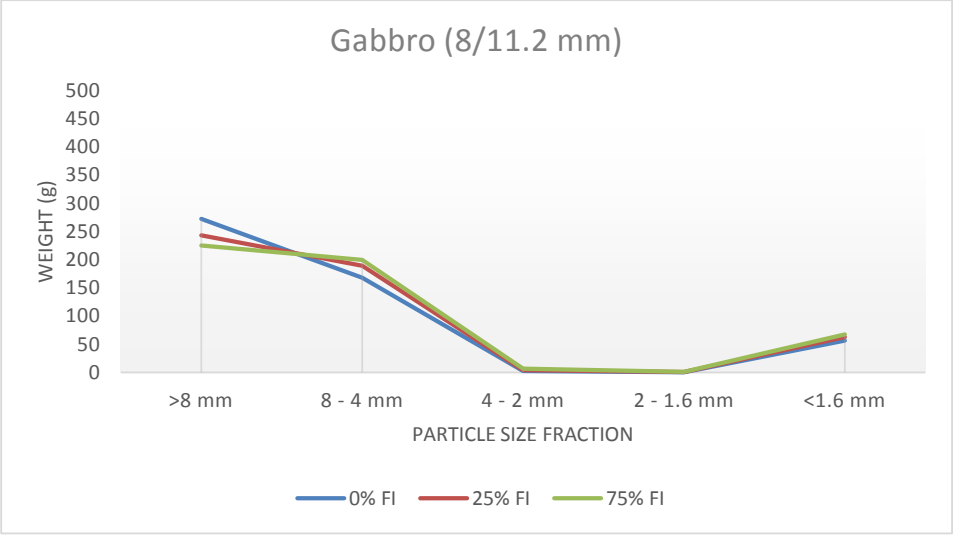

Figure D20: Gabbro size fraction 8/11.2 mm, sieve analysis of the micro-Deval test.

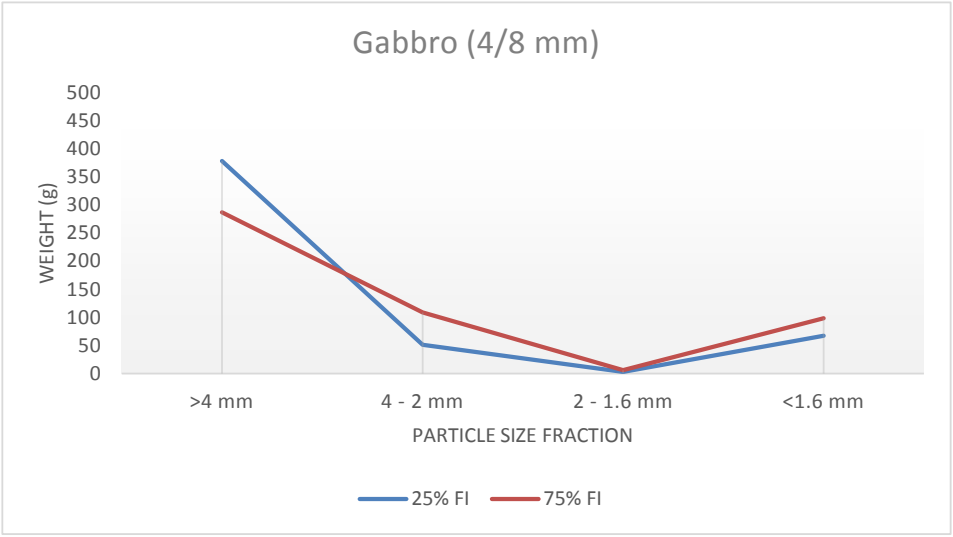

Figure D21: Gabbro size fraction 4/8 mm, sieve analysis of the micro-Deval test.

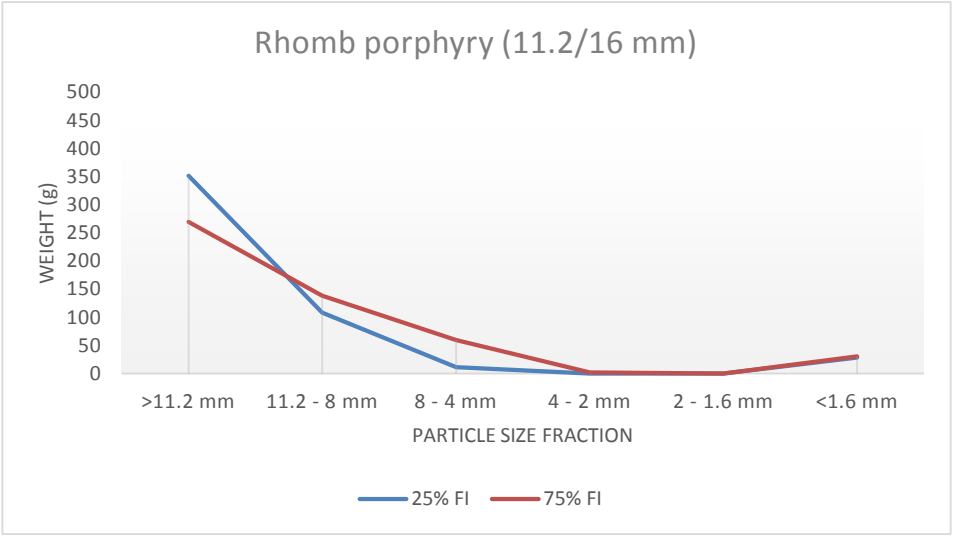

Figure D22: R. porphyry size fraction 11.2/16 mm, sieve analysis of the micro-Deval test.

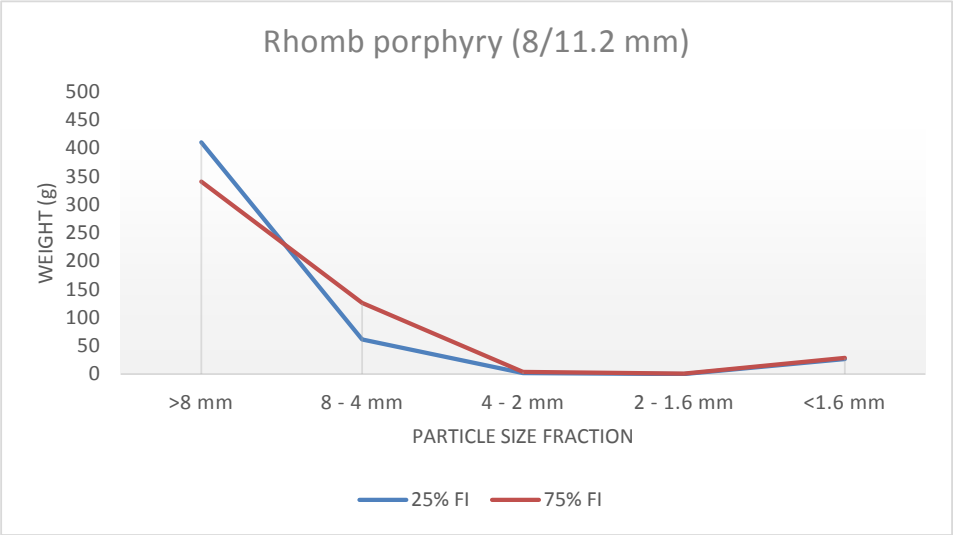

Figure D23: R. porphyry size fraction 8/11.2 mm, sieve analysis of the micro-Deval test.

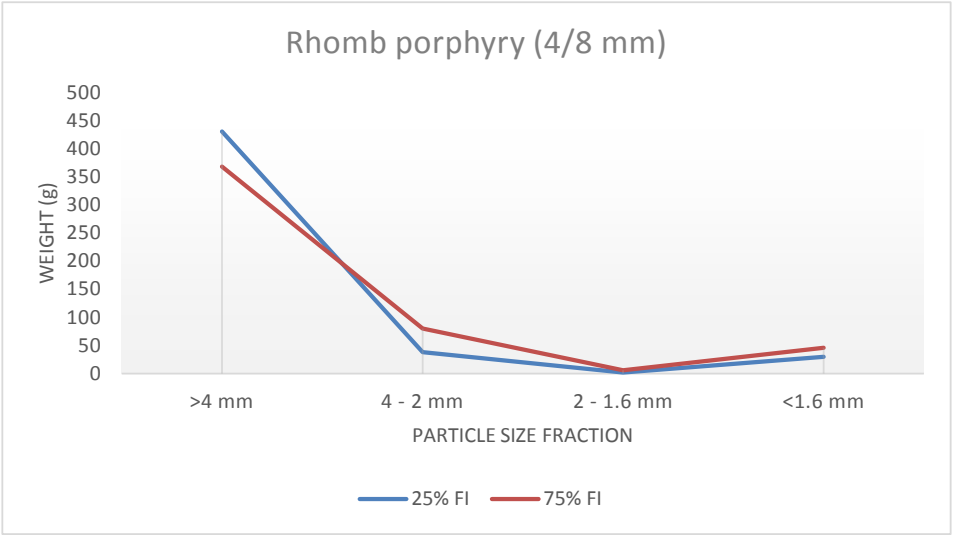

Figure D24: R. porphyry size fraction 4/8 mm, sieve analysis of the micro-Deval test.

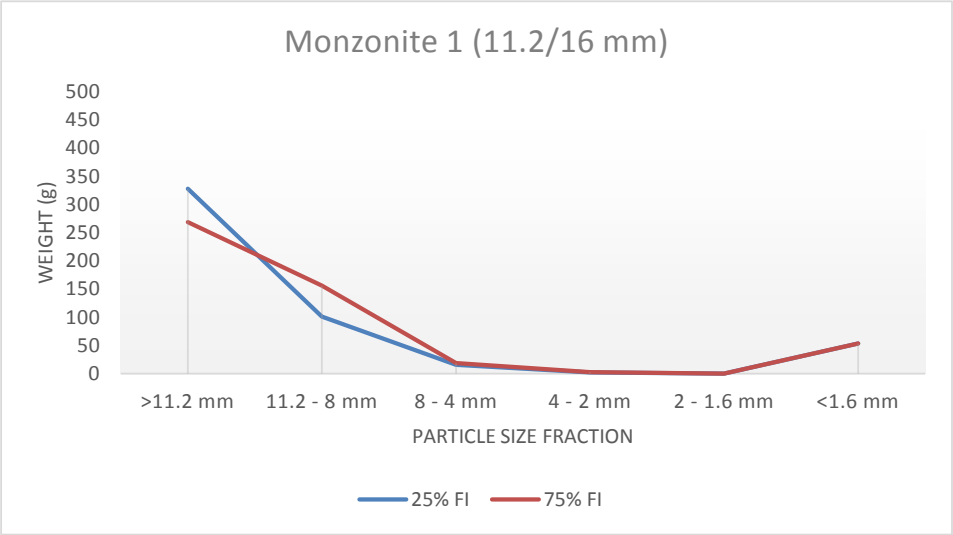

Figure D25: Monzonite 1 size fraction 11.2/16 mm, sieve analysis of the MD test.

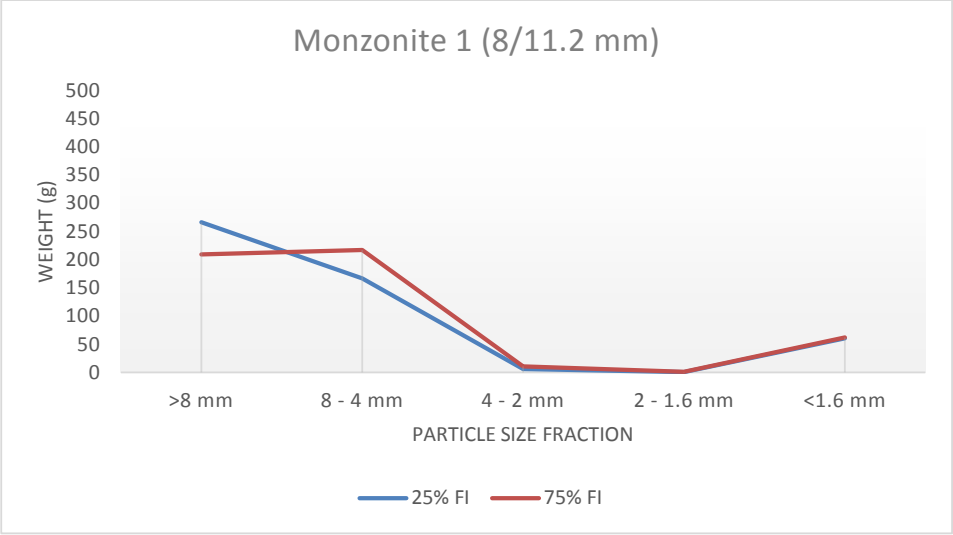

Figure D26: Monzonite 1 size fraction 8/11.2 mm, sieve analysis of the micro-Deval test.

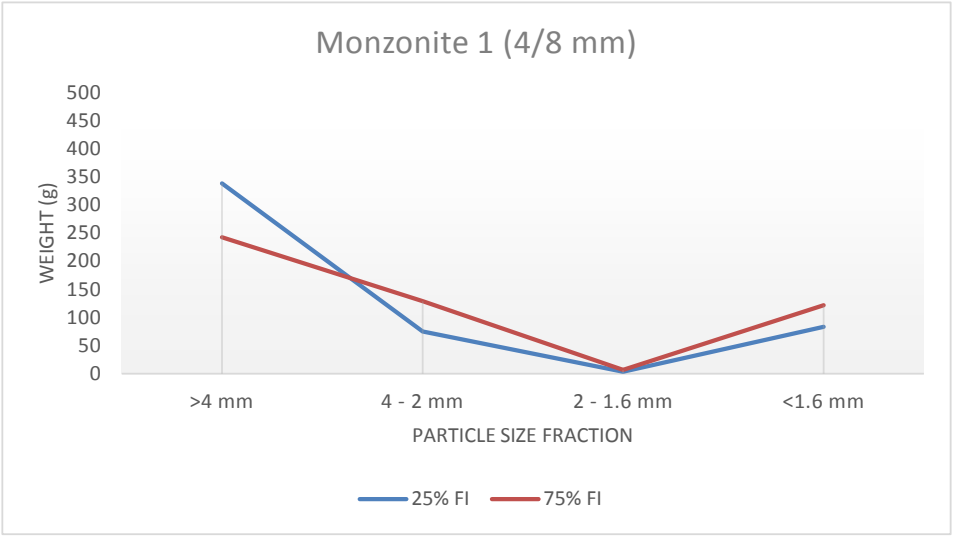

Figure D27: Monzonite 1 size fraction 4/8 mm, sieve analysis of the micro-Deval test.

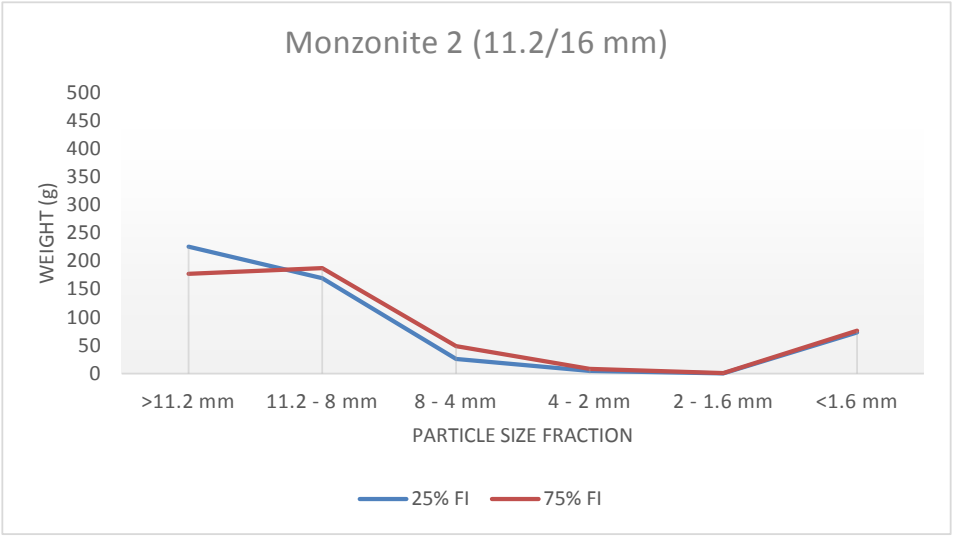

Figure D28: Monzonite 2 size fraction 11.2/16 mm, sieve analysis of the MD test.

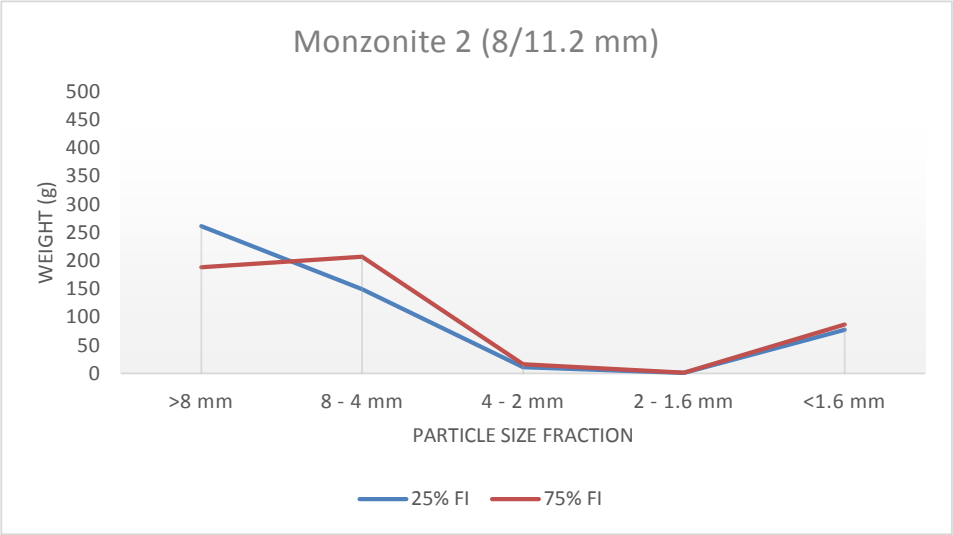

Figure D29: Monzonite 2 size fraction 8/11.2 mm, sieve analysis of the micro-Deval test.

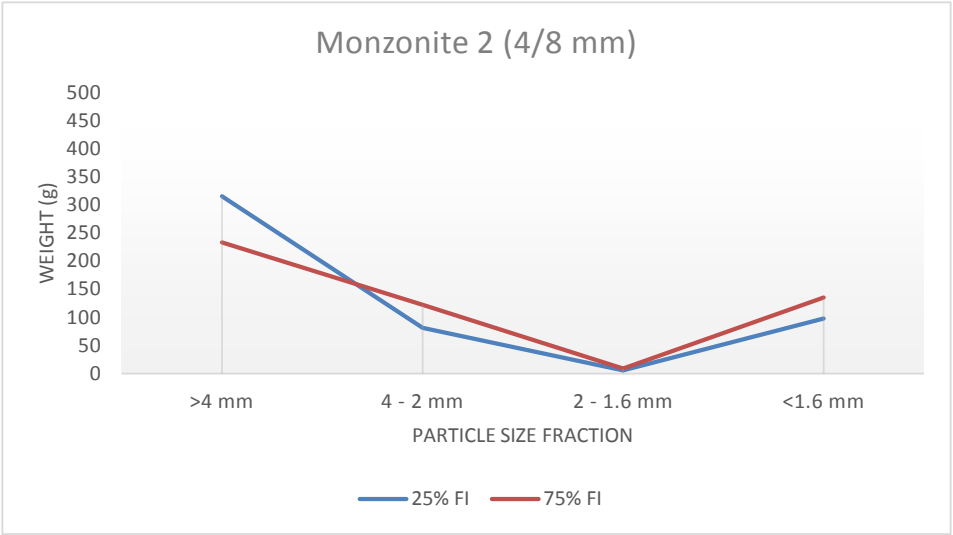

Figure D30: Monzonite 2 size fraction 4/8 mm, sieve analysis of the micro-Deval test.

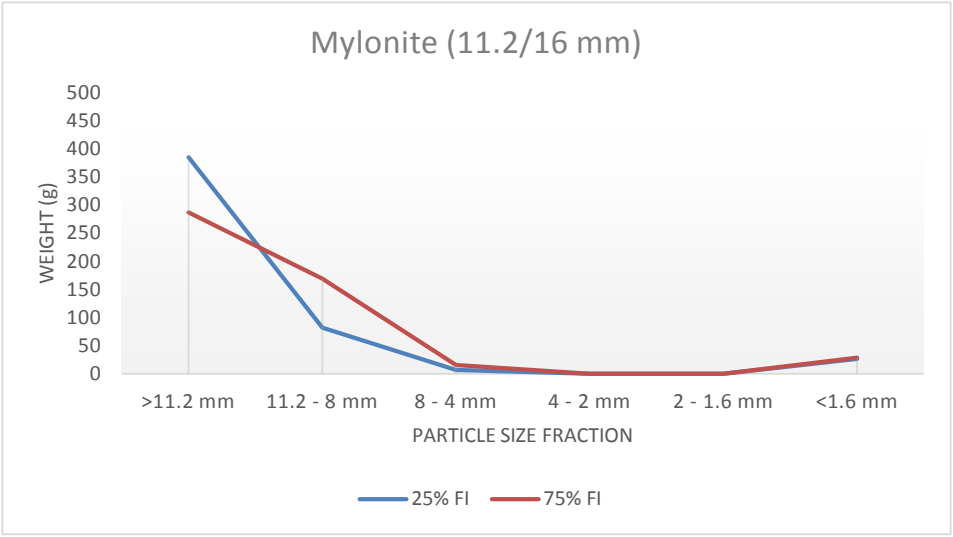

Figure D31: Mylonite size fraction 11.2/16 mm, sieve analysis of the micro-Deval test.

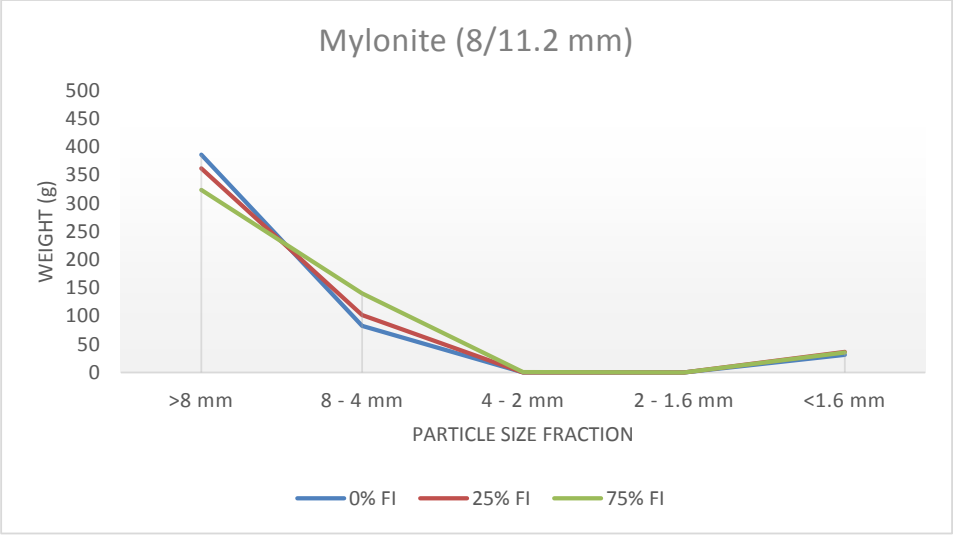

Figure D32: Mylonite size fraction 8/11.2 mm, sieve analysis of the micro-Deval test.

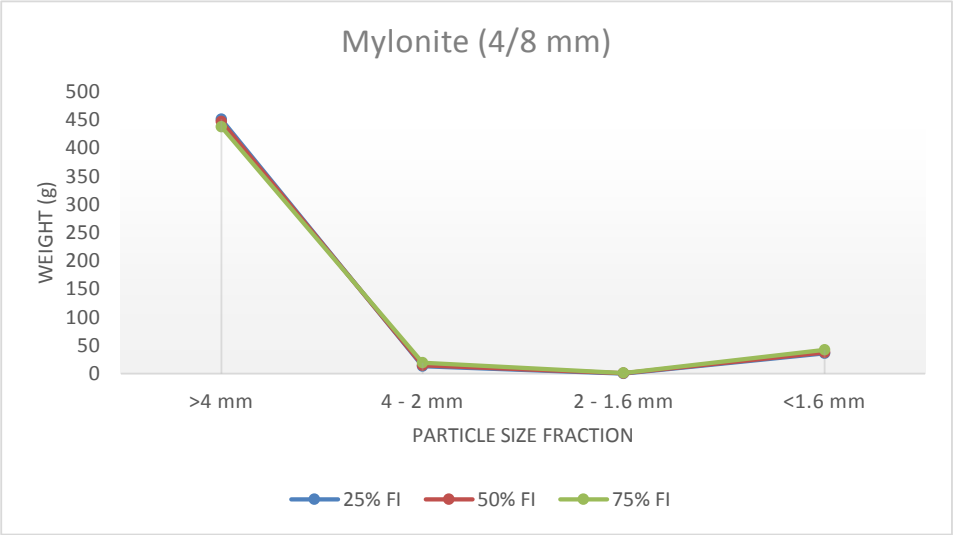

Figure D33: Mylonite size fraction 4/8 mm, sieve analysis of the micro-Deval test.

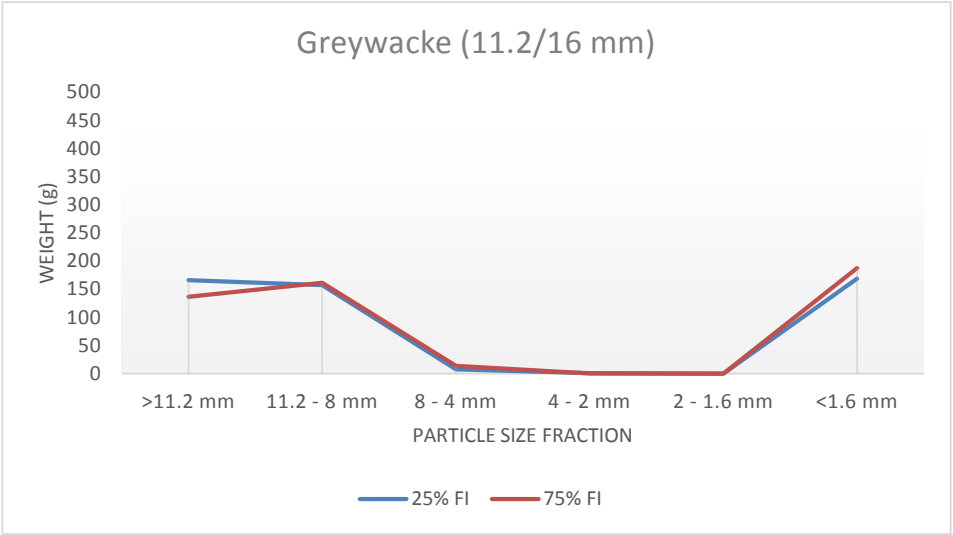

Figure D34: Greywacke size fraction 11.2/16 mm, sieve analysis of the micro-Deval test.

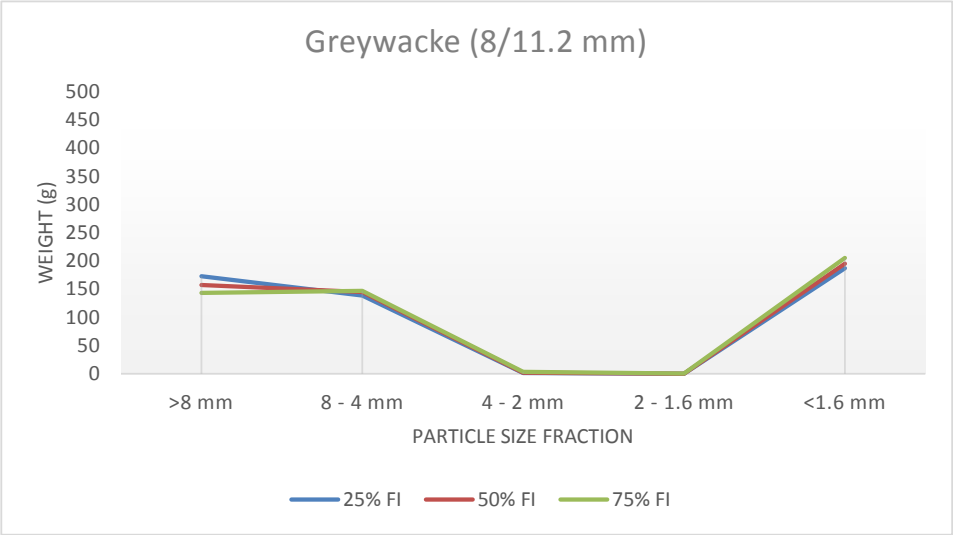

Figure D35: Greywacke size fraction 8/11.2 mm, sieve analysis of the micro-Deval test.

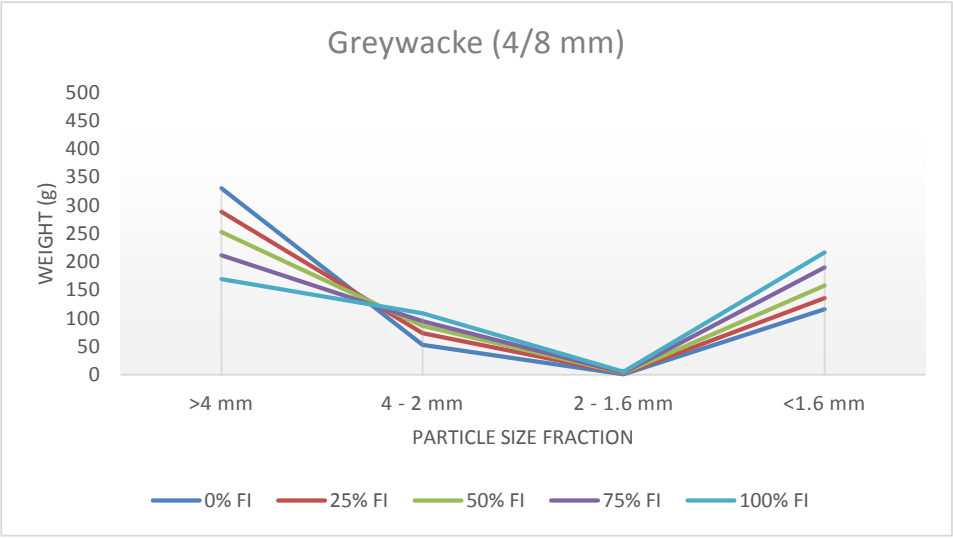

Figure D36: Greywacke size fraction 4/8 mm, sieve analysis of the micro-Deval test.